A molecular and functional analysis of the *Drosophila melanogaster* centrosome

DISSERTATION

zur Erlangung des akademischen Grades des

Doktors der Naturwissenschaften (Dr. rer. nat.)

eingereicht im Fachbereich Biologie, Chemie, Pharmazie

der Freien Universität Berlin

vorgelegt von

Karin Habermann

aus Berlin

April 2010

1. Gutachter: PD Dr. Bodo Lange
2. Gutachter: Prof. Dr. Wolfgang Schuster

Disputation am 22.06.2010

Contents

List of Publications

Habermann, K. and Lange B.M.H. (2010) Centrosomes: Methods for preparation. In: Encyclopedia of Life Sciences (ELS). John Wiley & Sons, Ltd: Chichester.

Hormeño S., Ibarra B., Chichón F.J., Habermann K., Lange B.M.H., Valpuesta J.M., Carrascosa J.L., Arias-Gonzalez J.R. (2009) Single centrosome manipulation reveals its electric charge and associated dynamic structure. *Biophysical Journal* **97**: 1022-1030.

Müller H., Mirgorodskaya E., Steinbrink S., Schmidt D., Lehmann V., Habermann K., Gustavsson N., Kessler T., Ploubidou A., Lehrach H., Gobom J., Boutros M., Lange B.M.H. (2010) Proteomic and functional analysis of the mitotic *Drosophila* centrosome. Embo J. *in revision*

Habermann K., Gobom J., Lehmann V., Müller H., Erdmann C., von Kries J., Lange B.M.H. (2010) Functional analysis of the centrosome phosphoproteome in *Drosophila.* JCB. *submitted*

1 Introduction

1.1 The centrosome

The centrosome is a membrane-less, single-copy organelle, which is present in all eukaryotic species with the exception of some female meiotic systems and the majority of higher plants. Ever since its discovery by Theodor Boveri in the late 19th century (Boveri, 1901), research has been dedicated to unraveling the structure, functions and molecular composition of this intriguing organelle. Today, the centrosome is primarily known as the major microtubule organizing centre (MTOC) of mammalian cells. However, evidence for its importance in other cellular processes, e.g. cell cycle regulation, stress response and tumorigenesis, has emerged in recent years and we are now beginning to recognize the functional complexity of this organelle and to understand the role of the centrosome in various pathologies (Badano et al., 2005; Nigg and Raff, 2009).

1.2 Centrosome structure

Mammalian centrosomes are approximately 1 µm in size. They are comprised of two orthogonally arranged centrioles that are embedded in an amorphous protein matrix, known as the pericentriolar material (PCM). The PCM is a lattice-like structure that anchors and nucleates microtubules and docks other protein complexes (Bornens, 2002). Its molecular composition is highly dynamic in that the number of PCM proteins increases dramatically as the cell prepares for mitosis (Kalt and Schliwa, 1993). Each centriole is composed of 9 microtubule triplets, which are arranged in a pinwheel-like structure. Mother and daughter centrioles are linked by interconnecting fibers and the mother centriole additionally carries subdistal and distal appendages which are required for the anchoring of cytoplasmic microtubules (Paintrand et al., 1992) (see Figure 1). It is important to note that the structure of centrioles and centrosomes, respectively, varies in different organisms. In *Drosophila melanogaster* and *Caenorhabditis elegans* embryos, centrioles are comprised of singlet or doublet microtubules and lack appendages (Moritz et al., 1995a; Gonzalez et al., 1998; O'Toole et al., 2003). *Chlamydomonas reinhardtii* centrioles are structurally very similar to human centrioles but they lack any appreciable PCM (Dutcher, 2003). Yeast cells do not possess centrioles but they developed a structure known as the spindle pole body, which is embedded in the nuclear membrane and is generally considered to be the functional analogue of the animal centrosome (Rout and Kilmartin, 1990; Jaspersen and Winey, 2004). Despite these structural differences, centrosome functions and many of its components are highly conserved among various species.

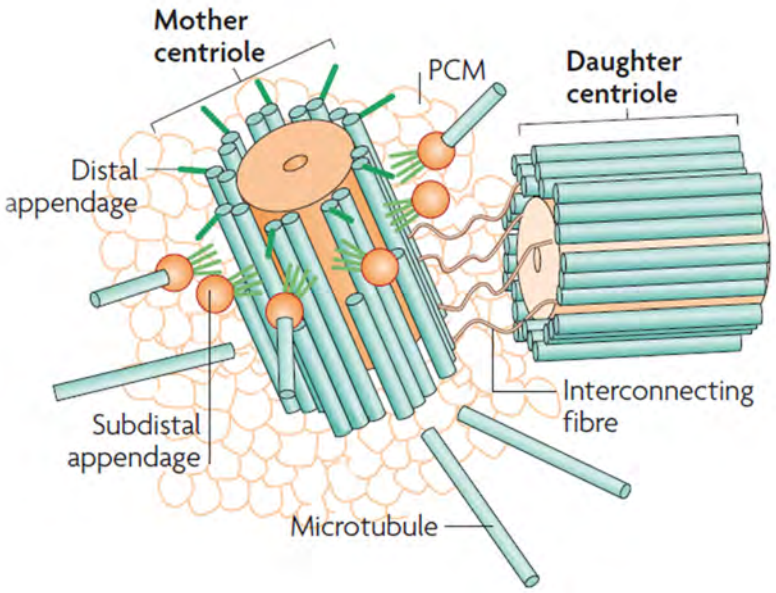

Figure 1: Schematic view illustrating the structure of the centrosome (from Bettencourt-Dias and Glover, 2007)

1.3 The centrosome cycle

In dividing cells, the centrosome duplicates once per cell cycle such that at the onset of mitosis, a cell contains two centrosomes that form the poles of the mitotic spindle. During cytokinesis, one centrosome is distributed to each daughter cell. Likewise, a cell replicates its DNA and following mitosis each daughter cell inherits one set of chromosomes. In order to ensure genomic stability, both the centrosome and chromosome duplication cycle need to progress in a synchronized and coordinated fashion (Meraldi and Nigg, 2002). Uncoupling of the two cycles can lead to centrosome amplification as a result of successive rounds of duplication in the same S-phase and may trigger chromosomal instability and malignant transformation (Nigg, 2002). The centrosome cycle is subdivided into 4 distinct steps, which are tightly linked to different stages of the cell cycle (see Figure 2).

(1) In G1, mother and daughter centriole lose their orthogonal orientation in a process termed centriole disengagement. This is an essential prerequisite for the growth of daughter centrioles and considered to be the licensing event which ensures that centriole duplication occurs only after cells have passed through mitosis (Wong and Stearns, 2003). Disengagement depends on the activity of the cysteine protease Separase and Plk1 (Tsou and Stearns, 2006; Tsou et al., 2009). The nucleolar protein nucleophosmin, which shuttles between the nucleus and centrosomes, is also implicated in this process. Phosphorylated nucleophosmin is released from the centrosome and this release is a prerequisite for centriole disengagement (Okuda, 2002). **(2)** At the G1/S transition, centrosome duplication is

initiated through the formation of procentrioles at the proximal end of each parental centriole. Pioneering studies in *C. elegans* early embryos have identified 5 essential proteins involved in the centriole duplication pathway, the kinase ZYG-1 and the coiled-coil proteins SPD-2, SAS-4, SAS-5 and SAS-6. Their timely ordered recruitment to the parental centriole results in the formation of procentrioles (Leidel and Gonczy, 2005; Delattre et al., 2006; Pelletier et al., 2006). This process is conserved in humans and flies, as orthologues of all proteins, except SAS-5, have been identified in these species. The kinase Plk4/Sak, the functional analogue of ZYG-1, and SAS-6 are master regulators of centriole duplication in human and *Drosophila* (Habedanck et al., 2005; Bettencourt-Dias et al., 2005). The mechanism by which the number of newly formed centrioles next to the parental centriole is restricted to one is not well understood. It has been shown that overexpression of Plk4 or SAS-6 induces the formation of extra centrioles around a single parent (Kleylein-Sohn et al., 2007; Leidel et al., 2005; Peel et al., 2007). Therefore it is likely that the number of centrioles produced during each S-phase depends on the limited presence of these proteins at centrosomes. Elongation of procentrioles proceeds throughout S-phase in concert with chromosome replication until maximal length is reached in late G2. It is not fully understood how the final length of the newly assembled daughter centriole is determined but the three proteins CP110, SAS-4 and POC1 appear to be involved in length control (Keller et al., 2009; Kohlmaier et al., 2009; Schmidt et al., 2009). **(3)** At the G2/M transition, centrosomes recruit several PCM components required for microtubule nucleation, a process termed maturation (Palazzo et al., 2000), and **(4)** eventually separate and move to opposite poles to assemble the bipolar mitotic spindle. Centrosome maturation is promoted through the coordinated activity of Plk1 and Aurora-A, which recruit several proteins involved in nucleation, anchorage and stability of microtubules, such as γ-TuRC components, Asp, TACC and MSPS (Blagden and Glover, 2003; Glover, 2005; Giet et al., 2002; Barros et al., 2005). The separation of duplicated centrosomes at the G2/M transition is triggered by the kinase Nek2, which upon phosphorylation of its substrate c-Nap1 releases the fibrous link between centrioles (Bahe et al., 2005; Yang et al., 2006).

Non-dividing cells often form a cilium, which is assembled from the mother centriole after the centrosome has migrated to the cell surface (ciliogenesis) (Satir and Christensen, 2007). Apart from the canonical (centriolar) pathway of centriole biogenesis, in which the mature centriole functions as a template, centrioles can also form de novo in the absence of pre-existing template centrioles (Khodjakov et al., 2002; Marshall et al., 2001). This acentriolar pathway is commonly seen in epithelial cells that can simultaneously generate hundreds of centrioles in order to form motile cilia, which are required for example in the fallopian tubes and trachea (Dirksen, 1991).

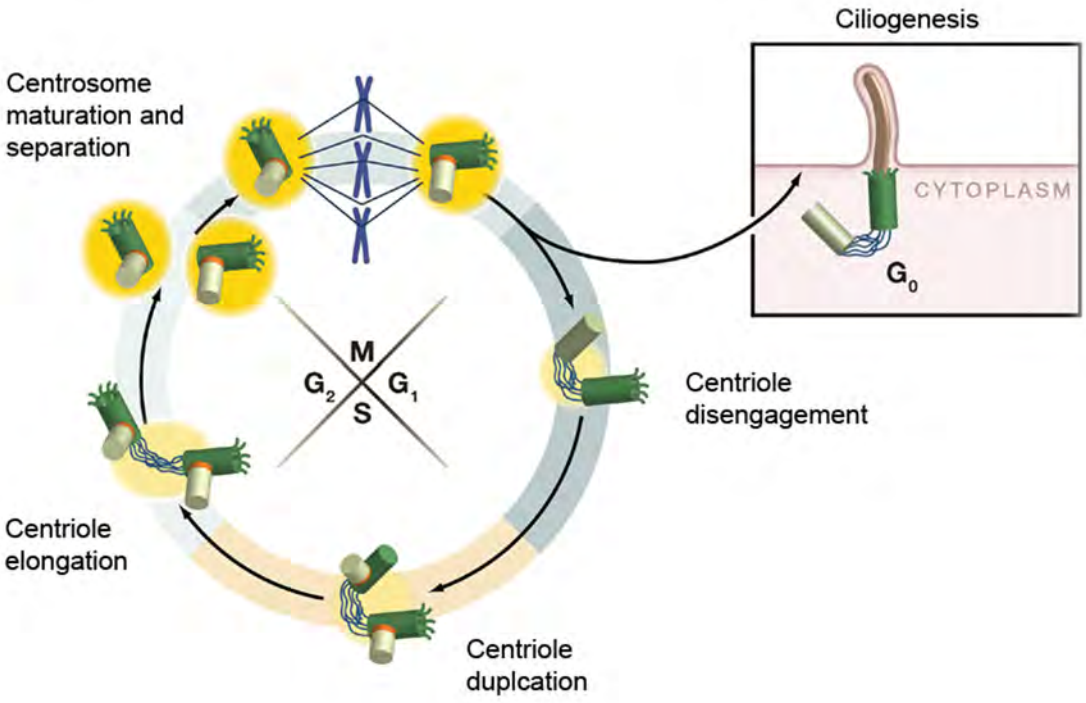

Figure 2 Schematic illustrations of centrosome duplication and ciliogenesis during the cell cycle (from Nigg and Raff, 2009)

1.4 Centrosome functions

1.4.1 Microtubule-dependent functions

The most prominent role of the centrosome is the nucleation and organization of microtubules and hence the coordination of all microtubule-dependent functions. In interphase cells, this includes the regulation of cell motility, adhesion and polarity, the maintenance of cell shape as well as intracellular transport and positioning of organelles. In proliferating cells, the centrosome facilitates the assembly of the bipolar mitotic spindle, which is required for efficient and correct segregation of duplicated chromosomes (Doxsey, 2001; Bettencourt-Dias and Glover, 2007; Schatten, 2008). Although the centrosome is implicated in mitotic spindle assembly, many cell types can divide normally without centrosomes. For instance, centrosomes are naturally absent from female germ cells of many species and from higher plants (Theurkauf and Hawley, 1992; Schmit, 2002). Furthermore, Basto and colleagues showed that mutant flies lacking centrosomes can develop into morphologically normal adults (Basto et al., 2006). In these systems, cell division is accomplished by using a centrosome-independent pathway for spindle formation, in which microtubules are nucleated in the vicinity of chromosomes and the minus ends are focused by microtubule motors and microtubule-bundling proteins (Wadsworth and Khodjakov, 2004). However, spindle assembly is slowed in mutant flies, suggesting that

centrosomes albeit not required, increase the efficiency of cell division. In contrast to these findings, centrosomes were shown to be required for efficient asymmetric cell divisions of *Drosophila* male germline stem cells and neuroblasts. They contribute to correct spindle orientation and thus ensure the precise distribution of fate determinants between the two daughter cells. (Yamashita et al., 2003; Basto et al., 2006; Gonczy, 2008)

1.4.2 Cilia formation

While centrosomes may be dispensable for spindle assembly in some cell types, they are absolutely essential for the organization of cilia and flagella. In non-dividing cells, mother centrioles can transform into basal bodies, which migrate to the cell cortex and form a cilium (Satir and Christensen, 2007). Two types of cilia are known. Motile cilia are composed of a ring of nine outer microtubule doublets and two central microtubule doublets. In humans, they are found in large numbers projecting from several epithelial tissues such as the bronchial tubes, where their coordinated movement sweeps debris out of the lung. Nonmotile cilia, also referred to as primary cilia, lack the central pair of microtubules. Most vertebrate cells possess a primary cilium but its important functions in many cellular and developmental processes have only recently been acknowledged. They play a role in chemical sensation and modulate several signaling pathways that are essential during development (Singla and Reiter, 2006). Ciliary defects are linked to a variety of diseases, such as abnormalities in left-right asymmetry (situs inversus) (Nonaka et al., 1998), polycystic kidney and liver disease and other ciliopathic genetic disorders like the Bardet-Biedl syndrome, which is caused by mutations in different basal body genes (Badano et al., 2006). Although many molecular components of basal bodies, cilia and flagella have been identified (Ostrowski et al., 2002; Keller et al., 2005; Li et al., 2004), currently little is known about the mechanisms that mediate the biogenesis of these structures.

1.4.3 Cell cycle regulation

As described above, the centrosome duplication cycle is intimately linked to cell cycle progression. Remarkably, in recent years it has been shown that the centrosome itself is involved in the orchestration of various cell cycle events, such as entry into mitosis, anaphase onset, cytokinesis and the G1 to S transition (Sluder, 2005). It has been proposed that control of the cell cycle is mediated by the centrosome via anchoring several cell cycle regulatory proteins. It thus functions as a scaffold which increases the local concentration of enzymes, positions them in proximity to their downstream targets or upstream modulators and ultimately increases the efficiency of signaling pathways (Doxsey et al., 2005a; Doxsey et al, 2005b).

G2 to M transition

The first evidence to link the centrosome with the regulation of mitotic entry came from the observation that the initial activation of the mitotic kinase Cdk1/Cyclin B takes place at centrosomes in early prophase. Activated Cdk1 then spreads from the centrosome to promote important mitotic events like nuclear envelope breakdown, chromosome condensation and spindle formation (Jackman et al., 2003). Subsequent studies have demonstrated that centrosomal kinases Aurora-A and Chk1 function as upstream positive and negative regulators of Cdk1, respectively and their association with centrosomes is important for the proper timing of the G2/M transition (Dutertre et al., 2004; Kramer et al., 2004). In *C. elegans*, the activity of centrosome-associated Aurora-A has furthermore been shown to be required for efficient breakdown of the nuclear envelope (Portier et al., 2007).

Metaphase to anaphase transition

In addition to the kinetochore, which is a highly conserved protein complex located at the centromere of chromosomes and a well-established regulator of the metaphase to anaphase transition, several lines of evidence indicate that centrosomes also play a role in anaphase onset. For instance, Cyclin B destruction is initiated at the centrosome and proceeds along the mitotic spindle. When centrosomes are detached from the spindle, Cyclin B degradation is inhibited at spindle microtubules and consequently cells fail to progress to anaphase (Wakefield et al., 2000). Furthermore, homologues of the centrosomal proteins γ-Tubulin and pericentrin in *A. nidulans* and *S. pombe*, respectively were shown to be involved in the regulation of the metaphase/anaphase transition (Prigozhina et al., 2004; Rajagopalan et al., 2004). Finally, Müller and colleagues demonstrated that in *Drosophila*, loss of γ-Tubulin or γ-TuRC proteins activates the spindle assembly checkpoint (Müller et al., 2006). In support of these findings, γ-TuRC was shown to promote spindle assembly through nucleation of microtubules at kinetochores in human cells (Mishra et al., 2010).

Cytokinesis

Several studies suggest a role for the centrosome in cytokinesis. In some human cell lines, the mother centriole transiently migrates to the midbody at the end of telophase upon which abscission of the two daughter cells occurs (Piel et al., 2000; Piel et al., 2001). When centrosomes are removed from cells, by either laser ablation or microsurgical cutting, they still form a cleavage furrow but frequently fail to complete cytokinesis (Hinchcliffe et al., 2001; Khodjakov and Rieder, 2001) suggesting that centrosomes deliver regulatory components (e.g. Plk1 and motor proteins) and/or membrane vesicles to the midbody that are required for the completion of cell separation.

G1 to S transition

In addition to cytokinesis defects or failure, experimentally induced centrosome loss as well as individual silencing of many centrosome components results in failure to replicate DNA and arrest in G1 phase of the cell cycle. These findings led the authors to propose a novel checkpoint at the G1/S transition that monitors centrosome integrity (Mikule et al., 2007). However, this hypothesis remains controversial as G1 arrest does not occur in the absence of p53 and p38 and therefore centrosome perturbation might rather trigger a stress response which in turn leads cells to arrest prior to entering S-Phase (Srsen et al., 2006; Uetake et al., 2007).

1.4.4 Stress response

Cellular stresses such as heat shock or DNA damage directly affect centrosome structure and function. When cells are exposed to elevated temperatures, centrosomes disperse and multipolar spindles are formed (Debec and Marcaillou; 1997). Similarly, centrosome fragmentation and inactivation has been shown to occur in response to impaired DNA integrity in both DNA damage checkpoint defective vertebrate cells and *Drosophila* embryos (Sibon et al, 2000; Takada et al., 2003; Hut et al., 2003; Castedo et al., 2004b). Moreover, heat shock proteins, e.g. Hsp90 (Lange et al., 2000) and components of the DNA damage checkpoint (Chk2, Chk1) are concentrated at the centrosome (Takada et al., 2003; Kramer et al., 2004). Taken together, these findings suggest that centrosomes are implicated in signaling pathways related to stress response. However, the molecular mechanisms which lead to disruption and inactivation of centrosomes in response to environmental perturbations remain to be fully understood. It is important to note though, that the inactivation of centrosomes as a consequence of DNA lesions in the absence of a checkpoint control contributes to chromosome segregation failures. This in turn triggers a process termed mitotic catastrophe, which leads to cell death by apoptosis and non-apoptotic pathways, respectively, a mechanism that is critical for the maintenance of genomic integrity, normal development and disease prevention (Roninson et al., 2001; Castedo et al., 2004a).

1.5 Centrosome aberrations and cancer

The equal partition of duplicated chromosomes during cell division is essential for maintaining ploidy of the genome. Errors in chromosome segregation lead to chromosomal instability, a hallmark of cancer cells (Cheng and Loeb, 1997). Nearly 100 years ago, Boveri (1914, 2008) first proposed that numerical centrosome aberrations, through the formation of multipolar spindles, lead to chromosomal instability and the ontogeny of cancer, a hypothesis which remains debatable until today. Indeed, cancer cells frequently display early

amplification of centrosome numbers. However, evidence for a direct causal link between centrosome aberrations and tumorigenesis has until recently been elusive (Nigg, 2002).

Two independent studies published in 2008 (Basto et al.; Castellanos et al.) demonstrated that centrosomal abnormalities can lead to tumor formation in flies. When larval brain cells from mutant flies harboring several different centrosome defects (extra centrosomes, reduced number of centrosomes or no centrosomes) were transplanted into the abdomen of normal flies, the transplanted tissue overproliferated and formed aggressive tumors that killed the host within weeks. These fly transplantation assays along with other studies in human cell lines also provided the first insights into the mechanisms that prevent the deleterious consequences of centrosome amplification and allow cancer cells with multiple spindle poles to survive. It was shown that cells with extra centrosomes can ultimately still divide in a bipolar fashion by clustering of extra centrosomes or partial inactivation of centrosomes that fail to cluster (Quintyne et al., 2005; Yang et al., 2008; Kwon et al., 2008; Basto et al., 2008). However, centrosome amplification can generate low-level chromosomal instability, even in the presence of clustering, due to simultaneous attachment of sister kinetochores to one spindle pole (merotelic chromosomal attachment, see Figure 3) (Ganem et al., 2009; Silkworth et al., 2009). In conclusion, our current understanding is that centrosome amplification is sufficient to promote tumor formation by inducing relatively low levels of chromosome missegregation. Yet direct genetic evidence for the implication of individual centrosomal proteins in cancer progression is still missing.

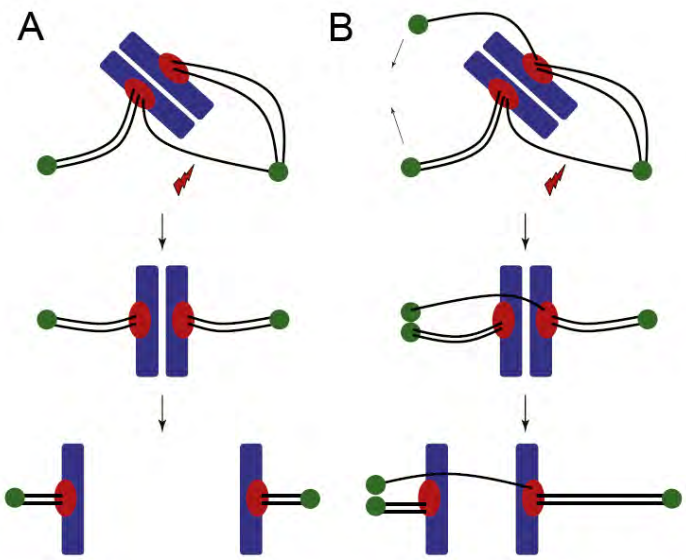

Figure 3 Extra centrosomes increase merotelic kinetochore–microtubule attachments (from Bakhoum and Compton, 2009)

(A) Normal diploid cells build bipolar spindles through the direction of two centrosomes (green). Spontaneously arising erroneous (merotelic) attachments of microtubules (black lines) to chromosomes (blue) at kinetochores (red) are corrected (red lightning bolt) prior to anaphase onset to prevent chromosome mis-segregation. (B) Extra centrosomes in cancer cells induce multipolar spindles prior to bipolarization through centrosome clustering (arrows). These multipolar spindles increase the incidence of merotelic kinetochore–microtubule attachments that persist into anaphase and cause chromosome lagging and mis-segregation.

1.6 Molecular composition of the centrosome

The development and improvement of new technologies such as RNA interference and mass spectrometry along with the sequencing and annotation of the complete genome of a variety of model organisms have provided us with a wealth of information on the molecular composition and functional properties of the centrosome. An important prerequisite for the identification of the centrosomal proteome was the development of protocols that allow for the isolation of biochemically meaningful quantities of this organelle. A comprehensive overview of centrosome preparation methods with emphasis on affinity purification of centrosomes from *Drosophila* embryos can be found in the first manuscript that is enclosed in this thesis (Habermann and Lange, 2010). This review also describes the most important MS-based proteomic, comparative genomics and genome-wide RNA interference (RNAi) studies that significantly increased our current knowledge of the composition of this large protein complex.

In general, all identified centrosome components can be classified into four main groups (Lange, 2002): (a) As the centrosome, unlike other cellular organelles, lacks a defined boundary, a major fraction of the PCM is comprised of scaffolding proteins that facilitate the

maintenance of centrosome structure (Schnackenberg et al., 1998; Moritz et al., 1998). Particularly proteins with coiled-coil domains, which are prone to localize to centrosomes, are thought to organize a lattice-like multi-protein scaffold to which other complexes can bind (Bornens, 2002). (b) The second group includes proteins that function in microtubule nucleation. The main representatives of this class are γ-Tubulin, Grip84 and Grip91, which comprise the γ-Tubulin small complex (γ-TuSC). The γ-TuSC associates with 4 other proteins, Grip71, Grip75, Grip128 and Grip163 to assemble the γ-Tubulin ring complex (γ-TuRC). This complex was first defined in *Drosophila* (Moritz et al., 2000) but structure and composition of the γ-TuRC are evolutionary conserved. (c) The third group includes anchor proteins that target different enzymes to the centrosome and thereby bring them into the proximity of their centrosomal substrates (Diviani and Scott, 2001). Identified members of this group are AKAP450, pericentrin and AKAP220 (Diviani et al., 2000; Reinton et al, 2000; Gillingham and Munro, 2000). (d) The last group is comprised of kinases, phosphatases and signaling molecules. More than 100 of these regulatory proteins have been shown to transiently or stably associate with centrosomes (Doxsey et al., 2005a). They control intrinsic functions of the centrosome, like its duplication, maturation, separation and microtubule nucleation capacity and they link the centrosome to other cellular signaling pathways. In the fourth manuscript that is enclosed in this thesis, centrosomal phosphoproteins were functionally characterized and interactions of the identified substrates with centrosome-associated kinases were investigated. Therefore, the following section introduces some members of the group of centrosomal regulatory proteins in greater detail.

1.6.1 Centrosome-associated regulatory proteins

Among other posttranslational modifications, reversible phosphorylation plays a key role in both regulating the centrosome cycle and progression through the cell cycle (Fry et al., 2000; Hinchcliffe and Sluder, 2001). This notion is supported by the finding that members of the 4 main mitotic kinase families, the Cyclin-dependent kinases, Polo-like kinases, Aurora kinases and NIMA-related kinases all localize to centrosomes, and their association with the centrosome is important for the orchestration of M-phase events (Nigg, 2001).

(a) Cdk1 (or Cdc2 in *Drosophila*) is considered to be the master regulator of mitosis. The activation of Cdk1/Cyclin B is initiated at centrosomes in prophase (Jackman et al., 2003). Activation of this complex depends on its dephosphorylation, which occurs when the activity of the phosphatase Cdc25 towards Cdk1 exceeds that of the opposing kinases Wee1 and Myt1 (Mueller et al., 1995a; Mueller et al., 1995b; Parker et al., 1992). The activated Cdk1/Cyclin B complex then phosphorylates numerous substrates. Cdk1 is directly involved in centrosome separation and spindle assembly via phosphorylation of kinesin-related motor proteins (Eg5) (Blangy et al., 1997) and other microtubule binding proteins. It phosphorylates

nuclear lamins, which induces destabilization and ultimately breakdown of the nuclear envelope (Peter et al., 1990). Cdk1 activity also contributes to chromosome condensation via phosphorylation of condensin (Kimura et al., 1998). Cdk1 participates in the activation of the anaphase promoting complex/cyclosome (APC/C), which ensures the ubiquitylation of proteins, including Cyclin B and securin, to target them for degradation by the proteasome at the metaphase-anaphase transition (Kramer et al., 2000). Cyclin B destruction inactivates Cdk1 upon which the cell exits mitosis and undergoes cytokinesis (Pines, 2006).

(b) The Polo-like kinases were named after the *Drosophila polo* gene (Sunkel and Glover, 1988). Members of this family share a phosphopeptide binding domain, referred to as polo-box at their carboxyl terminus (Elia et al., 2003). This sequence motif targets the enzymes to subcellular compartments and possibly mediates interactions with other molecules (Lee et al., 1998). Plk1, the vertebrate Polo homologue, is found at centrosomes, kinetochores, the central spindle and at the midbody (Golsteyn et al., 1995). It is required for centrosome maturation by promoting the recruitment of microtubule-organizing γ-TuRCs (Lane and Nigg, 1996). It has also been shown to activate the abnormal spindle protein (Asp), which is thought to sequester γ-TuRCs at the mitotic centrosome (do Carmo Avides et al., 2001). Plk1 is furthermore involved in the activation of Cdk1 through phosphorylation of the Cdk1-activating phosphatase Cdc25, which itself associates with centrosomes (Kumagai and Dunphy, 1996). It also plays a role in the metaphase-anaphase transition through contributing to the activation of APC/C-Cdc20 (Kraft et al., 2003; Hansen et al., 2004). *Drosophila* polo mutants display cytokinesis defects, demonstrating the role of this kinase in controlling the final step of cell division (Petronczki et al., 2008). Another Polo-like kinase family member, SAK/Plk4, is essential for centriole duplication (Habedanck et al., 2005).

(c) Aurora-A (*aurora* in *Drosophila*) localizes to centrosomes and adjacent spindle microtubules during mitosis. It has been shown to be required for centrosome maturation as well as bipolar spindle assembly and stability by mediating the recruitment of several PCM components, including γ-Tubulin, centrosomin, TACC and minispindles (MSPS) (Berdnik and Knoblich, 2002; Barros et al., 2005). Aurora-A also contributes to the G2/M transition by phosphorylating Cdc25, which is required for the activation of Cdk1/Cyclin B (Dutertre et al., 2004). It also phosphorylates histone H3 leading to mitotic chromatin condensation, a crucial event for the onset of mitosis (Crosio et al., 2002). Several studies indicated that Aurora-A functions in centrosome duplication and separation (Glover et al., 1995; Roghi et al., 1998; Meraldi et al., 2002). Separation may be triggered through Aurora-A mediated phosphorylation of the kinesin-like motor Eg5 (Giet et al., 1999), but the exact mechanism by which Aurora-A regulates duplication and separation of centrosomes remains to be identified.

(d) The best studied among the NIMA (named after Aspergillus nidulans Never in mitosis A protein kinase) family members is Nek2 (Fry, 2002; Prigent et al., 2005). It localizes to centrosomes and kinetochores. C-Nap, a Nek2 substrate, is a centriolar protein which binds the fiber-forming protein rootletin and thereby links the mother and daughter centriole. Phosphorylation of c-Nap by Nek2 releases this link and allows centrosomes to separate (Yang et al., 2006). Nek2 is inactivated by the phosphatase PP1 during interphase (Helps et al., 2000).

In the past three decades, advances in the identification of molecular components of the centrosomes and their functions have dramatically changed our view of this intriguing cell organelle. It is now evident that the centrosome reaches far beyond its classical role as an organizer of microtubules (Doxsey, 2001; Doxsey et al., 2005a; Lange, 2002). The future challenge will be to decipher the exact mechanisms of centrosome biogenesis, to learn how centrioles facilitate the conversion to basal bodies and the subsequent formation of primary cilia and how the centrosome coordinates cell cycle progression and responds to cellular stress signals. In order to better understand these processes, it will be necessary to define the dynamic changes in centrosome protein composition as well as posttranslational modifications of centrosomal proteins during different cell cycle stages and to analyze the consequences of these centrosomal signaling events on the respective pathways. This should not only increase our knowledge of basic cellular functions but also aid to better understand the centrosome’s role in various human pathologies, including cancer.

2 Aim of the project

Proteomic studies in various organisms have identified hundreds of proteins associated with the centrosome and related structures, such as the yeast spindle pole body, basal bodies, cilia and flagella (Wigge et al., 1998; Ostrowski et al., 2002; Andersen et al., 2003; Keller et al., 2005; Reinders et al., 2006). Genome-wide RNAi screens in *Drosophila* cultured cells furthermore identified a number of proteins that are directly implicated in centrosome biogenesis and spindle assembly (Goshima et al., 2007; Dobbelaere et al., 2008). However, a complete molecular inventory of the *Drosophila* centrosome and a comprehensive functional analysis of centrosome components have yet to be obtained.

Therefore, the overall goal of this project was the identification and subsequent functional characterization of the centrosomal proteome in *Drosophila melanogaster*. An essential prerequisite for this work was the development of an improved isolation technique for the production of highly enriched centrosome preparations from *Drosophila* syncytial embryos. The isolation of centrosomes was the initial part of the project and the current knowledge regarding this topic is summarized in the review article that is enclosed in the present thesis (Habermann and Lange, 2010). The centrosomal preparations subsequently provided the basis for the three studies that comprise my PhD project: (a) In the first study (Hormeño et al., 2009), isolated centrosomes were used to analyze the biophysical properties of this organelle, such as its electric charge and hydrodynamic behavior. (b) In the second study (Müller et al., in revision), isolated centrosomes were used for the mass spectrometry-based identification of the centrosomal proteome. Following the MS analysis, all identified candidate centrosomal proteins were functionally characterized through RNAi and immunofluorescence microscopy in *Drosophila* SL2 cells in order to reveal their role in the regulation of the centrosome cycle and cell cycle, respectively. To elucidate the functional conservation of a subset of proteins that were found to play a crucial role for centrosome structure maintenance and replication in *Drosophila*, human homologues of these proteins were analyzed via small interfering RNA (siRNA)-mediated silencing in HacaT cells. (c) The third study (Habermann et al., submitted) was aimed at identifying centrosomal kinase substrates by an MS-based phosphoproteomic approach and integrating phosphorylated proteins in signaling pathways relevant for centrosome duplication, maturation and separation as well as cell cycle progression. Furthermore, high content screening immunofluorescence microscopy following a combinatorial RNAi approach in SL2 cells was used to reveal functional interdependencies between all MS-identified phosphoproteins and 4 centrosome-associated kinases.

MANUSCRIPT 1

Centrosomes: Methods for preparation

Karin Habermann and Bodo M.H. Lange

Max Planck Institute for Molecular Genetics, Berlin, Germany

Encyclopedia of Life Sciences (ELS)

2010

John Wiley & Sons, Ltd

Publication available online: DOI: 10.1002/9780470015902.a0002597.pub2

3.1.2 Author contributions

I wrote the manuscript for this publication. Bodo Lange proofread and commented on the manuscript.

MANUSCRIPT 2

Single Centrosome Manipulation Reveals Its Electric Charge and Associated Dynamic Structure

S. Hormeño[1], B. Ibarra[1], F. J. Chichón[1], K. Habermann[2], B. M. H. Lange[2], J. M. Valpuesta[1], J. L. Carrascosa[1], and J. R. Arias-Gonzalez[1,3,4]

(1) Department of Macromolecular Structure, Centro Nacional de Biotecnología, CSIC, Madrid, Spain

(2) Department of Vertebrate Genomics, Max Planck Institute for Molecular Genetics, Berlin, Germany;

(3) Instituto Madrileño de Estudios Avanzados en Nanociencia, Madrid, Spain

(4) Author of correspondence

Biophysical Journal, Volume 97, Issue 4, 1022-1030

2009

Publication available online: DOI:10.1016/j.bpj.2009.06.004

3.2.3 Author contributions

For this study I carried out the immunoisolation of centrosomes from *Drosophila* embryos. This included the maintenance of flies in large population cages, the collection of embryos over several weeks and the sucrose gradient centrifugation of embryo homogenate for centrosome enrichment. The immunoisolation of centrosomes also required prior affinity-purification of an antibody. Furthermore I participated in discussions on the manuscript. J. R. Arias-Gonzalez and B. Lange conceived the experiments. S. Hormeño, B. Ibarra, F. J. Chichón, J. M. Valpuesta and J. L. Carrascosa performed the experiments. J. R. Arias-Gonzalez wrote the manuscript.

MANUSCRIPT 3

Proteomic and functional analysis of the mitotic *Drosophila* centrosome

Hannah Müller[1,5]; Ekaterina Mirgorodskaya[1,5]; Sandra Steinbrink[2,5]; David Schmidt[3,5]; Verena Lehmann[1]; Karin Habermann[1]; Niklas Gustavsson[1,4]; Thomas Kessler[1]; Aspasia Ploubidou[3]; Hans Lehrach[1]; Johan Gobom[1]; Michael Boutros[2]; Bodo M.H. Lange[1,6]

(1) Max-Planck Institute for Molecular Genetics, Department of Vertebrate Genomics, Berlin, Germany
(2) German Cancer Research Center, Division of Signaling and Functional Genomics, Heidelberg, Germany
(3) Leibniz Institute for Age Research - Fritz Lipmann Institute, Jena, Germany
(4) Current address: Novozymes Biopharma AB, Lund, Sweden
(5) These authors contributed equally to this work.
(6) Author for correspondence

Submitted to EMBO Journal
Currently in revision

Abstract

Structure maintenance, replication and segregation of the centrosome are integrated into cellular pathways that control cell cycle progression and growth. However on the molecular level, a comprehensive inventory of the centrosome's protein components providing links to these functions is missing. We analyzed the *Drosophila* centrosomal proteome using immunoisolation in combination with mass spectrometry. The 260 identified components were functionally characterized by RNA interference (RNAi). Among those, a core set of 11 proteins is critical for centrosome structure maintenance. Depletion of any of these proteins in *Drosophila* SL2 cells results in centrosome disintegration, revealing a molecular dependency of centrosome structure on components of the protein translational machinery, actin and nuclear proteins. In total we assigned novel centrosome related functions to 27 proteins and confirmed 14 of these in human HaCaT cells.

Keywords: cell cycle / *Drosophila* centrosome / mitosis / proteomics / RNAi

Introduction

Detailed biochemical and functional information about the centrosome is critical for better understanding of basic cellular organization, cell division, developmental processes and diseases resulting from loss or abnormal function of centrosomal proteins (Januschke and Gonzalez, 2008; Badano *et al*, 2005; Khodjakova and Rieder, 2001). However, an in depth biochemical characterization of the eukaryotic microtubule-organizing center (MTOC) has been hampered mainly by its low cellular abundance. Bioinformatic and proteomic studies have identified components of the yeast spindle pole body (Wigge *et al*, 1998) and of the *Chlamydomonas* basal body (Keller *et al*, 2005; Li *et al*, 2004), which is the structural and functional homologue of the centriole. In *Drosophila*, genetic approaches and genome-wide RNAi screening have identified a series of centrosomal proteins (Bettencourt-Dias and Glover, 2007; Goshima *et al*, 2007; Dobbelaere *et al*, 2008) but remained short of a comprehensive molecular characterization of the centrosome. In higher eukaryotic cells, centrosome components have been identified and characterized via bulk isolation methods (Komesli *et al*, 1989; Moritz *et al*, 1995; Palazzo & Vogel, 1999; Lange *et al*, 2000) and by combining mass spectrometry (MS) with protein correlation profiling (Andersen *et al*, 2003).

Three classes of proteins are thought to be required for the structural maintenance of the centrosome. First, centriole proteins are part of the centrosomal core structure, as shown by ablation or depletion of the centriolar proteins Ana1, Ana2, Asl and Spd-2, which result in ablation of the *Drosophila* centrosome (Goshima *et al*, 2007; Dix and Raff, 2007; Varmark *et al*, 2007). Second, proteins of the pericentriolar material (PCM), such as Cnn, are essential

for centrosome integrity, providing a possible link between the centriole and the PCM in *Drosophila* (Lucas and Raff, 2007). Proteins of the small γ-tubulin ring complex (γ-TuSC), such as Grip84, Grip91 and γ-tubulin, form an integral part of the PCM structure (Vérollet *et al*, 2006) in addition to their role in microtubule nucleation.

The protein composition of the PCM is changing during the cell cycle, qualitatively and quantitatively. The increase of PCM components, in the interphase to mitosis transition, is regulated by the proteins comprising the third class of molecules required for centrosomal structure maintenance. The cell cycle kinases Polo, Cdc2/Cdc2c and Aur control PCM recruitment and therefore affect overall centrosome size and structure (Bettencourt-Dias and Glover, 2007). In addition, the kinases SAK, Cdc2, Cdc2c, Grp, Mei41 and the ubiquitin ligase complex SCF control transition steps of centriolar and centrosomal replication and segregation (Bettencourt-Dias and Glover, 2007).

Although increase in PCM is well characterized, less is know on the reverse process, namely reduction of PCM during the mitosis to interphase transition. This is a process likely down-regulated in cancer cells, which harbour hypertrophic centrosomes (Lingle *et al*, 1998; Nigg, 2002) and is up-regulated in differentiation (Manandhar *et al*, 2000; Tassin *et al*, 1985) and in certain viral infections (Ploubidou *et al*, 2000; Jouvenet and Wileman, 2005; Ferralli *et al*, 2006). However, the inactivation of kinases alone, which induces PCM increase when activated, is not likely to be the only contributing factor but might also require posttranslational modifications of PCM components (e.g. ubiquitination, dephosphorylation) or the recruitment of proteins only present on centrosomes in interphase (Hansen *et al*, 2002; Graser *et al*, 2007).

The diverse functions of the centrosome, especially the regulatory ones, are also reflected by the shuttling of centrosomal components between the centrosome and other cell organelles/compartments. A number of molecules, previously described as components of the nucleus or the focal adhesion complexes or diverse membrane compartments, have been subsequently localized at the centrosome and found to exert a centrosome related function. In turn, several centrosomal proteins have been additionally localized at other cell organelles and have been shown to perform also non-centrosomal functions. Examples for the former are the nuclear protein axin (Fumoto *et al*, 2009), which is implicated in centrosome segregation; beta-catenin (Bahmanyar *et al*, 2008), an adherens junctions/nuclear protein and component of the wnt signaling pathway, involved in microtubule nucleation. In contrast, the centriolar protein centrin-2, required for centriolar

duplication (Salisbury *et al*, 2002), has been recently identified as component of the nuclear pore, implicated in mRNA and protein export (Resendes *et al*, 2008).

Taken together, centrosomal proteins controlling centrosome structure and microtubule nucleation events plus the centrosomal proteins localized both at the centrosome and at other subcellular compartments point to the tight coordination of centrosome structure and function with basic cellular processes that e.g. control cell cycle regulation and cell growth (Doxsey, 2001; Sibon *et al*, 2000; Lange, 2002).

This study describes the identification of the proteome of the *Drosophila* mitotic centrosome and its functional characterization (Figure 1). Centrosome immunoisolation from *Drosophila* preblastoderm embryos was followed by MS identification of the protein components. Subsequently, RNAi in *Drosophila* SL2 cells was employed in order to determine the function of the identified proteins, in centrosome structure and duplication, chromosome segregation and cell cycle progression, by analysis of 15 different phenotypic parameters. One of the functional groups identified, were proteins that upon depletion resulted in a striking “0” centrosome phenotype. Among these proteins were molecules with previously identified functions in RNA binding, translational control, or components of the actin cytoskeleton, revealing a new surprising function in maintaining centrosome structure. As centrosome stability is frequently compromised in human cancer cells or upon viral infection, this functional group was selected for localization studies through GFP-tagging in SL2 cells. Moreover, functional characterization of the human orthologues in HaCaT cells identified 5 proteins with conserved function in centrosome structure maintenance.

Results

Identification of 260 centrosomal candidate proteins from immunoisolated *Drosophila* embryo centrosomes

One of the major problems so far in defining the molecules involved in structure maintenance, replication and segregation of the centrosome was the limited quantity and relatively low purity of the available centrosome preparations. Here we used immunoisolation following sucrose gradient centrifugation (Lehmann *et al*, 2005) to improve the enrichment of centrosome proteins (Supplementary Figure S1). The resulting preparations were analyzed by liquid chromatography-MS. MS analysis of the immunoisolated centrosomes identified 260 proteins, of which 20 have been localized to the *Drosophila* centrosome in previous studies (Supplementary Table S1, http://flybase.bio.indiana.edu/). The fact that we identified low abundant centriolar proteins (Spd-2, Sas-4), centrosomal core components (e.g. Cnn, γ-TuRC proteins) and transiently associated centrosomal mitotic kinases (e.g. Aur, Polo) confirmed the enrichment of our centrosome preparations. To test the validity of newly identified candidate proteins, we carried out N- and C-terminal GFP-, TAP- (tandem affinity purification) tagging and (for 10 cases) antibody localization of 36 of the MS identified proteins. For the verification of the localization we selected an important core group of proteins that had a “0” centrosome phenotype (Table I, Supplementary Table S1) in our functional RNAi assay in *Drosophila* SL2 cells and a set of candidates that were annotated (http://www.ebi.ac.uk/interpro/) to have multiple coiled coil domains (Supplementary Table S1), a common feature in centrosome proteins. 30 GFP fusion proteins (Supplementary Table S4) could be expressed in SL2 cells, of which 17 proteins (including 5 controls) localized to the centrosome (12 proteins) or mitotic spindle (5 proteins) as shown in Figures 2, S2 and S3, confirming the validity of our immunoisolation approach. In addition we found microtubule, nuclear and cytoplasmic localization (Supplementary Table S3). In total we identified 8 new centrosome and 4 new spindle localizations (Table II).

Centrosome ablation by RNAi of 7 proteins reveals their centrosome structural maintenance function

The function of the identified proteins for centrosome structure, duplication and segregation was characterized by RNAi in SL2 cells (Bartscherer *et al*, 2006; Boutros *et al*, 2004). Using immunofluorescence microscopy, we analyzed centrosome phenotypes resulting from depletion of the 260 identified proteins. In addition, we selected 96 proteins from the UniProt database (http://www.uniprot.org/) via the search terms centrosome and *Drosophila* (Supplementary Table S1). From these 96 proteins we had identified 26 in our MS analysis. The rest (71), we functionally analyzed together with the 260 identified proteins in the RNAi experiment to test for phenotypical correlation between the MS identified proteins and

proteins already functionally related to the centrosome. Off-target effects were evaluated both bioinformatically and through a second round of RNAi experiments for functionally important proteins (Supplementary Table S2).

First we examined the effect of protein depletion for three classes of abnormal centrosome structure (Figure 3 B,D,F): (i) zero centrosomes (11/260), (ii) small centrosomes (5/260) and (iii) fuzzy centrosomes (8/260) (Supplementary Table S1). The most striking phenotype related to centrosome structure maintenance was centrosome loss ("0" centrosome phenotype) which resulted from depletion of: Act57B, eIF-4a, CG11943, CG31716, Lam, Rae1, Scra, while reduction of PCM (small centrosome phenotype) was the consequence of RNAi targeting Cup, Fib and RpS4 (Supplementary Table S1). Depletion of the proteins Act79B, Qm, RpL27, RpL3, RpL36, RpL6, RpL7A, RpS23 led to fuzzy centrosome appearance. In addition, we confirmed already known centrosomal proteins to affect centrosome structure: Cnn, Spd-2, Aur, Grip84.

The fact that centrosome structure was affected by the depletion of proteins involved in protein translation (e.g. eIF-4a) raised the question if global inhibition of this process causes a centrosome structure defect. Therefore we investigated in more detail the consequences of translation inhibition on the centrosome via RNAi depletion of the eIF-4e core component of the translation initiation complex eIF4F and treatment with cycloheximide that is known to block translation elongation. eIF-4e mediates mRNA cap binding, the first step of translation initiation (Gingras *et al*, 1999) and had not been detected in our centrosome preparations (Supplementary Table S1). We compared the effects of depleting eIF-4e with the phenotype resulting from depletion of eIF-4a (identified in our centrosome preparations), which is also known to be a part of the eIF4F complex and to function in translation initiation as a helicase with RNA-dependent ATPase activity (Gingras *et al*, 1999).

RNAi mediated depletion (confirmed by western blotting, Figure 4D) of both proteins gave two distinct phenotypes: eIF-4e knock down in SL2 cells resulted in a large proportion of cells (40%) with elevated centrosome numbers (> 2) as compared to the control (22%) while eIF-4a RNAi produced a "0" centrosome phenotype (46%, Figure 4A-C, G). Cycloheximide inhibition (Supplementary Figure S6) resulted in elevated levels of multiple centrosomes similar to eIF-4e depletion but again significantly different to the eIF-4a phenotype. These results support the hypothesis that the centrosome related effect of eIF-4a depletion is not likely to be caused by a general inhibition of translation. In addition, a detailed analysis of cell cycle stage changes induced by eIF-4a and eIF-4e depletion revealed a strong increase of cells in prophase in eIF-4a and to a much lesser extent in eIF-4e depleted cells (Figure 4F). This further supports the proposition that centrosome loss

through eIF-4a depletion is mechanistically distinct from the inhibition of protein translation after either eIF-4e depletion or cycloheximide treatment.

A second functional group of proteins involved in centrosome duplication and segregation

RNAi-mediated depletion of 51 MS identified proteins displayed centrosome aberrations in the form of single and/or abnormally large centrosomes, indicating malfunction of centrosome duplication and/or segregation (Table I, Supplementary Table S1). The group exhibiting both traits was the largest (23), with proteins known to affect centrosome replication and segregation: α- and β-tubulins, γ-TuRC components and motor proteins (Supplementary Table S1). In addition, depletion of ribosomal proteins, the RNA processing protein Crn and the DNA-binding protein CG6905 produced a single centrosome phenotype (Supplementary Table S1). We investigated the relationship between defects in centriolar and centrosomal replication with the MS-identified proteins Feo, a microtubule associated protein previously localized to the midspindle area (Verni *et al*, 2004; D'Avino *et al*, 2007) and Lat, a component of the origin recognition complex, that regulates DNA replication (Pinto *et al*, 1999). Depletion of Feo in SL2 cells caused large and unequal sized centrosomes, containing multiple centrioles as identified by immunofluorescence staining with an antibody against Cp309, a protein predominantly associated with the centriole (Martinez-Campos *et al*, 2004), (Supplementary Figure S4B). RNAi knock-down of Lat resulted in multiple centrosomes per cell (>3) all of which co-labeled with the Cp309 antibody suggesting to contain centriolar structures (Supplementary Figure S4).

Hence the identification of proteins in our centrosome preparations that are implicated in the processing and translation of proteins and DNA replication and that affect centrosome duplication or segregation suggests that these proteins could either be a structural part of the centrosome or have a functional role that is associated with the centrosome. Our control experiments showed that global inhibition of protein translation through cycloheximid (Supplementary Figure S6) and inhibition of DNA replication through aphidicolin (Supplementary Figure S7) result in over-replication of centrosomes. Hence the effect of Lat depletion on the centrosome (centrosome overreplication), in our experiments can not directly be differentiated from a general effect of blocked DNA replication. In contrast, depletion of the majority of ribosomal proteins leads to a single centrosome phenotype and is different to the multiple centrosome (>2) phenotype caused by cycloheximide treatment. This suggests that a set of ribosomal proteins is linked to a pathway required for centrosome duplication or segregation that is distinct from their global function in protein translation.

Link of the centrosome to cell cycle progression, cell proliferation pathways and cell viability

We characterized the effect of all MS-identified proteins (260) and control proteins (71) on cell cycle progression to correlate the detected phenotypes with events of cell cycle progression and to elucidate possible links of centrosomal proteins to cell proliferation pathways (Supplementary Table S1; Figure 3). DNA content- and mitotic index analysis by FACS and phospho-histone H3 labeling, respectively, revealed three major phenotypic groups. These were characterized by enrichment of cells with either (i) sub-G1-phase DNA content indicating decreased viability (26/260), (ii) more than G2 DNA content (20/260) suggesting cytokinesis defects and (iii) an increase number phospho-histone H3 expressing cells pointing to mitotic arrest (25/260). Subsequently, we analyzed the correlation of centrosome aberration phenotypes and cell cycle deregulation. In the group of proteins identified known to be implicated in the process of centrosome segregation we found α-tub, β-tub, Fzy, Msps, Pav also to affect cell viability. In addition we found that depletion of CG11148 (a not annotated protein we localized to the centrosome), Act42A, His4R, Nup153 and Ote resulted in an increased number of sub-G1 cells. An expected cytokinesis defect (more than G2 DNA content) was observed after knockdown of the proteins Pav and Cdc2. However, the strong cytokinesis defect induced by depletion of the Heph protein that contains a RNA recognition motif and is involved in notch signaling (Dansereau *et al*, 2002) was unexpected. The majority of cells arrested in mitosis also had a single centrosome phenotype suggesting that depletion of these proteins blocked both centrosome duplication/segregation and mitotic progression. We confirmed that a minor subgroup (4 of 25) were members of the γ-TuRC whose depletion caused mitotic arrest (Vérollet *et al*, 2006; Müller *et al*, 2006).

Functional conservation of *Drosophila* centrosome candidate proteins and their human orthologues

We assessed human orthologues of all proteins that yielded a centrosomal phenotype in the SL2 RNAi assay for functional conservation by short interfering RNA (siRNA) mediated silencing in human HaCaT cells. We confirmed a conserved centrosome related function for 40 of 95 proteins which we identified to have a function in *Drosophila* SL2 cells (Supplementary Table S1, Figure 3G-L, Supplementary Figure S8). The largest functional conservation occurs in the class of centrosome duplication and segregation (36) while less (5) had a conserved function in maintaining centrosome structure. In the group of proteins whose depletion affects centrosome segregation are two γ-TuRC components (Grip75, Grip128), molecular motors (Klp61F, Klp10A) together with Hsc70-3, the regulatory proteins Fzy, Stg, Mts and Pp2A and several ribosomal proteins (Supplementary Table S1 -

Drosophila & human phenotypes comparison). We found the following proteins to be required for centrosome structure maintenance in both SL2 and HaCaT cells: Cnn, γ-tubulin, Grip75, Grip84, Grip91. In addition we analyzed 10 human orthologues (Supplementary Table S1) of *Drosophila* genes in the osteosarcoma cell line U2OS, depletion of which resulted in the “0” centrosome phenotype in SL2 cells. We confirmed a function in the maintenance of centrosome structure for NUP205 (CG11943), CEP192 (Spd-2) and CNOT4 (CG31716) (Supplementary Figure S7, Supplementary Table S1). From these results we conclude that the functions of centrosome duplication and segregation are most strongly conserved between *Drosophila* and human cells.

In summary, the functional characterization of the centrosome proteome assigned a novel function to 27 proteins that are required for maintaining centrosome morphology and for centrosome duplication and segregation. We identified 18 proteins that were assigned a previously not described function in maintaining centrosome structure. Depletion of 7 of these proteins resulted in a distinct loss of centrosome (“0”) phenotype. Interspecies comparison reveals that mainly proteins involved in the process of centrosome duplication and segregation are functionally conserved.

Discussion

The analysis of the mitotic *Drosophila* centrosomal proteome, reported here, identified 260 components using immunoisolation in combination with MS. The currently estimated total number of centrosome proteins remains open. Andersen *et al* (2003) identified 114 centrosome/centrosome candidate proteins in the human interphase centrosome. The *centrosomeDB* database (Nogales-Cadenas *et al*, 2009) lists 383 centrosomal human genes based on a compilation from the literature and homologues of centrosome genes identified in various organisms. Indeed, taking different proteomic, bioinformatics and genetic studies into account, an estimate of over 300 centrosome candidate proteins has been proposed (Bettencourt-Dias and Glover, 2007). However, there are uncertainties attached to these numbers due to the fact that many proteins are only transiently associated with the centrosome (Kalt and Schliwa, 1993). In addition, the origin of the centrosome (isolated for example from somatic interphase cells or from highly mitotic embryonic tissue) is likely to contribute to major differences in the types and number of proteins identified. Based on the figures above, the work presented here covers possibly a major part of the structural centrosome proteins but will have missed a fraction of low abundant proteins in the MS analysis. This takes also into account that the cut-off level at the level of MS identification (Supplementary Information) was set high. The validity and robustness of our approach was confirmed by the MS identification of 20 from 35 known *Drosophila* centrosomal proteins in the analyzed preparations and by the fact that 12 identified proteins were assigned a previously not described localization at the centrosome and at the spindle (Table II). Major contaminants, as identified in our negative control experiments were the highly abundant yolk proteins (Yp1, Yp2, Yp3), Act5C, betaTub56D and Ef1alpha48D (for a complete list see Supplementary Table S1). The identification of γ-tubulin and Cnn in the negative control sample is likely to be a result of the control beads exposure to highly concentrated centrosome enriched sucrose fractions during the immuno-isolation protocol.

Centrosome structure maintenance depends on proteins implicated in RNA-binding and translation initiation, nuclear transport and actin-related processes

The RNAi analysis in SL2 cells shows a large fraction of the identified proteins to function in centrosome segregation/duplication and structure maintenance. The accuracy of our phenotypic scoring was confirmed by assaying proteins with a previously known centrosome related function (Supplementary Table S1) and by off-target controls (Supplementary Table S2). The high statistical cut-off levels implemented (significance level < 0.0001), allowed the robust identification of the molecules functioning in centrosome structure maintenance or centrosome duplication/segregation, albeit at the cost of potentially overlooking relatively weak phenotypes in the functional analysis experiments.

While the acquisition (maturation) of PCM material has been studied in detail (Dobbelaere *et al*, 2008; Palazzo *et al*, 2000) fewer factors have been identified that are required for maintaining centrosome structure (Mikule *et al*, 2007; Goshima *et al*, 2007). A main result of this work is the identification of proteins functioning in the maintenance of centrosomal structure, their depletion resulting in 0, small or fuzzy centrosomes. Knock-down of 7 proteins (Act57B, CG11943, CG31716, eIF-4a, Lam, Rae1, scra) resulted in the same phenotype ("0" centrosome) as depletion of the known structural centriolar protein Spd-2 (Dix and Raff, 2007) or major core PCM components cnn (Megraw *et al*, 1999), Grip84 (Colombié *et al*, 2006) and l(1)dd4 (Barbosa *et al*, 2000), indicating that the newly identified proteins have a structural role at the centrosome. This is consistent with the centrosomal localization of eIF-4a and Lam. Interestingly, some of proteins that we found to be important for maintaining centrosome structure have been implicated before in RNA-binding and initiation of translation: Rae1, CG31716, eIF-4a. (Sitterlin, 2004). This work also identified the functionally not yet annotated protein CG11943 (the nuclear porin NUP205 orthologue), depletion of which resulted in a "0" centrosome phenotype, implicating it in centrosome assembly either on a structural or regulatory level.

In order to test for possible alternative mechanisms, in which the observed PCM "0" centrosome phenotype could be due to global inhibition of protein translation, the eIF4F core component eIF-4e was depleted or cells were exposed to a range of cycloheximide concentrations. These experiments showed, that inhibition of protein translation results in a phenotype distinct from that caused by eIF-4a depletion. Because of its striking "0" centrosome depletion phenotype and localization of a fraction of eIF-4a to the centrosome we propose a regulatory or structural task for this helicase at the centrosome. Recently, the RNA helicase CG7033 has been described to play a role for mitotic spindle organization (Goshima *et al*, 2007; Hughes *et al*, 2008). In our experiments, CG7033 was MS-identified as component of the centrosome preparations, the subsequent functional analysis revealed a centrosome segregation/replication role and we confirmed its previously reported spindle localization (Hughes *et al*, 2008). Taken together, these results support a centrosome-related function of Rae1, CG31716, CG11943, eIF-4a, in addition to their previously annotated global roles in mRNA binding and translational control. Surprisingly, we found that Act57B, Scra (depletion of both results in a "0" centrosome phenotype) and Act79B (fuzzy centrosome phenotype), which were previously described to be involved in muscle differentiation and cytokinesis (Thomas and Wieschaus, 2004; Fyrberg *et al*, 1983), are also involved in centrosome structure maintenance. These results suggest that actin-related processes are not only required for centrosome separation in interphase (Stevenson *et al*,

2001) or clustering in mitosis (Kwon *et al*, 2008) but also for centrosome structure maintenance in SL2 cells.

The process of centrosome duplication/segregation is linked to transcriptional and translational control as well as cell viability

The functional analysis showed that 56 proteins, of the 260 MS-identified proteins, play a role in the process of centrosome duplication and/or segregation. Depletion of a subgroup of these proteins (23/56) led to large single centrosome phenotype implicating the identified proteins in centrosome segregation. This group includes 6 factors known to function in this process: α-/β-tubulins, γ-TuRC, Tum and the motor protein Klp10A (Zavortink *et al*, 2005; Goshima *et al*, 2007). Unexpectedly, knock-down of Hsc70-3 phenocopies the centrosome and chromosome segregation plus cytokinesis phenotypes of the two molecular motor proteins Pav and Klp61F (Adams *et al*, 1998; Gatt *et al*, 2005), providing evidence that these three proteins might share a common molecular pathway. A group of proteins that previously has been implicated in transcriptional and translational processes (CG6905, CG7033, Crn, ribosomal proteins), we identified to also function in centrosome segregation and duplication. Of these, we localized CG7033 and Crn to spindle, midbody and centrosome respectively. The association of mRNA (Lécuyer *et al*, 2007) and proteins of the transcription/translation machinery with the spindle and centrosome suggests that part of the centrosomal protein translation and its regulation occurs in close association with the centrosome or that these proteins (or their associated RNA) are structural components as has been suggested before (Blower *et al*, 2005). An alternative explanation that would take the translational cause of the described centrosome phenotypes into account, would be a specific molecular impairment in translation initiation, regulating the expression of selected mRNAs (Barna *et al*, 2008). However, we have no evidence for the involvement of such a process. Our results suggest multiple roles of mRNA associated proteins, for both protein translation and for centrosome structure maintenance and segregation.

The correlation of centrosomal and cell cycle phenotypes in SL2 cells after depletion of the newly identified and of control proteins, provided evidence that known centrosomal proteins, e.g. Fzy, Klp61F, Pav, Msps and the identified uncharacterized centrosome associated protein CG11148, are required for cell survival. The fact that most of the cell viability affecting knock-downs resulted in a “1” centrosome phenotype suggests that centrosome segregation and cell survival are interdependent in the majority of cases examined here.

Highest functional conversation between fly and human is a feature of proteins functioning in centrosome duplication and separation

We found the MS identified proteins Spd-2 (CEP192), CG11943 (NUP205) and CG31716 (CNOT4) to be conserved in their function for centrosome structure maintenance between SL2 and human U2OS cells. Overall the conservation in the class of proteins that function in centrosome structure maintenance was about 28% (17% in HaCaT cells). The functional conservation between HaCaT und SL2 was highest with about 75% in the class of proteins relevant for centrosome duplication and segregation. These data are consistent with previous published results from RNAi screens comparing the osteosarcoma U2OS cells and the cervix cancer derived HeLa cells with *Drosophila* cell cultures (Kittler *et al*, 2007). The previously stated overlap between human and *Drosophila* RNAi screens was 38% and between different human cell lines 10% (Kittler *et al*, 2007). The higher rate of overlap for the function of centrosome duplication and segregation (between HaCaT and SL2 cells) is possibly related to the fact that the examined proteins are identified components in a centrosome preparation rather than are analyzed from genome wide pool of targets (Supplementary Table S1).

Through the proteomic and functional characterization of the early *Drosophila* embryo centrosome this work provides a resource for further molecular characterization of the processes of centrosome duplication/segregation and centrosome structure maintenance. Our results assign a new centrosome related function to 27 proteins. As a core group we identified 11 proteins, whose depletion resulted in loss of centrosomes in SL2 cells. The function of 7 of these had not been previously related to centrosome structure maintenance. Future work will elucidate the protein-protein interaction maps within the centrosome and their links to regulatory proteins networks. Our results and developed technique will find future application in the combination of powerful *Drosophila* genetics with highly sensitive MS-technologies (Gstaiger & Aebersold, 2009) for the functional analysis of centrosome protein complexes.

Materials and methods

Further details of all experimental procedures can be found in Supplementary Information.

Centrosome Isolation

Embryo homogenate was prepared from *Drosophila* preblastoderm stage embryos and centrosomes were enriched through sucrose gradients centrifugation according to Moritz *et al,* (1995). Subsequent immunoisolation of centrosomes was performed as described previously (Lehmann *et al*, 2005) with modifications detailed in the Supplementary Materials and Methods section.

Nano LC-MALDI MS

Nano LC-MALDI MS was performed according to Mirgorodskaya *et al,* (2005). In brief, peptides were separated on an 1100 Series Nanoflow LC system (Agilent Technologies). Mass analysis of positively charged peptide ions was performed on an Ultraflex II LIFT MALDI-TOF/TOF mass spectrometer (Bruker Daltonics). Protein identification was performed using the Mascot software (Matrixscience), searching the FlyBase sequence database.

RNA Interference and Phenotype Analysis

RNAi knockdown in *Drosophila* SL2 and siRNA knockdown in human HaCaT or U2OS cells were each performed in two independent experiments, followed by immunofluorescence labeling of the cells or processing for FACS analysis. For SL2 and U2OS cells, in each experiment, on average, n=100 mitotic cells were analyzed for centrosome number and shape, n=2000 SL2 cells were analyzed for mitotic index calculation and n=35000 SL2 cells were subjected to DNA content analysis by FACS. For HaCaT cells, in each experiment, on average, n=550 mitotic cells were analyzed for centrosome number and area plus centrosomal γ-tubulin content, while n=29000 cells were subjected to mitotic index and DNA content analysis. The values measured were normalized to the corresponding average value of the quadruplicate negative control wells on the plate. Phenotypes were quantified using three different software algorithms.

Data Evaluation of RNA Interference Experiments

Each mitotic cell was assigned to phenotypic categories of centrosome number and morphology as shown in Figure 3 and specified in Supplementary Material and Methods. The resulting phenotype distributions of the two independent experiments were averaged and compared to the average distribution of the negative controls, by means of a non-parametric two-tailed chi square test. A significant deviation from the control distribution was assigned for significance levels $p<0.0001$ (list of p-values in Supplementary Table S2). For the knockdowns thus determined to cause significant effects on centrosome number, the phenotype was identified as the category that showed >2-fold increase compared to the

negative control. If this threshold was exceeded for two or more categories, a mixed phenotype was assigned, unless one of these categories was >2 fold the abundance of the second highest.

For all other data analysis, the values measured were normalized to the corresponding average value of the quadruplicate negative control wells on the plate. Phenotypes were considered to be statistically significant when a z-score ≥ 3 was obtained in both independent experiments and, for mitotic index and DNA-content analysis in HaCaT, when, in addition, the average z-score was ≥ 6. The values (z-scores) listed in Supplementary Table S2 represent the average distances between individual knock-downs and control, determined as described above, in fold standard deviation of the negative controls.

Acknowledgements

We would like to thank C.B. Chien, M. Gatti, D. Glover, T. Kaufman, K. Kwan, T. Orr-Weaver, N. Sonenberg and Y. Zheng for the gift of antibodies and DNA constructs, K. Nierhaus for advice on protein translation control experiments, J. Hamann and D. Schudde for assistance with HT methods and our colleagues for comments on the manuscript. The work was funded by: (a) B.L. laboratory: Berliner Senat für Kultur, Wissenschaft und Forschung, EFRE; NGFN2 SMP Protein; NGFN Plus, IG Mutanom; EU. (b) M.B. laboratory: DFG, European Commission; HFSP. (c) J.G. laboratory: Technologiestiftung Berlin (TSB); the Structural Fonds of the European Union within the project 2D/3D-ProteinChips, NGFN2 SMP Protein. Bruker Daltonics in Bremen is acknowledged for scientific collaboration. (d) A.P. laboratory: Leibniz Society.

Author contributions

E.M., N.G. and J.G. carried out the MS work and MS data analysis. H.M., S.S., V.L., K.H., D.S., T.K. and B.L. performed all other experiments. H.M., S.S., D.S., A.P. and B.L. analyzed the data. H.L., A.P., M.B. and B.L. supervised the experiments. B.L. designed the experiments and wrote the manuscript. All authors discussed the data and commented on the manuscript.

Figure legends

Figure 1. Experimental approach and main findings of the proteomic and functional characterization of the early preblastoderm *Drosophila* centrosome

Drosophila preblastoderm embryo extract was used as starting material for the immuno-isolation of mitotic centrosomes, followed by the identification of the centrosomal proteome components by mass spectrometry. The 260 identified proteins plus 71 controls were characterized by RNAi-mediated knock-down in *Drosophila* SL2 cells. Five centrosomal, chromosomal and cell cycle features were analyzed using immunofluorescence microscopy or FACS. Subsequently, localization analysis was performed (GFP-, TAP-tag expression and immunolocalization in SL2 cells) for the MS-identified proteins whose functional inhibition resulted in a “0” centrosome phenotype, for proteins with coiled-coil domains and for control proteins. Functional conservation of the identified proteins was confirmed in human HaCaT and U2OS cells. (Main experimental steps shown in red colour, experimental procedures and main findings in blue).

Figure 2. Confirmation of centrosomal or spindle localization of candidate MS-identified proteins and controls

Stable expression of GFP-fusion proteins in SL2 cells identifies new centrosomal and spindle localization of identified proteins while the GFP-control shows uniform distribution (A). A centrosome associated localization was identified for TFAM (B), Lam (C), Nup153 (D), Feo (E), eIF-4a (F), Cort (G), CG11148 (H) and Crn (I). Not previously known was the spindle localization of the proteins Nat1 (J), Cka (K), Lat (L) and Coro (M). Positive controls confirm known centrosomal localization of Grip91 (N), Grip84 (O), Spd-2 (P), CG1962 (Q) and the spindle localization of CG7033 (R). The GFP-tag is shown in green (upper panel, A-R), antibody staining against γ-tubulin (middle panel, A-O, Q, R) and Cp309 (P) in red and superimposition of both images with DNA labeled by DAPI in blue (lower panel, A-R).

Figure 3. Functional characterization of 260 MS-identified *Drosophila* centrosome candidate proteins plus 71 controls and 95 human orthologues identified centrosomal and cell cycle functions.

(A-L) Examples of the two phenotypic classes, aberrant centrosome structure (B,D,F,H,J,L) or centrosome duplication/segregation (C,E,I,K) revealed by RNAi mediated knock-down in SL2 and HaCaT cells. The RNAi target protein is indicated within each panel. A complete list of all *Drosophila* and human proteins and the result of their functional analysis can be found in Supplementary Table S1. Anti-γ-tubulin (green) and anti-phospho-histone 3 (red) antibodies were used to label centrosomes and mitotic chromosomes respectively.

(M-R) Examples of the cell cycle distribution profiles, determined by FACS analysis of dsRNA treated SL2 cells. The RNAi target proteins whose depletion is inducing each phenotype are listed on the right of the corresponding cell cycle distribution profile. A complete list including the cell cycle analysis of the human siRNA treated cells can be found in Supplementary Table S1. (M) control (EGFP dsRNA treated cells) cell cycle distribution, (N) Sub-G1, (O) G1/G0, (P) S-phase, (Q) G2/M, (R) more than G2 DNA content.

(S,T) Representative fields of SL2 cells displaying low (S) or high (T) mitotic index following dsRNA treatment. The RNAi target proteins whose depletion is inducing each phenotype are listed on the right of the corresponding image. DAPI (blue) and anti-phospho-histone 3 antibodies (red) were used to label DNA and mitotic chromosomes respectively. A complete list of the RNAi targets including the mitotic index analysis of the human siRNA treated cells can be found in Supplementary Table S1.

(U) Example of a cell showing an abnormal chromosome segregation phenotype. The RNAi target proteins whose depletion is inducing an aberrant chromosome segregation phenotype are listed on the right of the image. A complete list of the chromosome aberration analysis can be found in Supplementary Table S1. Anti-γ-tubulin (green) and anti-phospho-histone 3 (red) antibodies were used to label centrosome and mitotic chromosomes respectively.

Scale bars represent 10 µm in F and U, 20 µm in S and T.

Figure 4. The eukaryotic initiation factor 4a protein has a centrosome and cell cycle related function.

(A). Depletion of eIF-4a results in cells with small or no centrosomes (B, G, H), high mitotic index (E) and an accumulation of prophase cells (F), while eIF-4e knock-down led to cells with many centrosomes (B, G), normal mitotic index (E) and normal distribution of mitotic phases (F). Western blotting shows protein depletion by RNAi using anti-eIF-4a and eIF-4e antibodies. α-tubulin is used as loading control (D). The distinct differences between the eIF-4a and eIF-4e RNAi phenotypes strongly suggest that the effect on the centrosome resulting from depletion of eIF-4a is most likely not a consequence of global inhibition of translation.

(F: * could not be determined)

References

Adams RR, Tavares AA, Salzberg A, Bellen HJ, Glover DM (1998) Pavarotti encodes a kinesin-like protein required to organize the central spindle and contractile ring for cytokinesis. *Genes Dev* **12**: 1483-1494

Andersen JS, Wilkinson CJ, Mayor T, Mortensen P, Nigg EA, Mann M (2003) Proteomic characterization of the human centrosome by protein correlation profiling. *Nature* **426**: 570-574

D'Avino PP, Archambault V, Przewloka MR, Zhang W, Lilley KS, Laue E, Glover DM (2007) Recruitment of Polo kinase to the spindle midzone during cytokinesis requires the Feo/Klp3A complex. *PLoS One* **2**: e572

Badano JL, Teslovich TM, Katsanis N (2005) The centrosome in human genetic disease. *Nat Rev Genet* **6**: 194-205

Bahmanyar S, Kaplan DD, Deluca JG, Giddings TH Jr, O'Toole ET, Winey M, Salmon ED, Casey PJ, Nelson WJ, Barth AI (2008) beta-Catenin is a Nek2 substrate involved in centrosome separation. *Genes Dev* **22**: 91-105

Barbosa V, Yamamoto RR, Henderson DS, Glover DM (2000) Mutation of a Drosophila gamma tubulin ring complex subunit encoded by discs degenerate-4 differentially disrupts centrosomal protein localization. *Genes Dev* **14**: 3126-3139

Barna M, Pusic A, Zollo O, Costa M, Kondrashov N, Rego E, Rao PH, Ruggero D (2008) Suppression of Myc oncogenic activity by ribosomal protein haploinsufficiency. *Nature* **456**: 971-975

Bartscherer K, Pelte N, Ingelfinger D, Boutros M (2006) Secretion of Wnt ligands requires Evi, a conserved transmembrane protein. *Cell* **125**: 523-533

Bettencourt-Dias M, Glover DM (2007) Centrosome biogenesis and function: centrosomics brings new understanding. *Nat Rev Mol Cell Biol* **8**: 451-463

Blower MD, Nachury M, Heald R, Weis K (2005) A Rae1-containing ribonucleoprotein complex is required for mitotic spindle assembly. *Cell* **121**: 223-34

Boutros M, Kiger AA, Armknecht S, Kerr K, Hild M, Koch B, Haas SA, Paro R, Perrimon N, Heidelberg Fly Array Consortium (2004) Genome-wide RNAi analysis of growth and viability in Drosophila cells. Science **303**: 832-835

Colombié N, Vérollet C, Sampaio P, Moisand A, Sunkel C, Bourbon HM, Wright M, Raynaud-Messina B (2006) The Drosophila gamma-tubulin small complex subunit Dgrip84 is required for structural and functional integrity of the spindle apparatus. *Mol Biol Cell* **17**: 272-282

Dansereau DA, Lunke MD, Finkielsztein, A, Russell MA, Brook WJ (2002) Hephaestus encodes a polypyrimidine tract binding protein that regulates Notch signalling during wing development in Drosophila melanogaster. *Development* **129**: 5553-5566

Dix CI, Raff JW (2007) Drosophila Spd-2 recruits PCM to the sperm centriole, but is dispensable for centriole duplication. *Curr Biol* **17**: 1759-1764

Dobbelaere J, Josué F, Suijkerbuijk S, Baum B, Tapon N, Raff J (2008) A genome-wide RNAi screen to dissect centriole duplication and centrosome maturation in Drosophila. *PLoS Biol* **6**: e224

Doxsey S (2001) Re-evaluating centrosome function. *Nat Rev Mol Cell Biol* **2**: 688-698

Ferralli J, Ashby J, Fasler M, Boyko V, Heinlein M (2006) Disruption of microtubule organization and centrosome function by expression of tobacco mosaic virus movement protein. *J Virol* **80**: 5807-5821

Fumoto K, Kadono M, Izumi N, Kikuchi A (2009) Axin localizes to the centrosome and is involved in microtubule nucleation. *EMBO Rep* **10**: 606-613

Fyrberg EA, Mahaffey JW, Bond BJ, Davidson N (1983) Transcripts of the six Drosophila actin genes accumulate in a stage- and tissue-specific manner. *Cell* **33**: 115-23

Gatt MK, Savoian MS, Riparbelli MG, Massarelli C, Callaini G, Glover DM (2005) Klp67A destabilises pre-anaphase microtubules but subsequently is required to stabilise the central spindle. *J Cell Sci* **118**: 2671-2682

Gstaiger M, Aebersold R (2009) Applying mass spectrometry-based proteomics to genetics, genomics and network biology. *Nat Rev Genet* **10**: 617-627

Gingras AC, Raught B, Sonenberg N (1999) eIF4 initiation factors: effectors of mRNA recruitment to ribosomes and regulators of translation. *Annu Rev Biochem* **68**: 913-963

Gonzalez C (2008) Centrosome function during stem cell division: the devil is in the details. *Curr Opin Cell Biol* **20**: 694-698

Goshima G, Wollman R, Goodwin SS, Zhang N, Scholey JM, Vale RD, Stuurman N (2007) Genes required for mitotic spindle assembly in Drosophila S2 cells. *Science* **316**: 417-421

Graser S, Stierhof YD, Nigg EA (2007) Cep68 and Cep215 (Cdk5rap2) are required for centrosome cohesion. *J Cell Sci* **120**: 4321-4331

Hansen DV, Hsu JY, Kaiser BK, Jackson PK, Eldridge AG (2002) Control of the centriole and centrosome cycles by ubiquitination enzymes. *Oncogene* **21**: 6209-6221

Hughes JR, Meireles AM, Fisher KH, Garcia A, Antrobus PR, Wainman A, Zitzmann N, Deane C, Ohkura H, Wakefield JG (2008) A microtubule interactome: complexes with roles in cell cycle and mitosis. *PLoS Biol* **6**: e98

Januschke J, Gonzalez C (2008) Drosophila asymmetric division, polarity and cancer. *Oncogene* **27**: 6994-7002

Jouvenet N, Wileman T (2005) African swine fever virus infection disrupts centrosome assembly and function. *J Gen Virol* **86**: 589-594

Kalt A, Schliwa M (1993) Molecular components of the centrosome. *Trends Cell Biol* **3**: 118-28

Keller LC, Romijn EP, Zamora I, Yates JR 3rd, Marshall WF (2005) Proteomic analysis of isolated Chlamydomonas centrioles reveals orthologs of ciliary-disease genes. *Curr Biol* **15**: 1090-1098

Khodjakova A, Rieder CL (2001) Centrosomes Enhance the Fidelity of Cytokinesis in Vertebrates and Are Required for Cell Cycle Progression. *J Cell Biol* **153**: 237-242

Kittler R, Pelletier L, Heninger AK, Slabicki M, Theis M, Miroslaw L, Poser I, Lawo S, Grabner H, Kozak, Wagner J, Surendranath V, Richter C, Bowen W, Jackson A, Habermann B,

Hyman A, Buchholz F (2007) Genome-scale RNAi profiling of cell division in human tissue culture cells. *Nat Cell Biol* **9**: 1401-1412

Komesli S, Tournier F, Paintrand M, Margolis RL, Job D, Bornens M (1989) Mass isolation of calf thymus centrosomes: identification of a specific configuration. *J Cell Biol* **109**: 2869-2878

Kwon M, Godinho SA, Chandhok NS, Ganem NJ, Azioune A, Thery M, Pellman D (2008) Mechanisms to suppress multipolar divisions in cancer cells with extra centrosomes. *Genes Dev* **22**: 2189-2203

Lange BMH, Bachi A, Wilm M, Gonzalez C (2000) Hsp90 is a core centrosomal component and is required at different stages of the centrosome cycle in Drosophila and vertebrates. *EMBO J* **19**: 1252-1262

Lange BMH (2002) Integration of the centrosome in cell cycle control, stress response and signal transduction pathways. *Curr Opin Cell Biol* **14**: 35-43

Lécuyer E, Yoshida H, Parthasarathy N, Alm C, Babak T, Cerovina T, Hughes TR, Tomancak P, Krause HM (2007) Global analysis of mRNA localization reveals a prominent role in organizing cellular architecture and function. *Cell* **131**: 174-187

Lehmann V, Müller H, Lange BMH (2005) Immunoisolation of centrosomes from Drosophila melanogaster. *Curr Protoc Cell Biol* **29**: 3.17.1-3.17.13

Li JB, Gerdes JM, Haycraft CJ, Fan Y, Teslovich TM, May-Simera H, Li H, Blacque OE, Li L, Leitch CC, Lewis RA, Green JS, Parfrey PS, Leroux MR, Davidson WS, Beales PL, Guay-Woodford LM, Yoder BK, Stormo GD, Katsanis N, Dutcher SK (2004) Comparative genomics identifies a flagellar and basal body proteome that includes the BBS5 human disease gene. *Cell* **117**: 541-552

Lingle WL, Lutz WH, Ingle JN, Maihle J, Salisbury JL (1998) Centrosome hypertrophy in human breast tumors: implications for genomic stability and cell polarity. *Proc Natl Acad Sci USA* **95**: 2950-2955

Lucas EP, Raff JW (2007) Maintaining the proper connection between the centrioles and the pericentriolar matrix requires Drosophila centrosomin. *J Cell Biol* **178**: 725-732

Manandhar G, Simerly C, Schatten G (2000) Centrosome reduction during mammalian

spermiogenesis. *Curr Top Dev Biol* **49**: 343-363

Martinez-Campos M, Basto R, Baker J, Kernan M, Raff JW (2004) The Drosophila pericentrin-like protein is essential for cilia/flagella function, but appears to be dispensable for mitosis. *J Cell Biol* **165**: 673-683

Megraw TL, Li K, Kao LR, Kaufman TC (1999) The centrosomin protein is required for centrosome assembly and function during cleavage in Drosophila. *Development* **126**: 2829-2839

Mikule K, Delaval B, Kaldis P, Jurcyzk A, Hergert P, Doxsey S (2007) Loss of centrosome integrity induces p38-p53-p21-dependent G1-S arrest. *Nat Cell Biol* **9**: 160-170

Mirgorodskaya E, Braeuer C, Fucini P, Lehrach H, Gobom J (2005) Nanoflow liquid chromatography coupled to matrix-assisted laser desorption/ionization mass spectrometry: Sample preparation, data analysis, and application to the analysis of complex peptide mixtures. *Proteomics* **5**: 399-408

Moritz M, Braunfeld MB, Fung JC, Sedat JW, Alberts BM, Agard DA (1995) Three-dimensional structural characterization of centrosomes from early Drosophila embryos. *J Cell Biol* **130**: 1149-1159

Müller H, Fogeron ML, Lehmann V, Lehrach H, Lange BMH (2006) A centrosome-independent role for gamma-TuRC proteins in the spindle assembly checkpoint. *Science* **314**: 654-657

Nigg EA (2002) Centrosome aberrations: cause or consequence of cancer progression? *Nat Rev Cancer* **2**: 815-825

Nogales-Cadenas R, Abascal F, Díez-Pérez J, Carazo JM, Pascual-Montano A (2009) CentrosomeDB: a human centrosomal proteins database. *Nucleic Acids Res* **37**: D175-180

Palazzo RE, Vogel JM (1999) Isolation of centrosomes from Spisula solidissima oocytes. *Methods Cell Biol* **61**: 35-56

Palazzo RE, Vogel JM, Schnackenberg BJ, Hull DR, Wu X (2000) Centrosome maturation. *Curr Top Dev Biol* **49**: 449-470

Park AY, Shen TL, Chien S, Guan JL (2009) Role of focal adhesion kinase Ser-732 phosphorylation in centrosome function during mitosis. *J Biol Chem* **284**: 9418-9425

Pinto S, Quintana DG, Smith P, Mihalek RM, Hou ZH, Boynton S, Jones CJ, Hendricks M, Velinzon K, Wohlschlegel JA, Austin RJ, Lane WS, Tully T, Dutta A (1999) latheo encodes a subunit of the origin recognition complex and disrupts neuronal proliferation and adult olfactory memory when mutant. *Neuron* **23**: 45-54

Ploubidou A, Moreau V, Ashman K, Reckmann I, González C, Way M (2000) Vaccinia virus infection disrupts microtubule organization and centrosome function. *EMBO J* **19**: 3932-3944

Resendes KK, Rasala BA, Forbes DJ (2008) Centrin 2 localizes to the vertebrate nuclear pore and plays a role in mRNA and protein export. *Mol Cell Biol* **28**: 1755-69

Salisbury JL, Suino KM, Busby R, Springett M (2002) Centrin-2 is required for centriole duplication in mammalian cells. *Curr Biol* **12**: 1287-1292

Sibon OC, Kelkar A, Lemstra W, Theurkauf WE (2000) DNA-replication/DNA-damage-dependent centrosome inactivation in Drosophila embryos. *Nat Cell Biol* **2**: 90-95

Sitterlin D (2004) Characterization of the Drosophila Rae1 protein as a G1 phase regulator of the cell cycle. *Gene* **326**: 107-16

Stevenson VA, Kramer J, Kuhn J, Theurkauf WE (2001) Centrosomes and the Scrambled protein coordinate microtubule-independent actin reorganization. *Nat Cell Biol* **3**: 68-75

Tassin AM, Maro B, Bornens M (1985) Fate of microtubule-organizing centers during myogenesis in vitro. *J Cell Biol* **100**: 35-46

Thomas JH, Wieschaus E (2004) src64 and tec29 are required for microfilament contraction during Drosophila cellularization. *Development* **131**: 863-871

Varmark H, Llamazares S, Rebollo E, Lange B, Reina J, Schwarz H, Gonzalez C (2007) Asterless is a centriolar protein required for centrosome function and embryo development in Drosophila. *Curr Biol* **17**: 1735-1745

Vernì F, Somma MP, Gunsalus KC, Bonaccorsi S, Belloni G, Goldberg ML, Gatti M (2004) Feo, the Drosophila homolog of PRC1, is required for central-spindle formation and cytokinesis. *Curr Biol* **14**: 1569-1575

Vérollet C, Colombié N, Daubon T, Bourbon HM, Wright M, Raynaud-Messina B (2006) Drosophila melanogaster gamma-TuRC is dispensable for targeting gamma-tubulin to the centrosome and microtubule nucleation. *J Cell Biol* **172**: 517-528

Wigge PA, Jensen ON, Holmes S, Souès S, Mann M, Kilmartin JV (1998) Analysis of the Saccharomyces spindle pole by matrix-assisted laser desorption/ionization (MALDI) mass spectrometry. *J Cell Biol* **141**: 967-977

Zavortink M, Contreras N, Addy T, Bejsovec A, Saint R (2005) Tum/RacGAP50C provides a critical link between anaphase microtubules and the assembly of the contractile ring in Drosophila melanogaster. *J Cell Sci* **118**: 5381-5392

Table I – Function of MS-identified centrosome candidate proteins:

centrosome structure maintenance		centrosome duplication			
Gene D	**Gene name**	**GeneID**	**Gene name**	**GeneID**	**Gene name**
37368	Act57B	39130	alphaTub67C	34329	RpL13
33002	CG11943	40904	alphaTub84D	38983	RpL14
34416	CG31716	41183	alphaTub85E	31613	RpL17
36491	cnn	41446	aur	36985	RpL18A
37467	Rae1	37238	betaTub56D	37995	RpL19
33835	eIF-4a	43359	betaTub97EF	35453	RpL21
35696	scra	38062	CG6905	37628	RpL23
39850	spd-2	31838	CG7033	38208	RpL23A
32946	Grip84	31208	crn	34754	RpL24
48481	l(1)dd4	32015	feo	43103	RpL27
33782	Lam	33501	gammaTub23C	33654	RpL27A
40444	Act79B	32478	Grip128	38397	RpL28
41446	aur	39365	Grip163	41347	RpL3
33934	cup	35130	Grip71	44059	RpL30
37662	Fib	34441	Grip75	31483	RpL35
33501	gammaTub23C	318855	His2A:CG31618	31009	RpL36
32478	Grip128	318847	His3:CG31613	43349	RpL4
34441	Grip75	41773	His4r	43723	RpL6
36454	lat	32133	Hsc70-3	34352	RpL7
43864	Qm	32049	Klp10A	31588	RpL7A
38983	RpL14	36454	lat	44251	RpL8
43103	RpL27	50070	mask	34526	RpL9
41347	RpL3	32630	Nup153	34149	RpS13
31009	RpL36	38515	pav	39484	RpS4
43723	RpL6	34338	Pen	31700	RpS6
31588	RpL7A	2768940	Pp2A-29B	40859	sas-4
36576	RpS23	43864	Qm	36538	tum
39484	RpS4	39338	RpL10Ab	40687	RpL13A
		37235	RpL11		

Table I: Functional classification of the RNAi phenotypes in SL2 cells after depletion of MS-identified proteins

Significant phenotypes relating to centrosome structure (marked in green) and duplication (marked in brown) are listed, for the MS-identified centrosome-associated *Drosophila* proteins. The proteins, whose depletion resulted in a loss of centrosome (“0”) phenotype, are marked in yellow.

Table II - Proteins with new centrosomal/spindle localization and/or function

Drosophila SL2 cells				human HaCaT cells
Drosophila **Gene name**	**protein localization**	**centrosome duplication**	**centrosome structure maintenance**	**centrosomal function**
Nup153	centrosome, spindle	●		○
feo	centrosome	●		●
crn	centrosome, spindle	●		●
alphaTub84D	○	●		○
alphaTub85E	○	●		○
betaTub97EF	○	●		○
His4r	○	●		○
CG6905	nucleus	●		N
His2A:CG31618	○	●		●
His3:CG31613	○	●		●
mask	○	●		●
Pen	○	●		●
tum	○	●		●
Pp2A-29B	○	●		●
Hsc70-3	○	●	●	●
lat	spindle	●	●	N
cort	centrosome		●	*no human orthologue*
Lam	centrosome, spindle		●	N
eIF-4a	centrosome, spindle		●	●
CG11943	cytoplasm		●	N
CG31716	○		●	●
cup	○		●	*no human orthologue*
Fib	○		●	●
Rae1	nucleus		●	●
scra	nucleus		●	●
Act57B	○		●	○
Act79B	○		●	○
CG11148	centrosome, spindle	N	N	○
coro	spindle	N	N	○
Cka	spindle	N	N	○
TFAM	centrosome, chromosomes	N	N	○
Nat1	spindle	N	N	○

Table II: Localization and function of the new centrosomal proteins identified by MS, in SL2 and HaCaT cells

Significant phenotypes relating to centrosome structure and duplication are listed, for the MS-identified centrosome-associated *Drosophila* proteins and their human orthologues. Localization in SL2 cells, when known or tested (when antibody/clone available), is also indicated. The ● indicates new centrosomal function. The ○ indicates that clones were not available or could not be tested. N = no function or localization.

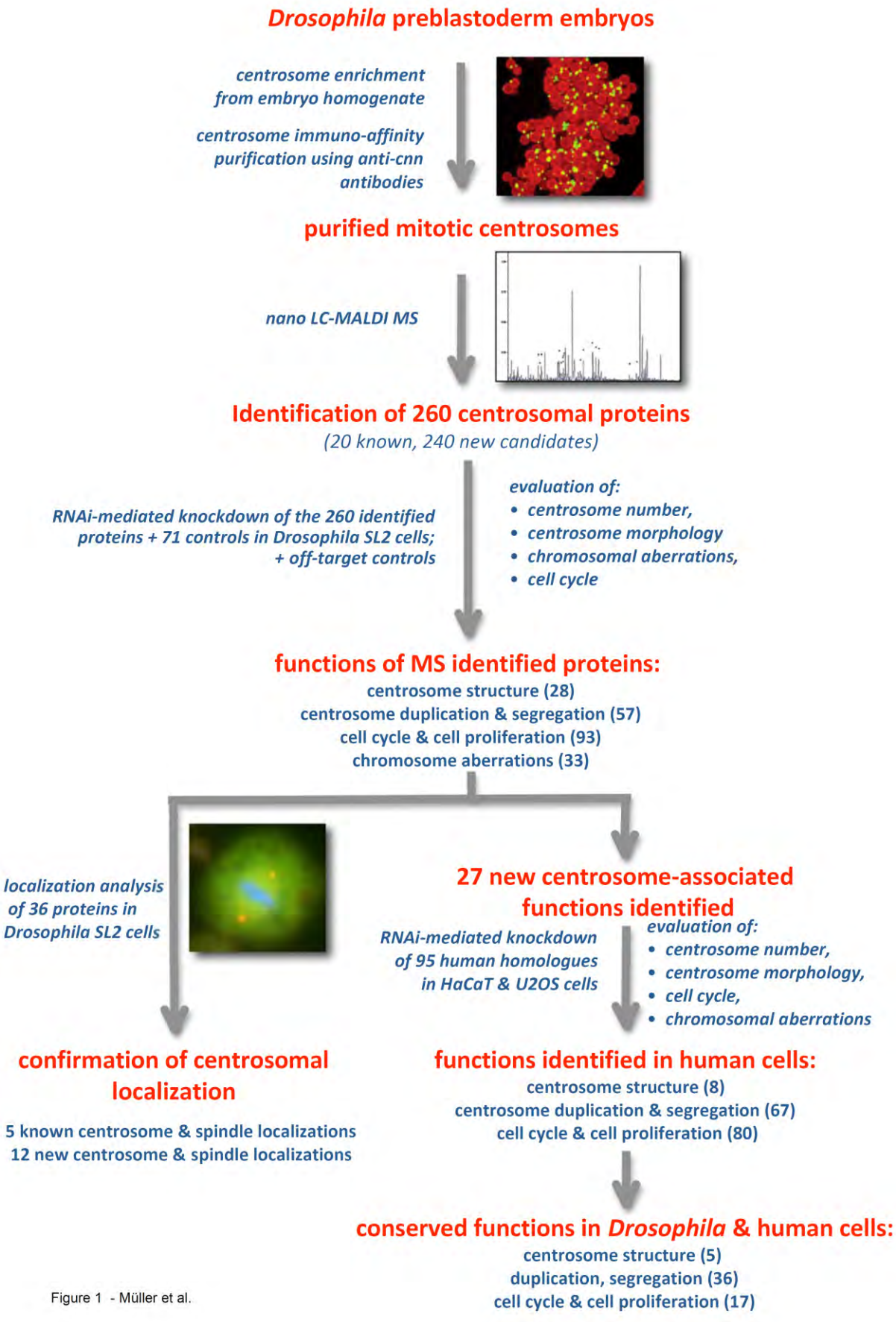

Figure 1 - Müller et al.

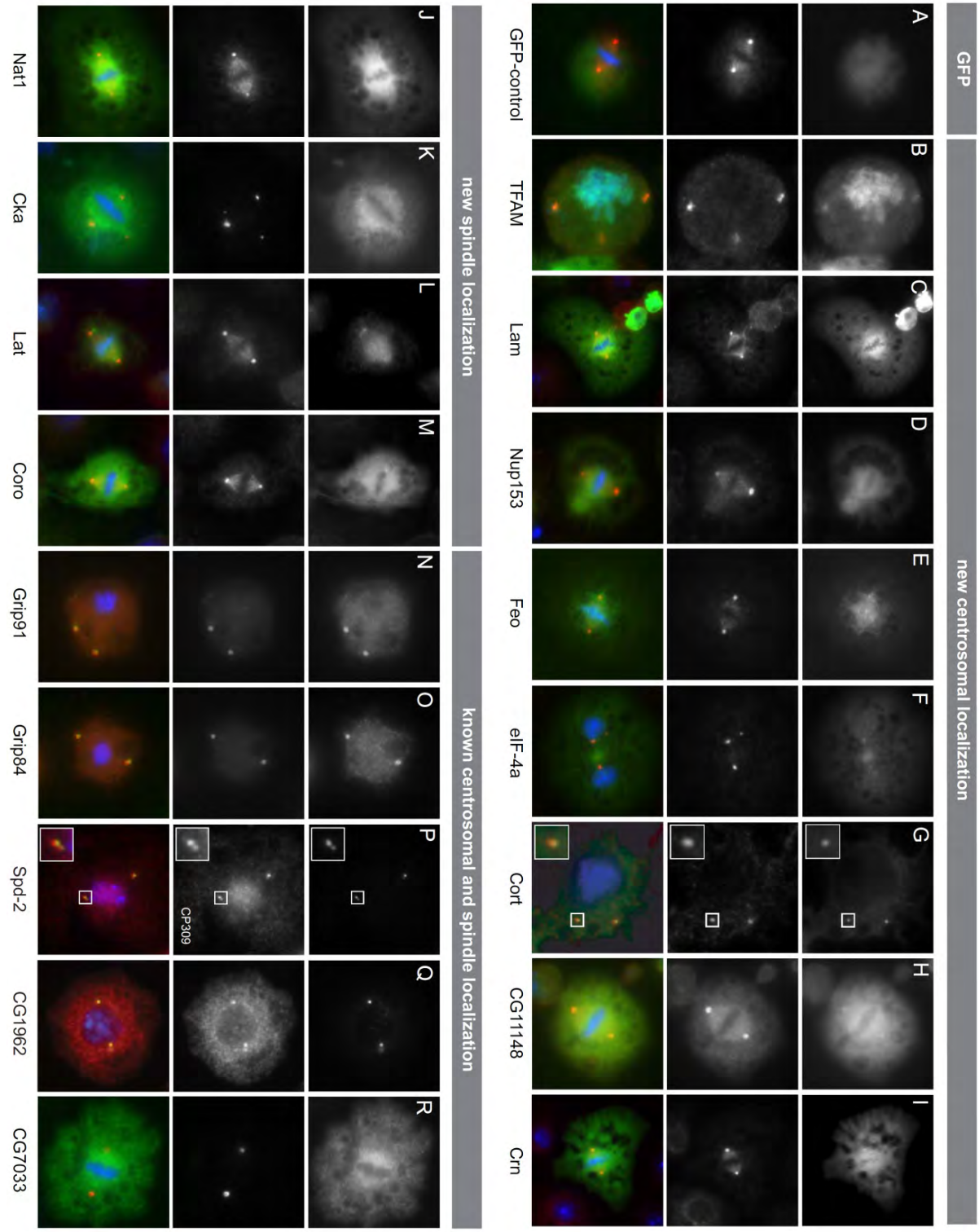

Figure 2 Müller et al

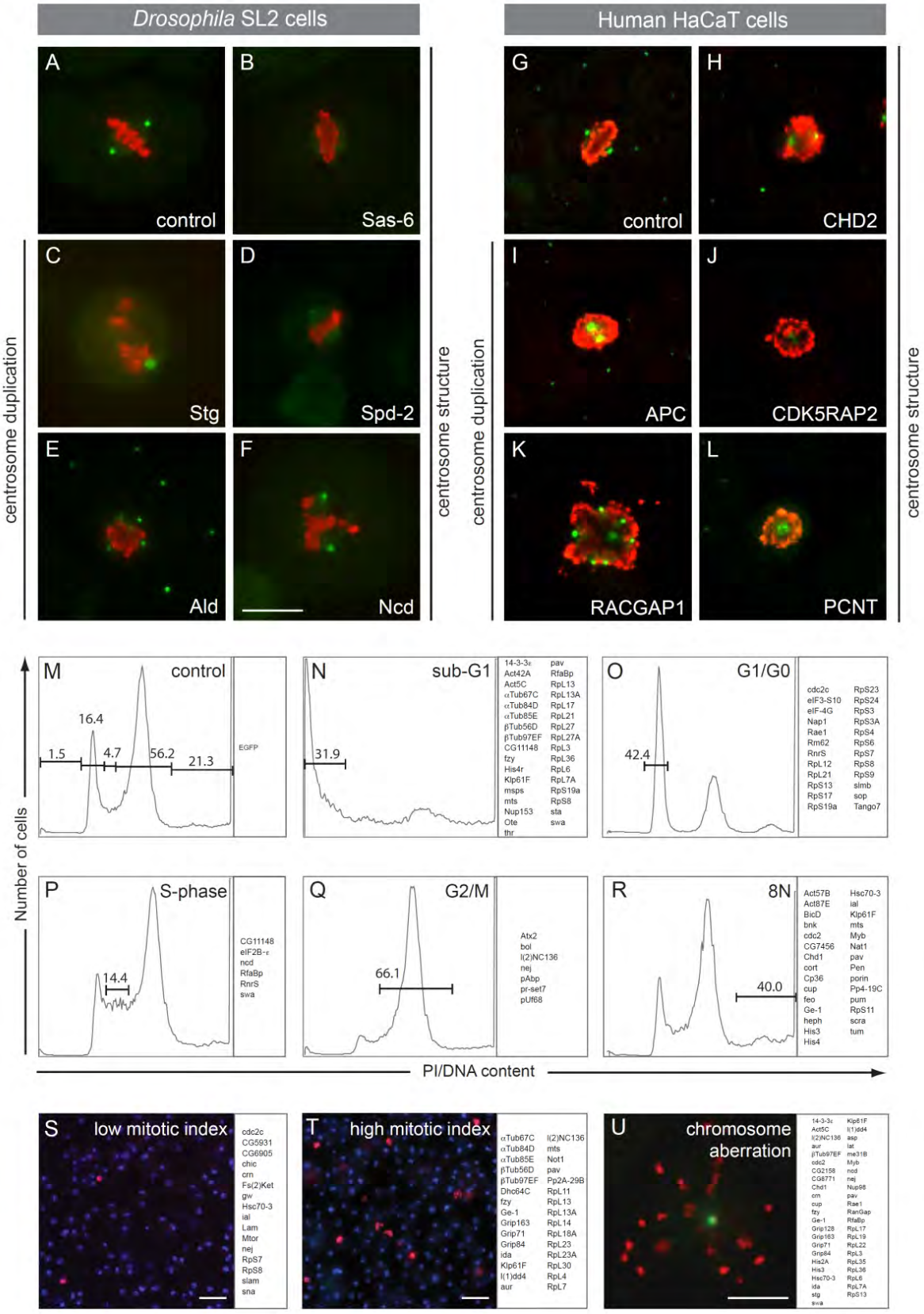

Figure 3
Müller et al.

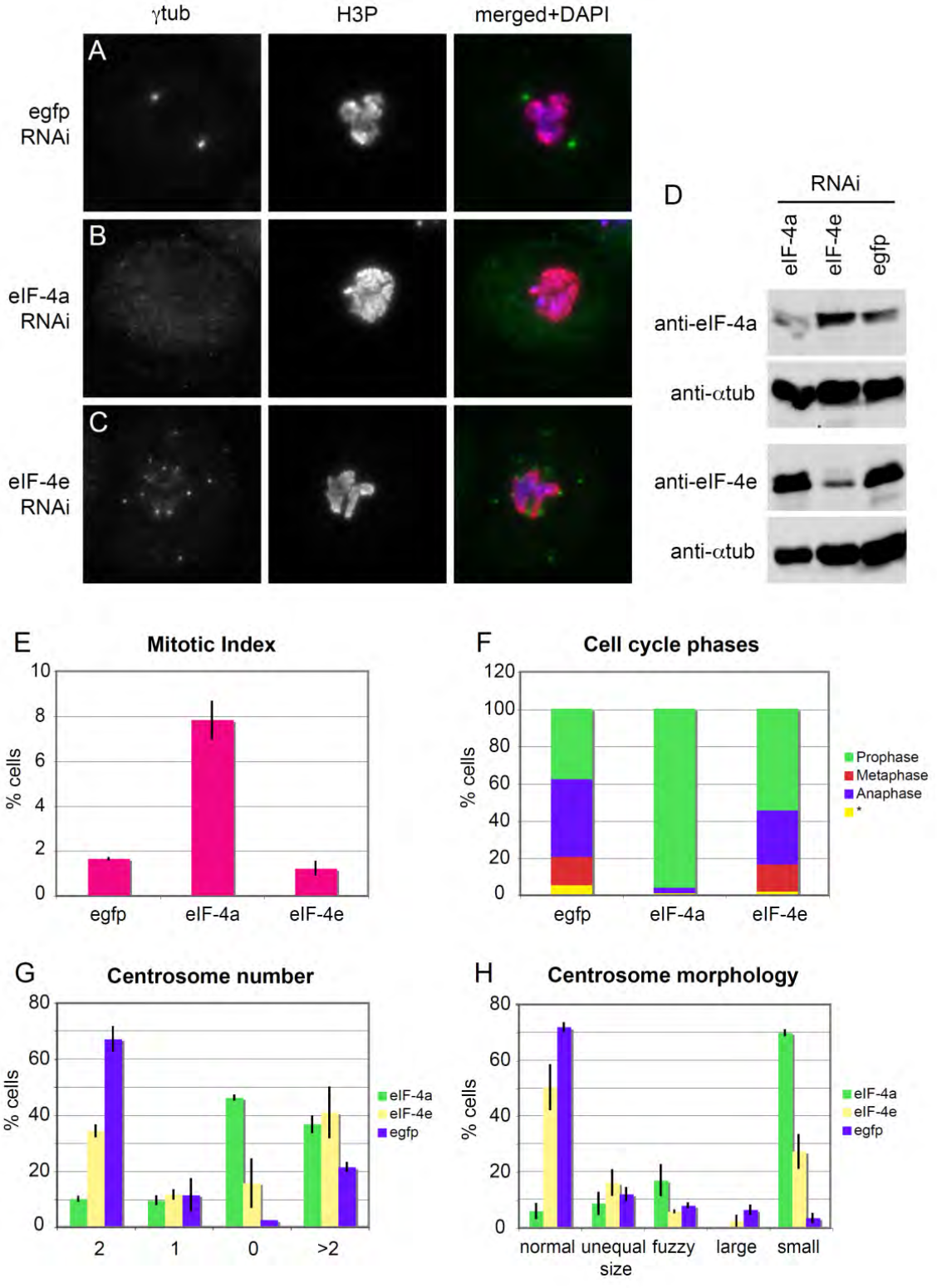

Figure 4
Müller et al

Supplementary Information

Supplementary Figures

- **S1**: Immunoisolation of centrosomes results in enrichment of centrosomal proteins and in reduction of cytoplasmic protein
- **S2:** Expression of TAP-tagged fusion proteins confirms centrosomal and spindle localization of candidate proteins
- **S3:** Centrosomal localization of candidate proteins is validated by antibody labeling
- **S4**: Centrosomal phenotypes related to abnormal centriolar replication
- **S5:** Effect of Feo RNAi or overexpression on centriole number and centrosome structure
- **S6**: Cycloheximide-induced inhibition of translation results in distinct centrosome phenotypes
- **S7:** Aphidicolin-induced inhibition of DNA replication results in centrosome over-replication and aberrant chromosome configurations
- **S8:** Depletion of the human orthologues of a subset of the centrosomal candidate proteins, in HaCaT and U2OS cells, affects centrosome shape and number

Supplementary Tables

- **S1**: Overview and comparison of phenotypes of *Drosophila* and human cells, following RNAi (*Microsoft Excel file*)
- **S2**: *Drosophila* RNAi and human siRNAs sequences; *p*-values and z-scores of statistical analysis (*Microsoft Excel file*)
- **S3**: Summary of localization of MS-identified proteins in SL2 cells
- **S4:** DNA constructs and cell lines created for the localization of MS-identified proteins in SL2 cells

Supplementary Materials and Methods

1. **CENTROSOME ISOLATION**
   - Cnn protein expression and purification
   - *Drosophila* embryo extract preparation
   - Calculation of centrosome isolation efficiency
2. **MASS SPECTROMETRY**
   - Chemicals
   - In-solution trypsinolysis of protein samples
   - SDS-PAGE
   - *In-situ* trypsinolysis
   - Nano LC-MALDI MS
   - Data processing
3. **MOLECULAR BIOLOGY**
   - DNA cloning
   - Cloning primer pairs
   - Synthetic clone
   - Generation of SL2 cell lines stably expressing centrosomal proteins
   - Production of double-stranded RNA (dsRNA)
4. **RNA INTERFERENCE**
   - Off-target effect control
5. **PHENOTYPE ANALYSIS and DATA EVALUATION**
   - Antibodies
   - Immunofluorescence microscopy
   - Mitotic index
   - Flow cytometry
   - Centrosome number and centrosome morphology analysis
   - Phenotypic scoring parameters
   - Cell cycle analysis
   - Drug treatment

Supplementary References

Supplementary Figures

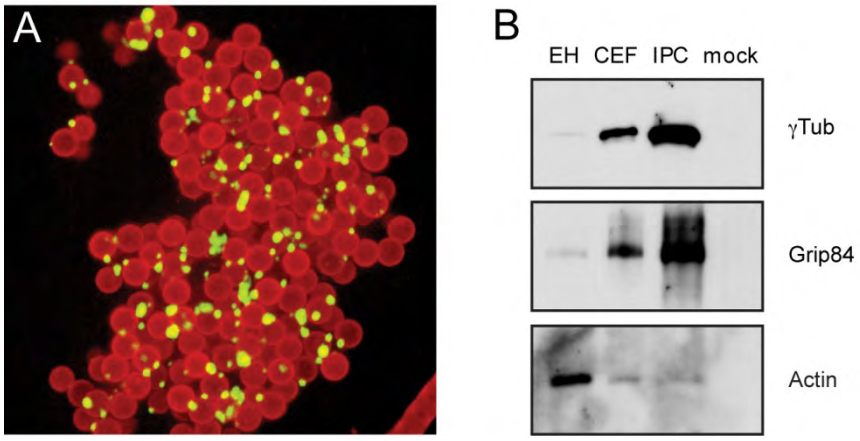

Figure S1: Immunoisolation of centrosomes results in enrichment of centrosomal proteins and in reduction of cytoplasmic protein

Immunoisolation of centrosomes results in highly enriched centrosome preparations. (A) Projection of a z-series of confocal microscopy images of centrosomes (yellow) immunoisolated on magnetic beads (red). (B) Western blotting analysis of different isolation stages shows an enrichment of centrosomal proteins (γ-tubulin, Grip84); (EH = embryo homogenate, CEF = centrosome enriched fraction, IPC = immunoisolated centrosomes, mock = negative control sample: magnetic beads coupled to preimmune serum incubated with CEF). The level of cytoplasmic protein actin is strongly reduced in the IPC fraction.

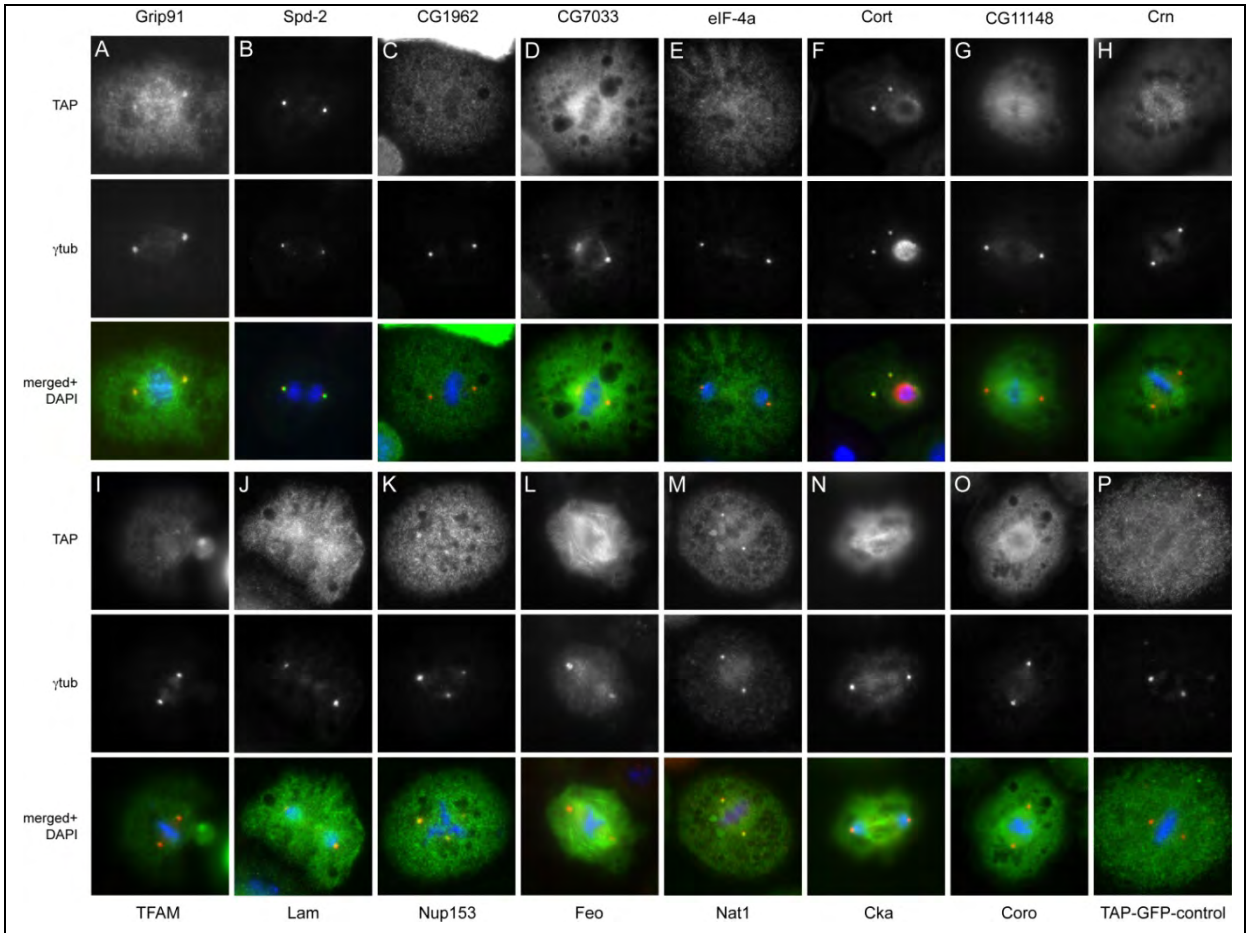

Figure S2: Expression of TAP-tagged fusion proteins confirms centrosomal and spindle localization of candidate proteins

TAP-tagged candidate protein expression in SL2 cells confirms centrosomal and spindle localization for the positive control proteins: Grip91 (A), Spd-2 (B), CG1962 (C), CG7033 (D) and new candidate proteins: eIF-4a (E), Cort (F), CG11148 (G), Crn (H), TFAM (I), Lam (J), Nup153 (K), Feo (L), Nat1 (M), Cka (N) and Coro (O). Expression of the TAP-GFP control vector shows uniform distribution in the cell (P) validating the specificity of candidate protein localization. The TAP-tag is shown in green (upper panel, A-P), antibody staining against γ-tubulin in red (middle panel, A-P) and composite of both together with DNA in blue (lower panel, A-P).

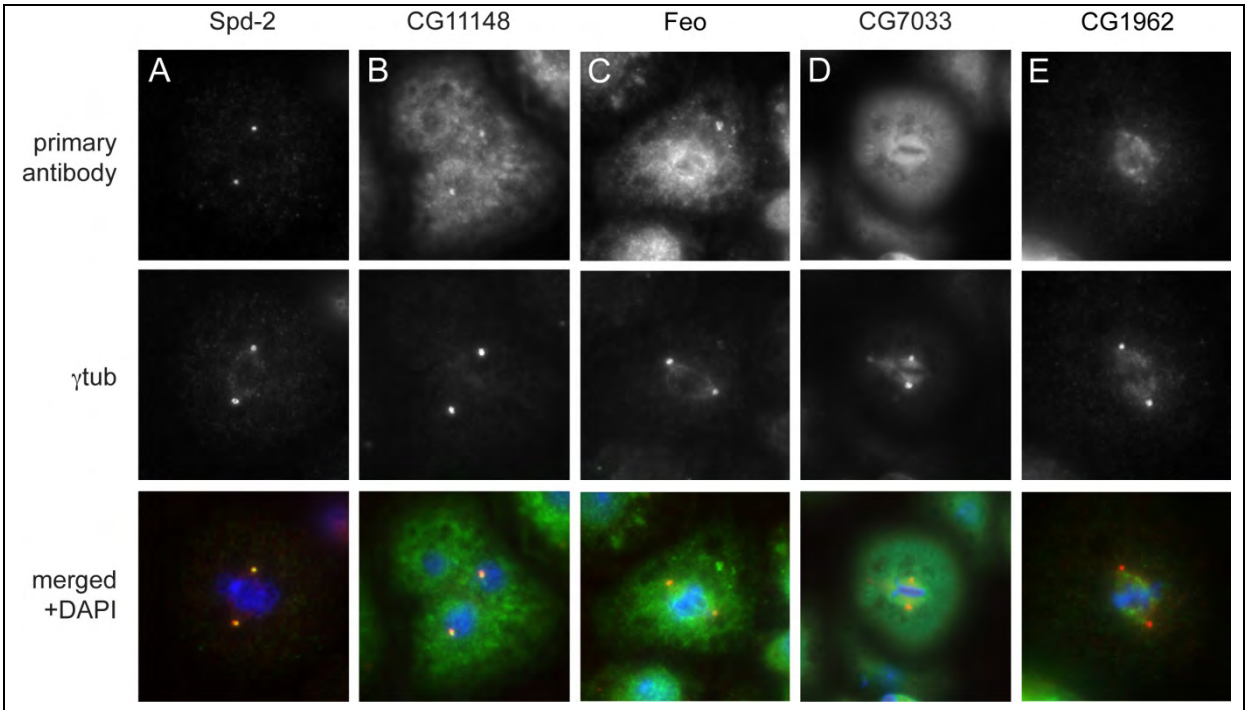

Figure S3: Centrosomal localization of MS-identified proteins is validated by antibody labeling.

Immunofluorescence microscopy after staining with antibodies against Spd-2 (A), CG11148 (B) and Feo (C) confirms centrosomal localization for those centrosome or candidate proteins, spindle localization is validated by antibody staining against CG7033 (D) and CG1962 (E). Antibodies against CG7033, CG11148, Spd-2 and CG1962 were generated as described in Supplemental Experimental Procedures, the anti-Feo antibody was kindly provided by M. Gatti.

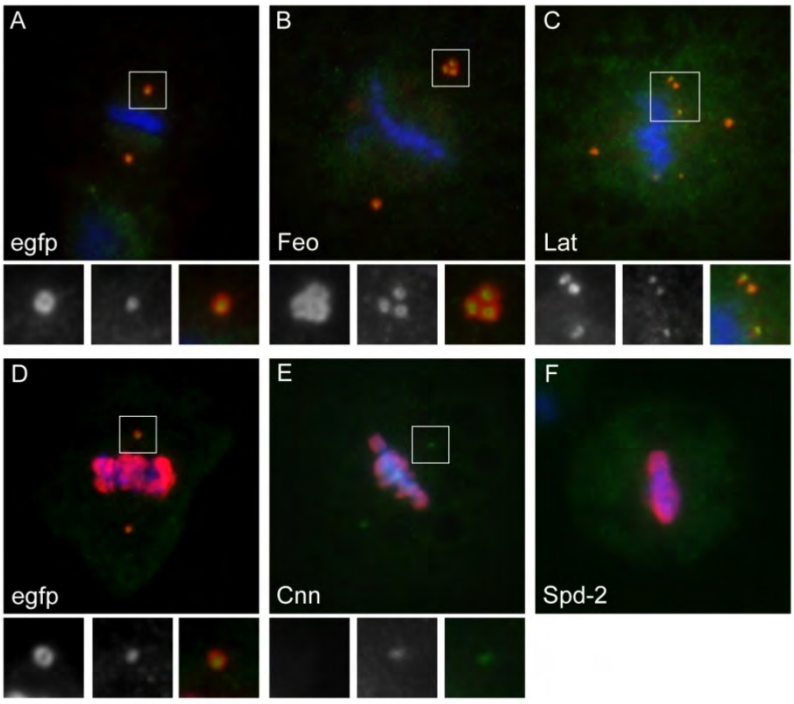

Figure S4: Centrosomal phenotypes are related to abnormal centriolar replication

Immunofluorescence microscopy of SL2 cells depleted of the proteins Feo, Lat, Cnn and Spd-2 shows the number of centrioles in centrosomes with altered size and number. The PCM is marked with an anti-γ-tubulin antibody (red), centrioles are labeled with an anti-Cp309 antibody (green) and DNA is labeled with DAPI (blue). EGFP was used as negative RNAi control. Below each main image the enlarged insert of one of the centrosomes is shown in the following sequence: γ-tubulin, Cp309, superimposed image. In the images D-F phospho-histone H3 was labeled together with γ-tubulin in the red channel to visualize three different antibody labels (γ-tubulin, phospho-histone H3, Cp309) at the same time in addition to DAPI. (A, D) A single centriolar signal can be detected within the PCM in EGFP control cells. (B) Large centrosomes after Feo depletion contain multiple centrioles demonstrating that centriole over-replication or cytokinesis failure has occurred. (C) Each centrosome fragment co-labels with the anti-Cp309 antibody indicating that multiple small centrosomes were generated through impaired centrosome number control rather than PCM fragmentation after Lat-RNAi. (E) Cnn depletion is causing PCM dispersion and centriole-like structures are still detected. (F) Spd-2 depletion causes complete PCM dispersion and absence of the centriolar marker Cp309.

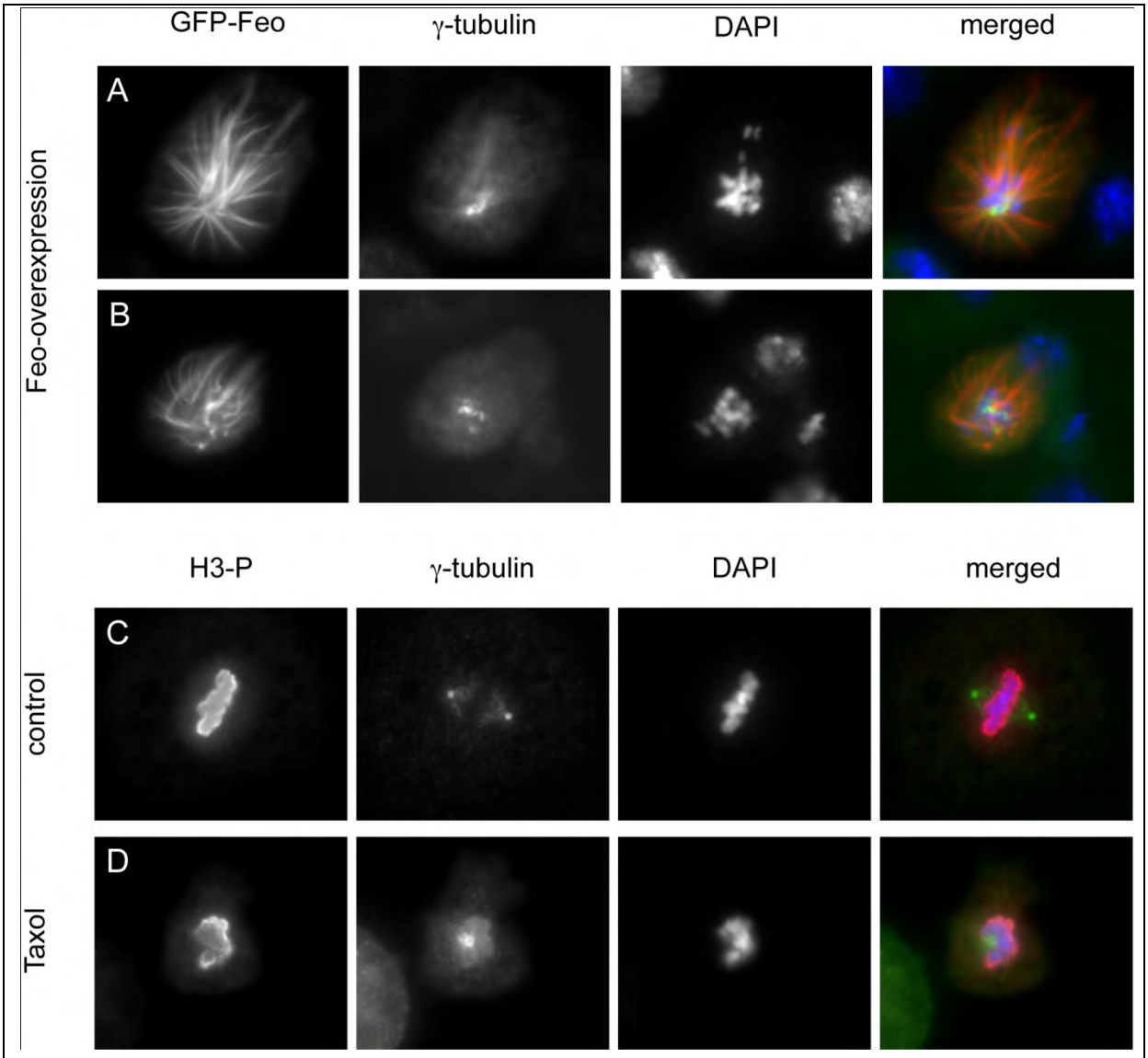

Figure S5: Over-expression of Feo leads to microtubule bundling and centrosome fragmentation

We analyzed the effect of Feo over-expression on the centrosome. Over-expression of N- or C-terminal GFP- (shown in A, B) or TAP-tagged Feo in SL2 cells leads to microtubule bundling as expected (Verni *et al*, 2004; D'Avino *et al*, 2007). However, in addition over-expression also leads to large structurally aberrant mitotic centrosomes (A, B; γ-tubulin) implying a more direct role of Feo in centrosome duplication or segregation. This is consistent with the fact that we find a fraction of the Feo protein associated with the centrosome (A; B composite, Figure S3 C). In order to test for a possible alternative mechanism, in which the observed PCM fragmentation is due to microtubule bundling-associated generation of free microtubule minus ends that capture PCM material, we induced microtubule bundling in mitotic SL2 cells by taxol-treatment (D). Taxol-treated cells (D) show a centrosome phenotype (single, large) that is clearly distinct from both, that of GFP-Feo expressing cells (fragmented centrosomes) (A, B) and from that of DMSO control treated cells (C).

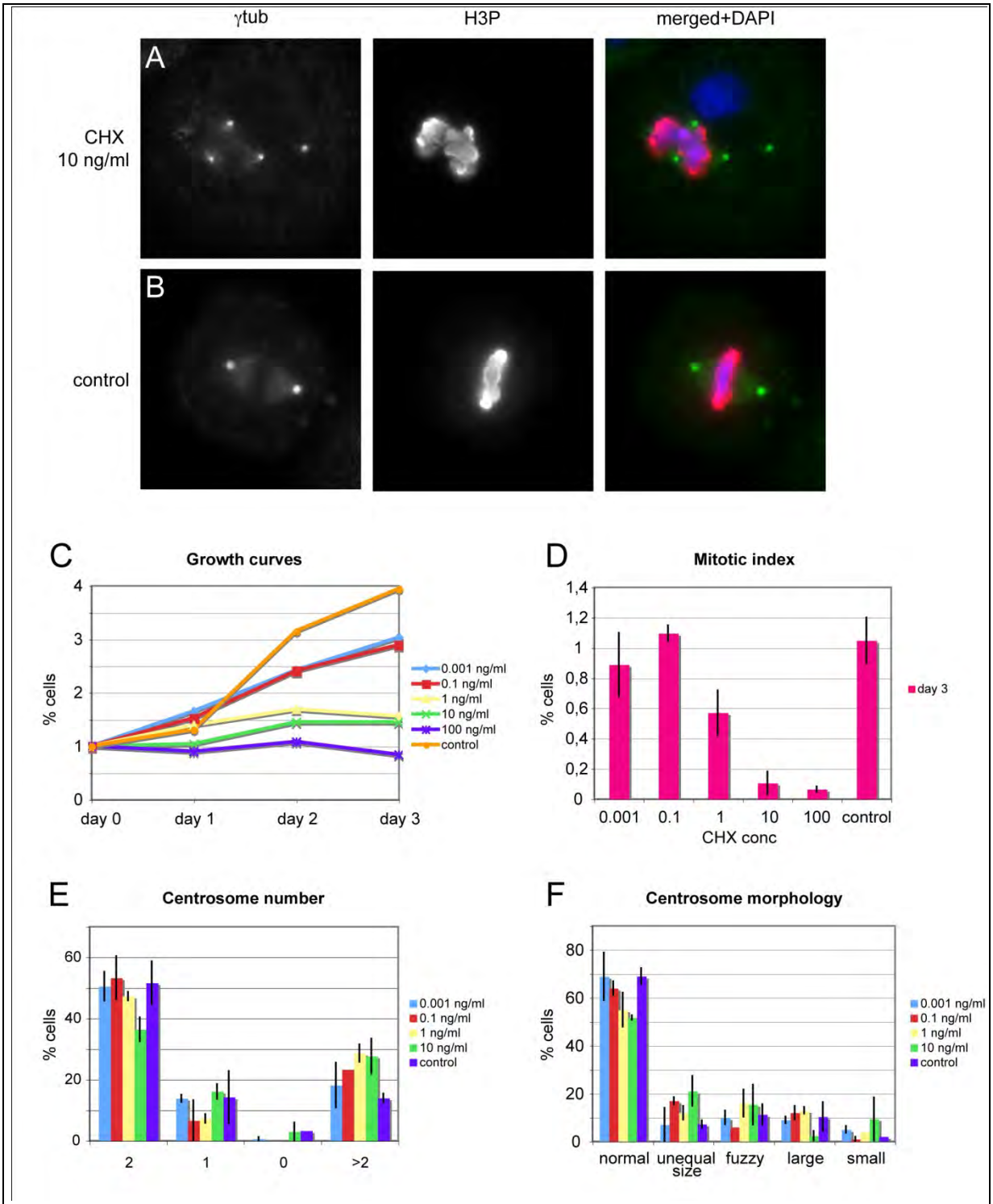

Figure S6: Cycloheximide-induced inhibition of translation results in distinct centrosome phenotypes.

Evaluation of growth curves (C) and mitotic index (D) of SL2 cells after treatment with 5 different cycloheximide (CHX) concentrations determined 10 ng/ml as the condition at which cells are affected by inhibited translation but remain viable over a period of 72 h. Phenotypic analysis and subsequent statistical evaluation revealed the formation of weak centrosomal abnormalities after inhibition of translation: Cells exhibited a slight increase in centrosome number (p-value 0,006; E) and in unequally sized or small centrosomes (p-value $2*10^{-5}$; F). Representative immunofluorescence microscopy images of cells treated with CHX or non-treated negative control are depicted in (A) and (B) respectively.

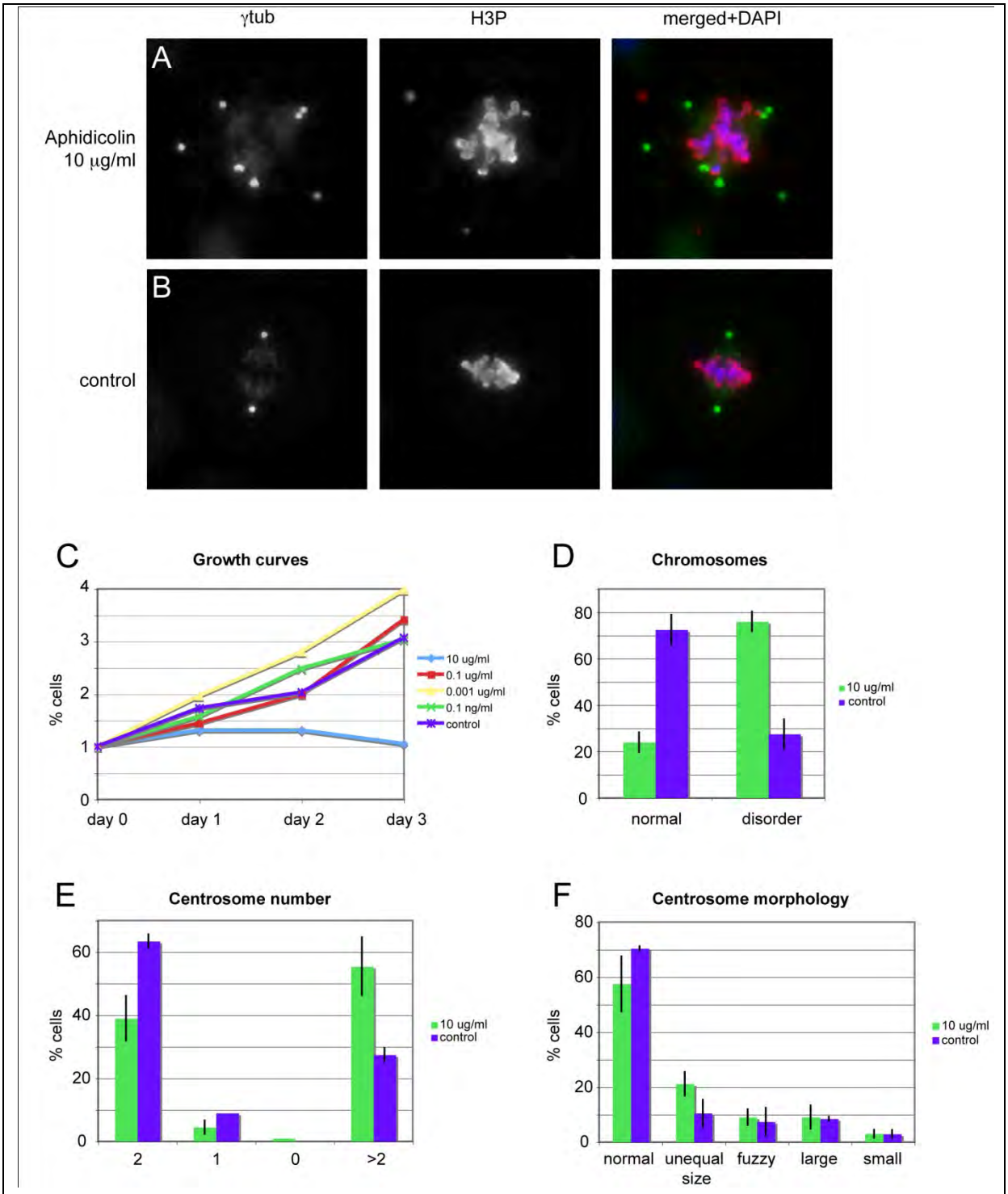

Figure S7: Aphidicolin-induced inhibition of DNA replication results in centrosome over-replication and aberrant chromosome configurations

Growth curves of SL2 cells after treatment with different concentrations of Aphidicolin over a period of 72 h indicate that cells are affected through inhibition of DNA replication at 10 µg/ml (C). Phenotypic scoring and statistical testing for significance of chromosome configuration, centrosome number and centrosome morphology in mitotic cells shows severe chromosomal aberrations after Aphidicolin treatment (p-value $1*10^{-17}$; D). A further consequence of Aphidicolin treatment was an increase in centrosome number (p-value $1*10^{-27}$; E) while centrosome morphology was largely unaffected (F). Representative immunofluorescence microscopy images of cells treated with Aphidicolin or DMSO-treated negative control are depicted in (A) and (B) respectively.

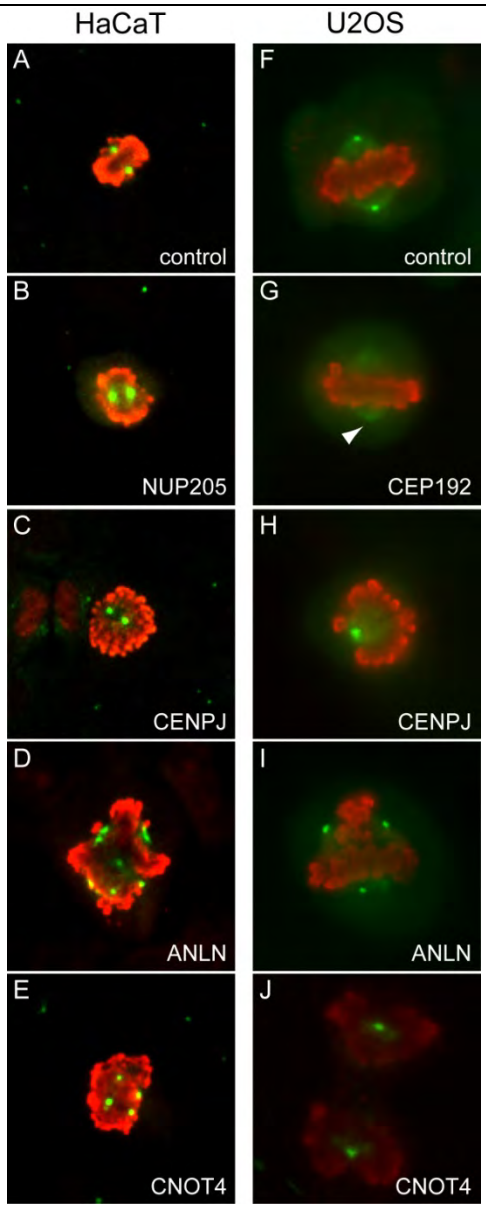

Figure S8: Depletion of the human orthologues of a subset of the centrosomal candidate proteins, in HaCaT and U2OS cells, affects centrosome morphology and number

Immunofluorescence microscopy images of mitotic U2OS and HaCaT cells show representative examples of the different centrosome abnormalities after protein depletion of human orthologues (corresponding *Drosophila* gene names are given in parenthesis below). Centrosomes are labeled with an anti-γ-tubulin antibody (green) and mitotic chromosomes with an anti-phospho-histone H3 antibody (red). (A, F) Non-specific control siRNA-transfected cells show normal metaphase chromosome alignment and two centrosomes at the spindle poles. (B, D, E) Depletion of NUP205 (CG11943), ANLN (Scra), CNOT4 (CG31716) in HaCaT cells and (I) depletion of ANLN (Scra) in U2OS produces a centrosome duplication or segregation phenotype (multiple and/or large centrosomes). (G, J) Knock-down of CEP192 (Spd-2) and CNOT4 (CG31716) results in a structural (small or fuzzy) centrosome phenotype. (H) Depletion of CENPJ (Sas-4) in U2OS produces a centrosome duplication ("1" centrosome) and structure (fuzzy) phenotype, while in HaCaT the centrosomes are like in control cells after depletion of CENPJ (C). These experiments show that the centrosome structure phenotypes observed after depletion of CEP192, CNOT4 and NUP205 in Drosophila SL2 cells are similar in human U2OS cells. In contrast, different cancer or tissue origin of cell lines might contribute to the fact that the depletion of NUP205, ANLN and CNOT4 do not result in structural centrosome abrogation but rather in duplication and segregation phenotypes in HaCaT cells. For a detailed comparison of phenotypes see table S1 - data sheet phenotype comparison.

Supplementary Tables

Table S1: (*Microsoft Excel file*)

Overview and comparison of phenotypes of *Drosophila* and human cells, following RNAi

Datasheet 1 "*Drosophila* SL2 phenotypes": List of all candidate and control *Drosophila* proteins, their localization and RNAi phenotype, a comparison with similar studies, protein domains, human orthologues and related diseases.

Datasheet 2 "human HaCaT phenotypes": List of human orthologues and the corresponding RNAi phenotypes analyzed in HaCaT and U2OS cells.

Datasheet 3 "phenotypes comparison": Comparative list of *Drosophila* and human cells RNAi phenotypes.

Phenotypic subgroups lists can be generated using the Excel "sort and filter" function by activating the sort function in row 6 on the arrow up and arrow down symbol selecting a relevant category for sorting in the pop down menu.

Table S2: (*Microsoft Excel file*)

***Drosophila* RNAi and human siRNA sequences; *p*-values and z-scores of statistical analysis**

Datasheet 1 "*Drosophila* RNAi": Sequence plus calculation of efficiency and specificity for each dsRNA used in the SL2 cell RNAi experiments. Corresponding z-scores (FACS analysis) and *p*-values (immunofluorescence microscopy analysis) for each knock-down.

Datasheet 2 "human siRNA": Sequence of the siRNA duplex pools used in the HaCaT and U2OS cell RNAi experiments. Each pool contains 4 independent oligos targeting the same gene transcript. In addition, z-scores and *p*-values for each knock-down are listed.

Table S3
Localization of MS-identified centrosome candidate and control proteins in SL2 cells

Drosophila gene name	Centrosome or spindle association	EGFP-localization		confirmed by	
		interphase	mitosis	TAP-tag	IF
Grip84	known	centrosome	centrosome	●	N/A
l(1)dd4	known	centrosome	centrosome	●	N/A
spd-2	known	cytoplasm	centriole	●	●
CG7033	known	cytoplasm	spindle	●	●
CG1962	known	cytoplasm	spindle, centrosome	●	●
gamma23C	known	N/A	N/A	N/A	●
CG11148	new	cytoplasm, nucleus	centrosome, spindle	●	●
feo	new centros., spindle known	nucleus, microtubules	MTs, spindle midzone, centrosome	●	●
Nup153	new	cytoplasm, nucleus	Centrosome, spindle	●	N/A
eIF-4a	new	cytoplasm, nucleus	centrosome, spindle	●	N
Nat1	new	cytoplasm, nucleus	spindle	●	N
crn	new	nucleus	centrosome, spindle, midbody	●	N/A
coro	new	cytoplasm, nuclear membrane	spindle, cytoplasm	●	N/A
Cka	new	cytoplasm, nucleus	spindle	●	N
TFAM	new	nucleus, mitochondria	centrosome, chromosomes	●	N/A
Lam	new	nuclear membrane	centrosome, spindle	●	N
lat	new	nucleus	spindle	●	N/A
cort	new	centrsosome	cytoplasm	●	N
CG3173	N	nucleus	vesicles	N/A	N/A
CG6455	N	cytoplasm, perinuclear	cytoplasm	N/A	N/A
CG6181	N	cytoplasm, perinuclear	cytoplasm	N/A	N/A
CG6905	N	nucleus, nucleolus, nuclear membrane	cytoplasm	N/A	N/A
CG10732	N	cytoplasmic spots	cytoplasm	N/A	N/A
CG11943	N	cytoplasm, perinuclear	cytoplasm	N/A	N/A
CG14235	N	nucleus	cytoplasm	N/A	N/A
Actin 57b	N	cytoplasm, perinuclear	cytoplasm	N/A	N/A

alt	N	cytoplasm, nuclear membrane	cytoplasm	N/A	N/A
Hsc70cb	N	cytoplasm	cytoplasm	N/A	N/A
Rae1	N	nucleus	cytoplasm	N/A	N/A
RpL17	N	nucleus, nucleolus	cytoplasm	N/A	N/A
RpL24	N	nucleus, nucleolus	cytoplasm	N/A	N/A
RpS17	N	nucleus, nucleolus	cytoplasm	N/A	N/A
scra	N	nucleus	cytoplasm	N/A	N/A
Sop2	N	cytoplasm, perinuclear	cytoplasm	N/A	N/A
Cup	N/A	N/A	N/A	N/A	N/A
fs(1)N	N/A	N/A	N/A	N/A	N/A

Table S3: Summary of localization of MS-identified proteins in SL2 cells

Localization of MS-identified proteins in SL2 cells, in interphase and mitosis, is indicated. The proteins were localized using GFP-fusion or TAP-fusion or antibodies, as available. (●=confirmed, N/A=antibody not available, N = not confirmed).

Table S4
DNA constructs & cell lines used for the localization of MS-identified proteins

Gene Name	Gateway entry vector	Gateway destination vector EGFP tag	stable cell line GFP tag	Gateway destination vector TAP tag	stable cell line TAP tag
CG1962	pDONR201 NT	pAGW NT EGFP	yes	pDEST NTAP	yes
	pDONR201 CT	pAWG CT EGFP	yes	pDEST CTAP	yes
CG3173	pDONR201 NT	pAWG CT EGFP	yes	pDEST NTAP	-
	pDONR201 CT	-	-	pDEST CTAP	-
CG6455	pDONR201 NT	pAGW NT EGFP	yes	-	-
	pDONR201 CT	-	-	-	-
CG6181	pDONR201 NT	pAGW NT EGFP	yes	-	-
	pDONR201 CT	pAWG CT EGFP	yes	-	-
CG6905	pENTR/D-Topo NT	pAGW NT EGFP	yes	pDEST NTAP	yes
	pENTR/D-Topo CT	pAWG CT EGFP	yes	pDEST CTAP	yes
CG7033	pENTR/D-Topo NT	pAGW NT EGFP	yes	pDEST NTAP	yes
	pENTR/D-Topo CT	pAWG CT EGFP	yes	pDEST CTAP	-
CG10732	pDONR201 NT	pAGW NT EGFP	yes	-	-
	pDONR201 CT	pAWG CT EGFP	yes	-	-
CG11148	pDONR201 NT	pAGW NT EGFP	yes	pDEST NTAP	yes
	pDONR201 CT	-	-	pDEST CTAP	yes
CG11943	pDONR201 NT	pAGW NT EGFP	yes	pDEST NTAP	-
	pDONR201 CT	-	-	pDEST CTAP	-
CG14235	pDONR201 CT	pAWG CT EGFP	yes	pDEST CTAP	-
CG17286	pDONR201 NT	pAGW NT EGFP	yes	pDEST NTAP	yes
	pDONR201 CT	pAWG CT EGFP	-	pDEST CTAP	yes
Actin 57b	pDONR201 NT	pAGW NT EGFP	yes	pDEST NTAP	-
	pDONR201 CT	-	-	pDEST CTAP	-
alt	pDONR201 NT	pAGW NT EGFP	yes	-	-

	pDONR201 CT	pAWG CT EGFP	yes	-	-
cka	pDONR201 NT	pAGW NT EGFP	yes	pDEST NTAP	yes
	pDONR201 CT	pAWG CT EGFP	yes	pDEST CTAP	-
coro	pDONR201 NT	pAGW NT EGFP	yes	pDEST NTAP	yes
	pDONR201 CT	pAWG CT EGFP	yes	pDEST CTAP	-
cort	pDONR201 NT	pAGW NT EGFP	yes	pDEST NTAP	yes
	pDONR201 CT	-	-	pDEST CTAP	yes
Cup	pENTR/D-Topo NT	pAGW NT EGFP	-	-	-
	pENTR/D-Topo CT	pAWG CT EGFP	-	-	-
crn	pDONR201 NT	pAGW NT EGFP	yes	pDEST NTAP	yes
	pDONR201 CT	pAWG CT EGFP	yes	pDEST CTAP	yes
eIF4a	pDONR221 NT	pAGW NT EGFP	yes	pDEST NTAP	yes
	pDONR221 CT	pAWG CT EGFP	-	pDEST CTAP	yes
feo	pENTR/D-Topo NT	pAGW NT EGFP	yes	pDEST NTAP	yes
	pENTR/D-Topo CT	pAWG CT EGFP	yes	pDEST CTAP	yes
fs(1)N	pDONR201 NT	pAGW NT EGFP	-	-	-
gamma23	pENTR/D-Topo NT	pAGW NT EGFP	-	-	-
C	pENTR/D-Topo CT	pAWG CT EGFP	-	-	-
Grip84	pDONR201 NT	pAGW NT EGFP	-	pDEST NTAP	yes
	pDONR201 CT	pAWG CT EGFP	yes	pDEST CTAP	yes
Grip91	pDONR201 NT	pAGW NT EGFP	yes	pDEST NTAP	-
	pDONR201 CT	-	-	pDEST CTAP	-
Hsc70cb	pDONR201 NT	pAGW NT EGFP	yes	-	-
	pDONR201 CT	-	-	-	
Lam	pDONR201 CT	pAWG CT EGFP	yes	pDEST CTAP	yes
lat	pDONR201 NT	pAGW NT EGFP	yes	pDEST NTAP	yes
	pDONR201 CT	pAWG CT EGFP	yes	pDEST CTAP	yes
Nat1	pDONR201 NT	pAGW NT EGFP	yes	pDEST NTAP	yes
	pDONR201 CT	pAWG CT EGFP	yes	pDEST CTAP	-
Nup153	pENTR/D-Topo NT	pAGW NT EGFP	yes	pDEST NTAP	yes
Rae1	pDONR201 NT	pAGW NT EGFP	yes	pDEST NTAP	-
	pDONR201 CT	pAWG CT EGFP	yes	pDEST CTAP	-
RpL17	pENTR/D-Topo NT	pAGW NT EGFP	-	-	-
	pENTR/D-Topo CT	pAWG CT EGFP	-	-	-
RpL24	pENTR/D-Topo NT	pAGW NT EGFP	-	-	-
	pENTR/D-Topo CT	pAWG CT EGFP	-	-	-
RpS17	pENTR/D-Topo NT	pAGW NT EGFP	-	-	-
	pENTR/D-Topo CT	pAWG CT EGFP	-	-	-
scra	pDONR201 NT	pAGW NT EGFP	yes	pDEST NTAP	-
	pDONR201 CT	pAWG CT EGFP	-	pDEST CTAP	-
Sop2	pDONR201 NT	pAGW NT EGFP	yes	pDEST NTAP	-
	pDONR201 CT	-	-	pDEST CTAP	-
TFAM	pDONR201 NT	pAGW NT EGFP	yes	pDEST NTAP	yes
	pDONR201 CT	pAWG CT EGFP	yes	pDEST CTAP	yes

Table S4 : DNA constructs and cell lines created for the localization of MS-identified proteins in SL2 cells

List of expression clones and stable SL2 cell lines generated, localization of the tag (NT = N-terminal tag, CT = C-terminal tag). The GFP-fusion protein expression is driven by the act5C promoter. TAP-tag fusion protein expression is driven by the metallothionein-inducible promoter.

Supplementary Materials and Methods

1. CENTROSOME ISOLATION

Cnn protein expression and purification

For antibody generation of exon 6 of Cnn the protein was expressed as a His-tagged fusion protein in Isopropyl-ß-D-thiogalactopyranoside (IPTG) induced BL 21 cells for 6 h at 30°C. The cell extract was prepared by resuspending the cell pellet in lysis buffer (10 mM ß-Mercaptoethanol, 10% Sucrose, 1x PBS, 0.8 M NaCl, 1 mM Imidazole ph 7.0, 1 mg/ml Lysozym) supplemented with a protease inhibitor mix (100 mg/ml Pefabloc SC Roche, 2.5 mM Phenylmethanesulfonyl fluoride (PMSF) and 1 mg/ml of Aprotinine, Leupeptine, Pepstatine A) sonicated and further incubated after adding 1% Triton X-100, 10 µg/ml DNase I, 10 mM $MgCl_2$ and 1 mM MnCl for 30 min. The inclusion bodies were recovered and solubilized by a protocol adapted from Sambrook and Russel (2001) and purified using TALON Metal Affinity Beads (BD) according to the manufacturers instructions. The eluted protein was precipitated with trichloracetic acid and used for immunization of rabbits and rats (Pineda) and affinity purification of antibodies on HiTrap NHS-activated columns (GE Healthcare) according to the manufactures instructions.

Drosophila embryo extract preparation

An average of 30-50 g of 0-3 h old *Drosophila* (strain W1118) embryos were collected per day on apple juice/molasses agar trays from large fly populations (>200000 flies) (Bonte and Becker, 1999). Embryo homogenate of the *Drosophila* preblastoderm stage embryos was prepared and centrosomes were enriched through sucrose gradients centrifugation, according to Moritz *et al* (1995). Subsequent immunoisolation of centrosomes was performed as described before (Lehmann *et al*, 2005) with the following modification: To improve the isolation efficiency, affinity purified antibodies against the centrosomal protein Cnn were bound to Protein G coupled magnetic beads (Dynal) and then cross-linked in two consecutive steps using dimethyl-pimelidate-dihydrochloride (Sigma).

Calculation of centrosome isolation efficiency

purification step	total protein [mg/ml]	centrosomes/ml	centrosomes/mg total protein
embryo homogenate	140	5 E6	0.03
centrosome-enriched fraction	6	50 E6	8.3
Immunopurified centrosomes	28	500 E6	17.9

Protein concentration of the embryo homogenate (EH) was determined by measuring the absorbance at 280 nm in a spectrophotometer. Protein concentrations of the centrosome enriched fraction (CEF) and the immunopurified fraction (IPC) were calibrated using SDS-PAGE gels, based on comparison to the known concentration of EH. Immunofluorescence microscopy was used to determine the number of centrosomes/ml. Equal volumes of sample from each purification step were centrifuged onto coverslips, labeled with anti-γ-tubulin antibody and centrosomes in ten fields of view (using the 63x PlanApo objective) per sample were quantified using the ImageJ software. The following equation was then used to calculate the concentration of centrosomes during the different purification steps:

$$\text{centrosomes/ml} = \frac{\frac{A^{\text{coverslip}}}{A^{\text{field of view}}} \times \text{average counts per field of view}}{\text{test volume}\,[\text{ml}]}$$

Centrosomes/mg total protein was calculated as a ratio of centrosomes/ml to total protein concentration of the respective sample. N-fold change in this quantity during a purification step should be equal to the n-fold enrichment of centrosomes relative to total protein. Total enrichment during the isolation procedure is found to be at least 600-fold, based on comparison of data for embryo homogenate and the immunopurified fraction. Centrosome enrichment was confirmed using western blot analysis against the centrosomal protein markers, while cytoplasmic actin was strongly reduced (Figure S1).

2. MASS SPECTROMETRY

Chemicals

The peptide calibration standards, angiotensin I and ACTH 18-39 were purchased from Bachem (Heidelberg, Germany). Acetonitrile (HPLC Gradient Grade, Carl Roth GmbH (Karlsruhe, Germany). Trifluoroacetic acid (TFA), tetrahydrofuran (THF), n-octylglucopyranoside (nOGP), α-cyano-4-hydroxycinnamic acid (CHCA), and water used for HPLC solvents and MALDI matrix solutions were purchased from Fluka Chemie (Buchs, Switzerland). Porcine trypsin was purchased from Promega (Mannheim, Germany), dithiothreitol (DTT), iodoacetamide (IAA), from Sigma (Sigma-Aldrich, St. Louis, MO), citric acid and 2,2'-thiodiethanol from Aldrich (Sigma-Aldrich, St. Louis, MO)

In-solution trypsinolysis of protein samples

Samples from the immunopurified centrosomes (3.3 µg) and the control experiment (sample from mock-isolation using pre-immune serum, instead of anti-Cnn antibody, cross-linked to magnetic beads) were subjected to trypsinolysis. Lyophylized samples were dissolved in 10 µl 100 mM NH_4HCO_3, 20 mM n-OGP. For reduction of cysteines, 2 µl of 20 mM DTT were added and samples were incubated at 37°C for 30 min. Cysteine carbamidomethylation was performed by adding 2 µl of 50 mM IAA and incubating the samples at room temperature for 30 min. 26 µl of 100 mM NH_4HCO_3 were added followed by 1 µl of trypsin solution (0.05 µg/µL, in 1 mM HCl) and the samples were incubated at 37°C over night. To terminate trypsinolysis, the samples were acidified by addition of 1 µl 10% TFA (v/v).

SDS-PAGE

Due to the high complexity of the samples, the proteins were separated by SDS-PAGE prior to trypsinolysis. Proteins from the centrosome purification and from the control experiment (using 4 times larger volume to achieve more stringent control conditions) were separated by SDS-PAGE on a 10 cm gel (vertical SDS-PAGE chamber, EMBL workshop, Heidelberg). The proteins were stained with colloidal Coomassie Blue G250 (Serva) and each lane was cut into 25 slices of different width, with smaller sizes at the high MW region (3 mm for the first 10 slices, 4 mm for the next ten slices, and 5 mm for the last 5 slices). Each gel sample was further cut into smaller pieces and washed by incubation with 800 µl 50% ethanol (v/v), 50 mM NH_4HCO_3 (wash solution) for 30 min. The wash solution was removed and the gel samples were dehydrated by incubation with 800 µl ethanol for 5 min. The ethanol was aspirated and the samples were stored at –20°C prior to *in-situ* trypsinolysis.

In-situ trypsinolysis

The samples were prepared as described under section SDS-PAGE. For reduction of cysteine disulfides, 400 µl 10 mM DTT, 50 mM NH_4HCO_3 were added and the samples were incubated for 30 minutes at 37 °C. The supernatants were removed and the samples were dehydrated by incubation with 800 µl ethanol for 5 min, after which the ethanol was removed. For alkylation of cysteines, 400 µl 20 mM IAA, 50 mM NH_4HCO_3 were added and the samples were incubated for 30 min at room temperature in the dark. The supernatants were aspirated and excess IAA was inactivated by incubating the gel samples in 400 µl 20 mM 2,2'-thiodiethanol for 10 min at room temperature. The liquid was removed and the samples washed by incubation with 800 µl wash solution for 5 min. The wash solution was removed and the washing procedure was repeated once followed by incubation with 800 µl ethanol (100%) for 10 minutes. After removing the liquid, the samples were dried in a vacuum centrifuge for 60 min. For trypsinolysis, 20 µl trypsin (2.5 ng/µl in 50 mM NH_4HCO_3, pH 7.8) were added to the dry gel pieces. After 30 min incubation on ice, additional volumes of 50 mM NH_4HCO_3 (pH 7.8), necessary to just cover the gel pieces, were added to the gel followed by incubation over night at 37°C. For peptide extraction, 100 µl of 0.1% TFA, 0.2 mM n-OGP were added and the gel samples were placed on a shaker for 10 min. The supernatants were collected into fresh vials and the extraction procedure was repeated twice using 100 µl 0.1 % TFA, 50 % ACN. The pooled extracts were dried in a vacuum centrifuge and stored at -20°C prior to further analysis.

Nano LC-MALDI MS

Nano LC-MALDI MS was performed as described recently (Mirgorodskaya *et al*, 2005). In brief, peptide samples were analyzed on an 1100 Series Nanoflow LC system (Agilent Technologies). The mobile phases used for the reversed-phase separation were Buffer A: 1% ACN (v/v), 0.05% TFA (v/v) and Buffer B: 90% ACN (v/v), 0.04% TFA (v/v). The samples were first loaded onto a trapping column (ZORBAX 300 SB C18, 0.3 mm $\times$ 5 mm, Agilent Technologies), using Buffer A, delivered by the loading pump with a flow-gradient according to the manufacturer's recommendation. After 5 min, the

trapping column was connected to the nanoflow path and the samples were eluted onto the analytical separation column (ZORBAX 300 SB C18, 75 µm × 150 mm, Agilent Technologies), using a binary pump operated at 300 nl/min. For fractionation, the LC effluent was deposited onto pre-formed microcrystalline layers of CHCA prepared on prestructured MALDI sample supports (AnchorChip 600/384, Bruker Daltonics). The matrix solution was CHCA (100 g/l) in 90% tetrahydrofuran, 0.001% TFA (v/v), 50 mM citric acid, containing the two calibration standards angiotensin I (1 pmol/µl) and ACTH 18-39 (2 pmol/µl). Thin layers of CHCA were prepared by spreading 200 µl of matrix solution over the target surface with a Teflon rod (Mirgorodskaya *et al*, 2005).

Mass analysis of positively charged peptide ions was performed on an Ultraflex II LIFT MALDI-TOF/TOF mass spectrometer (Bruker Daltonics). Positively charged ions in the *m/z* range 500 – 4,500 Da were analyzed automatically in the reflector mode. Sums of 50 single-shot spectra were acquired from 14 different sample spot positions (700 in total from each sample). Fixed laser attenuation was used, the optimal value of which was determined prior to analysis by evaluation of a few fractions. MALDI-TOF/TOF analysis was performed on the Ultraflex II instrument operated in the LIFT mode. MS/MS spectra were acquired automatically with fixed laser attenuation and fixed laser power boost. Up to 15 MS/MS spectra, each consisting of a total sum of 4,100 laser single-shot spectra, were acquired from a single MALDI sample. Additionally, manual spectra acquisition of signals for which parent ion isolation failed in the automatic mode was performed when sample availability permitted.

Data processing

Automatic detection of the peptide monoisotopic signals was performed using the algorithm SNAP, implemented in the FlexAnalysis software (Bruker Daltonics). Internal mass correction was performed using the signals of two peptides (Angiotensin I, MH^+ 1,296.6853 (monoisotopic mass), and ACTH (18-39), MH^+ 2,465.1989) included in the MALDI matrix solution, as reference masses.

Selection of precursor ions was performed based on the entire MS data set using a beta-version of the WARPLC software (collaboration with Bruker Daltonics), with manual corrections when necessary. Protein identification was performed using the Mascot software (Matrixscience), searching the FlyBase sequence database (http://flybase.bio.indiana.edu/). The following settings were used for the searches: mass error tolerance for the precursor ions: 30 ppm; mass error tolerance for the fragment ions: 0.8 Da; fixed modification: carbamidomethylation; variable modification: methionine oxidation; number of missed cleavage sites: 1; type of instrument: MALDI-TOF-PSD.

3. MOLECULAR BIOLOGY

DNA Cloning

For antibody production, Exon 6 of the *cnn* gene was amplified by PCR from genomic DNA of the *Drosophila* W1118 strain. The amplified DNA sequence was first cloned into the entry vector pENTR/D-Topo (Invitrogen) and then recombined with the destination vector pDest 17 (Invitrogen) for His-tagged protein expression.

For localization studies, all genes listed in the following subsection were PCR-amplified using clones from the DGRC collections as templates and attB sites were attached. The attB-flanked PCR products were then recombined with the Gateway donor vector pDONR201 (Invitrogen) or cloned into the entry vector pENTR/D-Topo (Invitrogen) and subsequently shuttled into the EGFP expression vectors pAGW (N-terminal EGFP tag) and pAWG (C-terminal EGFP tag), which were obtained from the DGRC *Drosophila* Gateway vector collection, and into the TAP expression vectors pDEST NTAP (N-terminal TAP tag) and pDEST CTAP (C-terminal TAP tag). A detailed overview of all constructs generated can be found in Table S4.

pDEST-CTAP and pDEST-NTAP vectors were constructed by converting pMK33-NTAP and pMK33-CTAP (Veraksa *et al*, 2005) into Gateway destination vectors. To generate pDEST-CTAP, pMK33-CTAP was linearized with SpeI, 5'overhangs were filled in using Klenow to form blunt ends and the vector was ligated with the blunt-ended Reading Frame Cassette C.1 (Invitrogen). pMK33-NTAP was converted into pDEST-NTAP by linearization with XhoI, 5'overhangs were filled in and the vector was ligated with Reading Frame Cassette B (Invitrogen).

Cloning Primer Pairs

Gene Name	CG-ID	Primer Sequence
cnn	CG4832	5'CACCAGTGACAACGAGGCCAGCTCCCAGG 3'CTACTCTGACTTTGCCTTTGGACTCGCT
spd-2	CG17286	5'CACCGACAGTAGCAGTGGAAGCCAA (N-term.) 3'TTAAAATTTAAAACTAATCGGGACA (N-term.)
		5'CACCATGGACAGTAGCAGTGGAAGC (C-term.) 3'AAATTTAAAACTAATCGGGACACTG (C-term.)
cort	CG11330	5'GGGGACAAGTTTGTACAAAAAAGCAGGCTTCCCTGGCATATGCAGTCCCGT (N-term.) 3'GGGGACCACTTTGTACAAGAAAGCTGGGTCTCACCGTATGCCTTTGTACA (N-term.)
		5'GGGGACAAGTTTGTACAAAAAAGCAGGCTACCATGGGTCCTGGCATATGCAGTCC (C-term.) 3'GGGGACCACTTTGTACAAGAAAGCTGGGTCCCGTATGCCTTTGTACAGGC (C-term.)
CG11148	CG11148	5'GGGGACAAGTTTGTACAAAAAAGCAGGCTTCAGATCGGCGCCTGGTCTGGC (N-term) 3'GGGGACCACTTTGTACAAGAAAGCTGGGTCTTATGGTCCTTCGACGTAGT (N-term)
		5'GGGGACAAGTTTGTACAAAAAAGCAGGCTACCATGGGTAGATCGGCGCCTGGTCTGGC (C-term) 3'GGGGACCACTTTGTACAAGAAAGCTGGGTCTGGTCCTTCGACGTAGTCTC (C-term)
CG1962	CG1962	5'GGGGACAAGTTTGTACAAAAAAGCAGGCTTCGAGGAATCCAATCACGGTTC (N-term) 3'GGGGACCACTTTGTACAAGAAAGCTGGGTCTTACTTTTGACGAAACTGAT (N-term)
		5'GGGGACAAGTTTGTACAAAAAAGCAGGCTACCATGGAGGAATCCAATCACGG (C-term) 3'GGGGACCACTTTGTACAAGAAAGCTGGGTCCTTTTGACGAAACTGATGAT (C-term)
CG3173	CG3173	5'GGGGACAAGTTTGTACAAAAAAGCAGGCTTCGATCGCGGGAAAGGAAGCGG (N-term) 3'GGGGACCACTTTGTACAAGAAAGCTGGGTCTTAATAGCCATGCTGGATCA (N-term)
		5'GGGGACAAGTTTGTACAAAAAAGCAGGCTACCATGGATCGCGGGAAAGGAAGCGG (C-term) 3'GGGGACCACTTTGTACAAGAAAGCTGGGTCATAGCCATGCTGGATCACTA (C-term)
CG6455	CG6455	5'GGGGACAAGTTTGTACAAAAAAGCAGGCTTCTATCGGCTAGCGGTGCGAGA (N-term) 3'GGGGACCACTTTGTACAAGAAAGCTGGGTCCTACAAATACAATAGTCCGC (N-term)
		5'GGGGACAAGTTTGTACAAAAAAGCAGGCTACCATGGGTTATCGGCTAGCGGTGCGAGA (C-term) 3'GGGGACCACTTTGTACAAGAAAGCTGGGTCCAAATACAATAGTCCGCTGG (C-term)
CG6181	CG6181	5'GGGGACAAGTTTGTACAAAAAAGCAGGCTTCTTAATCGCGCTCTTCGCGCT (N-term) 3'GGGGACCACTTTGTACAAGAAAGCTGGGTCTCATTTTAGCTGATCGCGGT(N-term)
		5'GGGGACAAGTTTGTACAAAAAAGCAGGCTACCATGGGTTTAATCGCGCTCTTCGCGCT (C-term) 3'GGGGACCACTTTGTACAAGAAAGCTGGGTCTTTTAGCTGATCGCGGTACG (C-term)
CG7033	CG7033	5'GGGGACAAGTTTGTACAAAAAAGCAGGCTTCGAGATGTCCTTGAATCCCGT (N-term) 3'GGGGACCACTTTGTACAAGAAAGCTGGGTCCTAGCAGTAGCCCCTGTCGG (N-term)
		5'GGGGACAAGTTTGTACAAAAAAGCAGGCTACCATGGAGATGTCCTTGAATCC (C-term) 3'GGGGACCACTTTGTACAAGAAAGCTGGGTCGCAGTAGCCCCTGTCGGGAA (C-term)
CG10732	CG10732	5'GGGGACAAGTTTGTACAAAAAAGCAGGCTTCGCGCCGCCGCCCAAGGTAGT (N-term) 3'GGGGACCACTTTGTACAAGAAAGCTGGGTCCTATTCGAGACTGACGTCCT (N-term)
		5'GGGGACAAGTTTGTACAAAAAAGCAGGCTACCATGGCGCCGCCGCCCAAGGT (C-term) 3'GGGGACCACTTTGTACAAGAAAGCTGGGTCTTCGAGACTGACGTCCTGTT (C-term)
CG11943	CG11943	5'GGGGACAAGTTTGTACAAAAAAGCAGGCTTCGATGTCGACAAGGAGTGCGC (N-term) 3'GGGGACCACTTTGTACAAGAAAGCTGGGTCCTAAAGAGCACCTGCACCAG (N-term)
		5'GGGGACAAGTTTGTACAAAAAAGCAGGCTACCATGGATGTCGACAAGGAGTGCGC (C-term) 3'GGGGACCACTTTGTACAAGAAAGCTGGGTCAAGAGCACCTGCACCAGTTG (C-term)
CG14235	CG14235	5'GGGGACAAGTTTGTACAAAAAAGCAGGCTTCTCGGCGGCCCGCCTGCCCTA (N-term) 3'GGGGACCACTTTGTACAAGAAAGCTGGGTCCTACTTGACCAGCGGCCGCT (N-term)
		5'GGGGACAAGTTTGTACAAAAAAGCAGGCTACCATGGGTTCGGCGGCCCGCCTGCCCTA (C-term) 3'GGGGACCACTTTGTACAAGAAAGCTGGGTCCTTGACCAGCGGCCGCTTGC (C-term)
Actin57B	CG10067	5'GGGGACAAGTTTGTACAAAAAAGCAGGCTTCTGCAAGGCCGGTTTCGCCGG (N-term) 3'GGGGACCACTTTGTACAAGAAAGCTGGGTCTTAGAAGCACTTGCGGTGGA (N-term)
		5'GGGGACAAGTTTGTACAAAAAAGCAGGCTACCATGGGTTGCAAGGCCGGTTTCGCCGG (C-term) 3'GGGGACCACTTTGTACAAGAAAGCTGGGTCGAAGCACTTGCGGTGGACGA (C-term)
alt	CG18212	5'GGGGACAAGTTTGTACAAAAAAGCAGGCTTCGACTTCCACATACTGATCGT (N-term) 3'GGGGACCACTTTGTACAAGAAAGCTGGGTCCTATTCTCCGTTTGAGGCAT (N-term)
		5'GGGGACAAGTTTGTACAAAAAAGCAGGCTACCATGGACTTCCACATACTGAT (C-term) 3'GGGGACCACTTTGTACAAGAAAGCTGGGTCTTCTCCGTTTGAGGCATGCT (C-term)

Cka	CG7392	5'GGGGACAAGTTTGTACAAAAAAGCAGGCTTCGGCACCAATTCGGGAGCCAC (N-term) 3'GGGGACCACTTTGTACAAGAAAGCTGGGTCTTAGACAAAGACCTTGGCGA (N-term)
		5'GGGGACAAGTTTGTACAAAAAAGCAGGCTACCATGGGCACCAATTCGGGAGC (C-term) 3'GGGGACCACTTTGTACAAGAAAGCTGGGTCGACAAAGACCTTGGCGAGGC (C-term)
coro	CG9446	5'GGGGACAAGTTTGTACAAAAAAGCAGGCTTCTCATTTCGCGTAGTGCGCAG (N-term) 3'GGGGACCACTTTGTACAAGAAAGCTGGGTCCTAGTCCTCGTCCTTTGACG (N-term)
		5'GGGGACAAGTTTGTACAAAAAAGCAGGCTACCATGGGTTCATTTCGCGTAGTGCGCAG (C-term) 3'GGGGACCACTTTGTACAAGAAAGCTGGGTCGTCCTCGTCCTTTGACGTTC (C-term)
cort	CG11330	5'GGGGACAAGTTTGTACAAAAAAGCAGGCTTCCCTGGCATATGCAGTCCCGT (N-term) 3'GGGGACCACTTTGTACAAGAAAGCTGGGTCTCACCGTATGCCTTTGTACA (N-term)
		5'GGGGACAAGTTTGTACAAAAAAGCAGGCTACCATGGGTCCTGGCATATGCAGTCC (C-term) 3'GGGGACCACTTTGTACAAGAAAGCTGGGTCCCGTATGCCTTTGTACAGGC (C-term)
crn	CG3193	5'GGGGACAAGTTTGTACAAAAAAGCAGGCTTCGAGCGGCCACAGAAGATGCC (N-term) 3'GGGGACCACTTTGTACAAGAAAGCTGGGTCTCAGTCACCGCTATCCGTCG (N-term)
		5'GGGGACAAGTTTGTACAAAAAAGCAGGCTACCATGGAGCGGCCACAGAAGAT (C-term) 3'GGGGACCACTTTGTACAAGAAAGCTGGGTCGTCACCGCTATCCGTCGTAT (C-term)
Grip84	CG3917	5'CACCAGTAAACCCCATGCGCTGCGCGGTG (N-term) 3'TTAGCCAATGGCATCCTCTACACAC (N-term)
		5'GGGGACAAGTTTGTACAAAAAAGCAGGCTACCATGGGTTACGCACTGCTGGTGTT (C-term) 3'GGGGACCACTTTGTACAAGAAAGCTGGGTCGCCAATGGCATCCTCTACAC (C-term)
Grip91	CG10988	5'GGGGACAAGTTTGTACAAAAAAGCAGGCTTCTCGCAGGACAGGATCGCCGG (N-term) 3'GGGGACCACTTTGTACAAGAAAGCTGGGTCCTATTCCTGAGTGGACGGCG (N-term)
		5'GGGGACAAGTTTGTACAAAAAAGCAGGCTACCATGGGTTCGCAGGACAGGATCGC (C-term) 3'GGGGACCACTTTGTACAAGAAAGCTGGGTCTTCCTGAGTGGACGGCGTAC (C-term)
Hsc70CB	CG6603	5'GGGGACAAGTTTGTACAAAAAAGCAGGCTTCTCCGTGATTGGCATCGATTT (N-term) 3'GGGGACCACTTTGTACAAGAAAGCTGGGTCTCACTCCACTTCCATGGAGG (N-term)
		5'GGGGACAAGTTTGTACAAAAAAGCAGGCTACCATGGGTTCCGTGATTGGCATCGATTT (C-term) 3'GGGGACCACTTTGTACAAGAAAGCTGGGTCCTCCACTTCCATGGAGGGAT (C-term)
Lam	CG6944	5'GGGGACAAGTTTGTACAAAAAAGCAGGCTTCTCGAGCAAATCCCGACGTGC (N-term) 3'GGGGACCACTTTGTACAAGAAAGCTGGGTCTTACATAATGGCGCACTTCT (N-term)
		5'GGGGACAAGTTTGTACAAAAAAGCAGGCTACCATGGGTTCGAGCAAATCCCGACGTGC (C-term) 3'GGGGACCACTTTGTACAAGAAAGCTGGGTCCATAATGGCGCACTTCTCGT (C-term)
lat	CG4088	5'GGGGACAAGTTTGTACAAAAAAGCAGGCTTCGATCCCACCATTTCAGTGTC (N-term) 3'GGGGACCACTTTGTACAAGAAAGCTGGGTCCTACCAGGTTAATCGAGTGG (N-term)
		5'GGGGACAAGTTTGTACAAAAAAGCAGGCTACCATGGATCCCACCATTTCAGT (C-term) 3'GGGGACCACTTTGTACAAGAAAGCTGGGTCCCAGGTTAATCGAGTGGCAT (C-term)
Nat1	CG12202	5'GGGGACAAGTTTGTACAAAAAAGCAGGCTTCCCTTCTAGCGATCCCCTGCC (N-term) 3'GGGGACCACTTTGTACAAGAAAGCTGGGTCCTAAGACGCTGCCGCTGCCG (N-term)
		5'GGGGACAAGTTTGTACAAAAAAGCAGGCTACCATGGGTCCTTCTAGCGATCCCCTGCC(C-term) 3'GGGGACCACTTTGTACAAGAAAGCTGGGTCAGACGCTGCCGCTGCCGTGG (C-term)
Rae1	CG9862	5'GGGGACAAGTTTGTACAAAAAAGCAGGCTTCTTTGGCGCCACACAATCGAC (N-term) 3'GGGGACCACTTTGTACAAGAAAGCTGGGTCTCAGTTAATGCGCGGCTTGA (N-term)
		5'GGGGACAAGTTTGTACAAAAAAGCAGGCTACCATGGGTTTTGGCGCCACACAATCGAC (C-term) 3'GGGGACCACTTTGTACAAGAAAGCTGGGTCGTTAATGCGCGGCTTGAGCT (C-term)
scra	CG2092	5'GGGGACAAGTTTGTACAAAAAAGCAGGCTTCGACCCGTTTACTCAGCACAT (N-term) 3'GGGGACCACTTTGTACAAGAAAGCTGGGTCTCAGTGGGTGGTTCCCCAGG (N-term)
		5'GGGGACAAGTTTGTACAAAAAAGCAGGCTACCATGGACCCGTTTACTCAGCACAT (C-term) 3'GGGGACCACTTTGTACAAGAAAGCTGGGTCGTGGGTGGTTCCCCAGGCGC (C-term)
Sop2	CG8978	5'GGGGACAAGTTTGTACAAAAAAGCAGGCTTCGCCGAGACATACACCTTTGG (N-term) 3'GGGGACCACTTTGTACAAGAAAGCTGGGTCCTAGATCTGCAGGTTGCGCA (N-term)
		5'GGGGACAAGTTTGTACAAAAAAGCAGGCTACCATGGCCGAGACATACACCTTTGG (C-term) 3'GGGGACCACTTTGTACAAGAAAGCTGGGTCGATCTGCAGGTTGCGCATGC (C-term)
TFAM	CG4217	5'GGGGACAAGTTTGTACAAAAAAGCAGGCTTCATCTACACCACAACACTGAT (N-term) 3'GGGGACCACTTTGTACAAGAAAGCTGGGTCCTATATATCTTTGGAGGCCA (N-term)
		5'GGGGACAAGTTTGTACAAAAAAGCAGGCTACCATGGGTATCTACACCACAACACTGAT (C-term) 3'GGGGACCACTTTGTACAAGAAAGCTGGGTCTATATCTTTGGAGGCCAGCG (C-term)
fs(1)N		5'GGGGACAAGTTTGTACAAAAAAGCAGGCTTCCTAATTTGGCACCTGCTGCT (N-term)

	CG11411	3'GGGGACCACTTTGTACAAGAAAGCTGGGTCTCATGGGCACTGGAGCCACG (N-term)
		5'GGGGACAAGTTTGTACAAAAAAGCAGGCTACCATGGGTCTAATTTGGCACCTGCTGCT (C-term) 3'GGGGACCACTTTGTACAAGAAAGCTGGGTCTCATGGGCACTGGAGCCACG (C-term)
CG6906	CG6905	5'CACCCCGCGAATAATGATCAAGGGC (N-term) 3'TTACGCTTCCTGGTCGGGCAGGAGT (N-term)
		5'CACCATGCCGCGAATAATGATCAAG (C-term) 3'CGCTTCCTGGTCGGGCAGGAGTTGC (C-term)
cup	CG11181	5'CACCGACCCTATGAAAGAGGAGGCG (N-term) 3' TTAATGAAACTCATCCCCGCTGTTG (N-term)
		5' CACCATGGACCCTATGAAAGAGGAG (C-term) 3' ATGAAACTCATCCCCGCTGTTGGGC (C-term)
feo	CG11207	5'CACCAACTCGCCGAGCGCCATTGCG (N-term) 3'CTAGAACTGTCTGCGCGGCTGCACG (N-term)
		5'CACCATGAACTCGCCGAGCGCCATT (C-term) 3'GAACTGTCTGCGCGGCTGCACGATC (C-term)
gamma23C	CG3157	5' CACCCCAAGTGAAATAATTACTTTG (N-term) 3' CTAGGAACCGGCGCTGGTCACAGAT (N-term)
		5' CACCATGGGTCCAAGTGAAATAATTACT(C-term) 3' GGAACCGGCGCTGGTCACAGATCGA (C-term)
Nup153	CG4453	5'CACCGAGGATGCACAGGAGCAAAGG (N-term) 3'CTACCGGGGCGGCAAACGGCGTACG (N-term
		5'CACCATGGAGGATGCACAGGAGCAA (C-term) 3'CCGGGGCGGCAAACGGCGTACGGGG (C-term)
Rpl17	CG3203	5' CACCGGCCGTTACTCACGCGAGTCA (N-term) 3' TTATTCAGAACGCAACATCTTCTCC (N-term)
		5' CACCATGGGCCGTTACTCACGCGA (C-term) 3' TTCAGAACGCAACATCTTCTCCTTT (C-term)
Rpl24	CG9282	5' CACCAAAATTGGCTTGTGCGCATTC (N-term) 3' TTACCGCTTGCCTCCGACGCGGGGA (N-term)
		5'CACCATGGGTAAAATTGGCTTGTGCGCA (C-term) 3' CCGCTTGCCTCCGACGCGGGGAGCA (C-term
RPS17	CG3922	5' CACCGGTCGCGTACGAACCAAGACG (N-term) 3' TTAGTTGCGACGACCAAAGTTGTTG (N-term)
		5' CACCATGGGTCGCGTACGAACCAAG (C-term) 3' GTTGCGACGACCAAAGTTGTTGGTG (C-term)

Synthetic clone

The Gateway compatible entry clone for the gene eIF-4a, with and without stop codon, in pDONR221, was generated by the company Geneart.

Generation of SL2 cell lines stably expressing centrosomal proteins

The EGFP Gateway vectors carrying the target genes were stably co-transfected with the pCoBlast vector (Invitrogen, carrying a Blasticidin resistance marker) in *Drosophila* SL2 cells by calcium phosphate transfection (Invitrogen) for 24 h using $3x10^6$ cells per well in a 6-well plate. Selection for the plasmid resistance marker was started five days after transfection with 75 µg/ml Blasticidin. After two weeks, resistant cells were maintained in medium containing 10 µg/ml Blasticidin.

Production of double-stranded RNA (dsRNA)

Long dsRNA for the *Drosophila* RNAi experiments were generated by using ~500bp long PCR fragments from a genome-covering *Drosophila* library as templates (Hild *et al*, 2003). The amplicons contain T7 promoter sites flanked by unique tag sequences and are amplified using tag-specific primers (Boutros *et al*, 2004). The resulting T7-PCR fragments are used as templates for in vitro transcription reactions, followed by DNaseI digestion and ethanol precipitation to purify the RNA (Boutros *et al*, 2004). Primer and amplicon sequence information are shown in Table S2 and are available from http://rnai.dkfz.de/.

4. RNA INTERFERENCE

SL2 cells were cultured in „Schneider's *Drosophila* Medium" (Invitrogen) with 10% FBS (Foetal bovine serum, Invitrogen) at 25°C. DsRNA treatment of cells was performed essentially according to Clemens *et al* (2000). Differing from this protocol, $1x10^6$ cells were incubated with 10 µg dsRNA for 1 h at 25°C. After 72 h a second dsRNA treatment was carried out to ensure maximum depletion of proteins. The cells were analyzed via immunofluorescence microscopy and FACS.

HaCaT cells (CLS) were cultured in DMEM (Biowest) supplemented with 10% FBS (Biowest) and 2 mM glutamine (Biowest) at 37°C in 5% CO_2. Transfection complexes were formed in 96-well microscopy plates (BD Falcon) by incubating 10 µl siRNA duplexes (500 nM siRNA pool, each pool contains 4 independent oligos targeting the same gene transcript, the sequences are listed in Table S2) with 10 µl of 1.25 % Interferin (Polyplus Transfection) in OptiMEM (Invitrogen), for 15 minutes at room temperature. As negative control, a pool of non-targeting siRNAs was used (see Table S2), in 4 replicate wells per plate. 4500 cells per well in a total volume of 180 µl growth medium were added onto the transfection complexes using an automatic dispenser (Biotek) and incubated for 72 hr at 37°C.

U2OS cells were cultured in DMEM (Invitrogen) with 10% FBS (Invitrogen) and 2mM L-glutamine at 37°C in 5% CO_2. For reverse siRNA transfection 8 µl siRNA (500nM stock; Pool of 4; Dharmacon) were spotted in each well of a 96-well glass bottom sensoplate (Greiner). DharmaFECT transfection reagent (0.2 µl/well) was prediluted in 19.8 µl/well RPMI (Invitrogen), after 10 min incubation at room temperature further diluted with 40 µl/well RPMI, added to siRNA and incubated for 30 min. 10000 cells in 130 µl DMEM were added to each well and incubated for 72 h.

Off-target effect control

We investigated potential off-target effects both by bioinformatics analysis and by carrying out a second round of independent RNAi experiments for selected functionally important targets. Using the E-RNAi database http://www.dkfz.de/signaling2/e-rnai/ we calculated gene specificity, transcript specificity and RNAi efficiency for all target genes listed in Table S2. In addition we carried out a second round of RNAi experiments with an independent set of dsRNA non-overlapping with the original dsRNA chosen. The dsRNA were selected in the E-RNAi database that had both the least predicted off-target effects and the highest target efficiency. We positively confirmed the phenotypes of 11/13 selected functionally important proteins (Table S2).

5. PHENOTYPE ANALYSIS and DATA EVALUATION

Details of the cellular processes scored, following immunofluorescence labeling of the cells, are presented in the following sections. Phenotypic scoring was carried out either by visual inspection of the samples at a Zeiss Imager Z1 or LSM 510 Meta microscope (SL2 and U2OS cells), or by the analysis of images acquired with an ArrayScan VTI microscope (Cellomics), using algorithms designed with the associated vHCS software (HaCaT cells). Images of SL2 or U2OS cells were acquired using a Zeiss MRM CCD camera or a Photometrics Coolsnap HQ slow scan CCD camera and Axiovision image acquisition software.

The values listed in Table S2 represent the *p*-values and/or average distances in fold standard deviation of the controls (z-scores), determined as described in the following sections.

Antibodies

His-tagged fusion protein corresponding to *cnn* exon 6 was used to raise and affinity purify rat and rabbit polyclonal antibodies (Pineda). Anti-peptide antibodies in rabbits were custom-made and affinity purified (Eurogentec) against the following peptides:

Gene Name	Peptide Antigen
Cp309	**C+2447-246**: C+KSPGDSPRKSPRADF- CONH2 (15 AA) **C+1014-1028:** C+KFYERQQGDDDYKPA- CONH2 (15 AA)
CG11148	**52-66:** H2N-RNLFPEYRYGREEML-CONH2 (15 AA) **1564-1579:** H2N-AEGRINVGIRDYVEGP-CONH2 (16 AA)
Nat1	**626-641:** H2N-HQKSKQQANQETDPDC-CONH2 (16 AA) **283-298:** H2N-FQEQYPRALCPRRLPL-CONH2 (16 AA)
CG7033	**221-234:** H2N-DKKPGVHQPQRIEN-CONH2 (16 AA) **149-162:** H2N-SSSDEKFRNDLLNI-CONH2 (16 AA)
CG1962	**93-108:** H2N-N+QRLNLEKNRDKKQIKTLC-CONH2 (19 AA) **783-786:** H2N-CQHN+GANIRKSHHHQFRQK-COOH (19 AA)
spd-2	**518-532:** H2N-C+VKEPSRRVRRTKISP-CONH2 (16 AA) **1112-1127:** H2N-VRLLRSPRQDLLEREP-CONH2 (16 AA)

For western blotting and immunofluorescence labeling, the following antibodies were used: mouse monoclonal anti-γ-tubulin (clone GTU-88) (Sigma), rabbit polyclonal anti-γ-tubulin (Sigma), rabbit polyclonal anti-Grip84, rat monoclonal anti-Actin (Babraham), rabbit polyclonal anti-phosphorylated (S10) histone H3 (Upstate), mouse monoclonal anti-phosphorylated (S10) histone H3 (Abcam). Primary antibodies were detected with the secondary antibodies Alexa Fluor 488-conjugated anti-mouse and anti-rabbit, Alexa Fluor 546-conjugated anti-mouse and Alexa Fluor 594-conjugated anti-rabbit (all purchased from Invitrogen), plus FITC-conjugated anti-rat (Jackson ImmunoResearch).

Immunofluorescence microscopy

SL2 cells were settled on Concanavalin A (Sigma) coated coverslips (Rogers *et al*, 2002), and fixed with 4% para-formaldehyde (Applichem) for 20 min at room temperature followed by methanol for 1h at -20°C. Centrosomes were visualized with the mouse monoclonal anti-γ-tubulin GTU-88 (Sigma) or rat Cnn (custom-made, Pineda) antibody. Centrioles were visualized with the custom-made rabbit polyclonal anti-Cp309 antibody. Mitotic chromosomes were labeled with a rabbit anti-phosphorylated (S10) histone H3 antibody (Upstate) and DNA was labeled with diamidino-2-phenylindoldihydrochloride (DAPI) (Applichem).

U2OS cells in 96-well glass bottom plates were processed as described above for SL2 cells. They were labeled with the mouse monoclonal anti-γ-tubulin antibody GTU-88 (Sigma), the rabbit anti-phosphorylated (S10) histone H3 antibody (Upstate) and DAPI (Applichem).

HaCaT cells were fixed with 3% para-formaldehyde (Applichem) in PBS for 3 min at room temperature followed by methanol for at least 20 minutes at -20°C. Centrosomes and mitotic chromosomes were labeled using a rabbit-anti-γ-tubulin antibody (Sigma) and a mouse anti-phosphorylated (S10) histone H3 antibody (Abcam), respectively. For DNA and whole cell labeling, diamidino-2-phenylindoldihydrochloride (DAPI) (Applichem) and whole cell stain red (Perbio) were used.

The preparation of figures, image processing and annotation was done using the ImageJ, Adobe Photoshop and Adobe Illustrator software.

Mitotic index

The mitotic index was determined as the ratio of phosphorylated histone H3 positive cells to total cell number. The percentage of mitotic cells was determined using the image processing software ImageJ (http://rsb.info.nih.gov/ij/) and custom-made macros available for downloading from our webpage: http://www.molgen.mpg.de/~ag_lange/links.html. An average of n=2000 cells per knock-down and experiment was analyzed. The evaluation of significant deviation of the mitotic index was done in the following way: the arithmetic mean of mitotic indices of all control samples were subtracted from the arithmetic mean of mitotic index of each sample. An arithmetic mean whose standard deviation was out of the range of two times the standard deviation of the control was considered statistically significant.

HaCaT cells were processed and labeled as described in the *Immunofluorescence microscopy* section. Automated identification of single cells and segmentation of cell clumps was based solely on whole cell labeling, in order to avoid artifacts caused by excessive segmentation of cells containing more than one nucleus. An average of n=29000 cells per knock-down and experiment were analyzed. Phenotypes were considered to be statistically significant when a z-score ≥ 3 was obtained in both independent experiments and when, in addition, the average z-score was ≥ 6.

Flow cytometry

SL2 cells were fixed in ice-cold 70% ethanol overnight and stained with propidium iodide staining solution [50 µg/ml pancreatic RNaseA (Sigma) and 50 µg/ml propidium iodide (Calbiochem) in PBS] for 1.5 h at 37°C. The DNA content of an average n=35000 cells per knock-down and experiment was quantified on a flow cytometer (BD FACSArray Bioanalyzer System, BD Biosciences) and analyzed using FlowJo software (Tree star). The cell populations were gated and quantified within the different cell cycle phases. The average of two replicates was calculated and the z-scores were assessed for each sample. The z-score signifies the number of standard deviation a specific phase in the cell cycle differs from the mean of the EGFP controls. Specifically, z-scores represent the ratio of the sample value minus the mean of the control divided by the standard deviation of the control.

Centrosome number and centrosome morphology analysis

The analysis was performed in SL2, HaCaT and U2OS mitotic cells, which were processed and labeled as described in the *Immunofluorescence microscopy* section.

Phenotypic scoring was carried out by visual inspection of the SL2 and U2OS cell samples; on average n=100 mitotic cells per knock-down and experiment were analyzed. In the case of HaCaT cells, centrosomes were identified using a filtering method that specifically detects fluorescent foci of a radius typical for mitotic HaCaT centrosomes (~1.6µm). This method strongly reduces the identification of labeling artifacts and allows the exclusion of the mitotic spindle (which is also γ-tubulin positive) from the selection. In order to accurately measure the fluorescence intensity of γ-tubulin labeling at the centrosome, the determined values were corrected for the intensity of cytoplasmic (soluble) γ-tubulin labeling. For each mitotic cell, the centrosome number per cell as well as the area per centrosome in pixels and the total fluorescence intensity of γ-tubulin labeling per centrosome were determined. An average of n=550 mitotic cells per knock-down and experiment was analyzed. A z-score of 3 was used as the significance threshold.

For the analysis of centrosome number, each mitotic cell was assigned to one of the categories: 0, 1, 2, 3, >3 centrosomes/cell. The resulting distributions of the two independent experiments were averaged and compared to the average distribution of the negative controls by means of a non-parametric two-tailed chi square test. A significant deviation from the control distribution was assigned for significance levels $p<0.0001$ (list of p-values in Table S2). For the knockdowns thus determined to cause significant effects on centrosome number, the phenotype was identified as the category that showed >2-fold increase compared to the negative control. If this threshold was exceeded for two or more categories, a mixed phenotype was assigned, unless one of these categories was >2 fold the abundance of the second highest.

Phenotypic scoring parameters

The accuracy of our phenotypic scoring (parameters summarized in the table below) was confirmed by validating previously known centrosome related function of centrosomal proteins: Examples are Grip75 (Vérollet *et al*, 2006), Grip84, Grip91 (Barbosa *et al*, 2003) and Cnn (Megraw *et al*, 1999), whose depletion resulted in a phenotype of single or no centrosomes. RNAi of Asp (do Carmo Avides and Glover, 1999), Ncd (Endow *et al*, 1994) and Aur (Giet *et al*, 2002) also confirmed the known morphological phenotype classes for structure and segregation.

SL2 and U2OS cells		HaCaT cells	
centrosome structure parameters	**centrosome duplication/segregation parameters**	**centrosome structure parameters**	**centrosome duplication/segregation parameters**
0 centrosomes	3 centrosomes	0 centrosomes	3 centrosomes
small centrosomes	>3 centrosomes	area reduction	>3 centrosomes
fuzzy centrosomes	1 centrosome	intensity reduction	1 centrosome
	large centrosomes	area increase & intensity reduction/no change	area increase
		intensity reduction & area increase/no change	intensity increase

Cell cycle analysis

The analysis was performed in HaCaT cells processed and labeled as described in the section *Immunofluorescence microscopy*. The cell cycle distribution was calculated based on DNA content measurements as follows: the fluorescence intensity of DAPI-labeling was integrated over the area of the nucleus/chromatin ("total nuclear DAPI fluorescence intensity") for each cell. For each 96-well plate, an average distribution of the total nuclear DAPI fluorescence intensity was calculated from the measurements of negative control wells. The intensity value corresponding to the highest peak of this "control" distribution was defined as G1/G0-peak intensity (IG1/G0) for this plate. The bins corresponding to G1/G0-phase and G2/M-phase were defined as [IG1/G0 ± 0.25 * IG1/G0] and [2 * IG1/G0 ± 0.25 * IG1/G0], respectively. Intensity values below, in-between or above these bins, respectively, were defined as sub-G1, S-phase and over G2. In order to correctly determine the DNA content of multinucleated cells, touching nuclei were not segmented but identified as a single nucleus.

An average of n=29000 cells per knockdown and experiment were analyzed. Phenotypes were considered to be statistically significant when a z-score $\geq$3 was obtained in both independent experiments and when, in addition, the average z-score was $\geq$6. This relatively high significance threshold, of 6 times the standard deviation of the negative controls, was chosen due to the fact that the position of the G1/G0-peak for some knockdowns was slightly shifted compared to the average distribution of the on-plate negative controls, used to define the bins for all cell cycle phases. Similar observations have been reported previously (Kittler *et al*, 2007).

Drug treatment

SL2 cells with a starting concentration of $1*10^6$ cells/ml were treated with 0.001, 0.1, 1, 10 and 100 ng/ml Cycloheximide (CHX) each 24 h for a period of 72 h. To determine the CHX concentration at which cells are viable for 72 h and show an effect of inhibited translation, growth curves and mitotic indices were calculated.

SL2 cells were treated with Aphidicolin at 0,01 ng/ml, 0,001 µg/ml 0,1 µg/ml and 10 µg/ml for 72h to block DNA replication. The effect of the different drug concentrations on cell growth was monitored through growth curves with only 10 µg/ml affecting the cells. This concentration was then selected for treatment and subsequent phenotypic characterization. For both drug treatments the subsequent phenotypic analysis was carried out as described for RNAi-treated cells. SL2 cells were treated for 4h with 35 µM Taxol to induce microtubule bundling in mitotic cells. Negative control cells were incubated with equal amounts of DMSO as in the Taxol and Aphidicolin samples.

Supplementary References

D'Avino PP, Archambault V, Przewloka MR, Zhang W, Lilley KS, Laue E, Glover DM (2007) Recruitment of Polo kinase to the spindle midzone during cytokinesis requires the Feo/Klp3A complex. *PLoS One* **2**: e572

Barbosa V, Gatt M, Rebollo E, Gonzales C, Glover DM (2003) Drosophila dd4 mutants reveal that gamma-TuRC is required to maintain juxtaposed half spindles in spermatocytes. *J Cell Sci* **116**: 929-941

Bettencourt-Dias M, Giet R, Sinka R, Mazumdar A, Lock WG, Balloux F, Zafiropoulos PJ, Yamaguchi S, Winter S, Carthew RW, Cooper M, Jones D, Frenz L, Glover DM (2004) Genome-wide survey of protein kinases required for cell cycle progression. *Nature* **432**: 980-987

Bjoerklund M, Taipale M, Varjosalo M, Saharinen J, Lahdenperä J, Taipale J 2005 Identification of pathways regulating cell size and cell-cycle progression by RNAi. *Nature* **439**: 1009-1013

Bonte E, Becker PB (1999) Preparation of chromatin assembly extracts from preblastoderm *Drosophila* embryos. *Methods Mol Biol* **119**: 187-194

Boutros M, Kiger AA, Armknecht S, Kerr K, Hild M, Koch B, Haas SA, Paro R, Perrimon N, Heidelberg Fly Array Consortium (2004) Genome-wide RNAi analysis of growth and viability in Drosophila cells. *Science* **303**: 832

Clemens JC, Worby CA, Simonson-Leff N, Muda M, Maehama T, Hemmings BA, Dixon JE (2000) Use of double-stranded RNA interference in Drosophila cell lines to dissect signal transduction pathways. *Proc Natl Acad Sci USA* **97**: 6499-6503

do Carmo Avides M, Glover DM (1999) Abnormal spindle protein, Asp, and the integrity of mitotic centrosomal microtubule organizing centers. *Science* **283**: 1733-1735

Endow SA, Chandra R, Komma DJ, Yamamoto AH, Salmon ED (1994) Mutants of the Drosophila ncd microtubule motor protein cause centrosomal and spindle pole defects in mitosis. *J Cell Sci* **107**: 859-867

Giet R, McLean D, Descamps S, Lee MJ, Raff JW, Prigent C, Glover DM (2002) Drosophila Aurora A kinase is required to localize D-TACC to centrosomes and to regulate astral microtubules. *J Cell Biol* **156**: 437-451

Goshima G, Wollman R, Goodwin SS, Zhang N, Scholey JM, Vale RD, Stuurman N (2007) Genes required for mitotic spindle assembly in Drosophila S2 cells. *Science* **316**: 417-421

Hild M, Beckmann B, Haas SA, Koch B, Solovyev V, Busold C, Fellenberg K, Boutros M, Vingron M, Sauer F, Hoheisel JD, Paro R (2003) An integrated gene annotation and transcriptional profiling approach towards the full gene content of the Drosophila genome. *Genome Biol* **5**: R3

Kao LR, Megraw TL (2009) Centrocortin cooperates with centrosomin to organize Drosophila embryonic cleavage furrows. *Curr Biol* **19**: 937-942

Kittler R, Pelletier L, Heninger AK, Slabicki M, Theis M, Miroslaw L, Poser I, Lawo S, Grabner H, Kozak K, Wagner J, SurendranathV, Richter C, Bowen W, Jackson AL, Habermann B, Hyman AA, Buchholz F (2007) Genome-scale RNAi profiling of cell division in human tissue culture cells. *Nat Cell Biol* **9**: 1401-12

Lehmann V, Müller H, Lange BMH (2005) Immunoisolation of centrosomes from Drosophila melanogaster. *Curr Protoc Cell Biol* Supplement **29**: 3.17.1-3.17.13

Megraw TL, Li K, Kao LR, Kaufman TC (1999) The centrosomin protein is required for centrosome assembly and function during cleavage in Drosophila. *Development* **126**: 2829-2839

Mukherji M, Bell R, Supekova L, Wang Y, Orth AP, Batalov S, Miraglia L, Huesken D, Lange J, Martin C, Sahasrabudhe S, Reinhardt M, Natt F, Hall J, Mickanin C, Labow M, Chanda SK, Cho CY, Schultz PG (2006) Genome-wide functional analysis of human cell-cycle regulators. *Proc Natl Acad Sci USA* **103**: 14819-14824

Mirgorodskaya E, Braeuer C, Fucini P, Lehrach H, Gobom J (2005) Nanoflow liquid chromatography coupled to matrix-assisted laser desorption/ionization mass spectrometry: Sample preparation, data analysis, and application to the analysis of complex peptide mixtures. *Proteomics* **5**: 399-408

Moritz M, Braunfeld MB, Fung JC, Sedat JW, Alberts BM, Agard DA (1995) Three-dimensional structural characterization of centrosomes from early Drosophila embryos. *J Cell Biol* **130**: 1149-1159

Rines DR, Gomez-Ferreria MA, Zhou Y, DeJesus P, Grob S, Batalov S, Labow M, Huesken D, Mickanin C, Hall J, Reinhardt M, Natt F, Lange J, Sharp DJ, Chanda SK, Caldwell JS (2008) Whole genome functional analysis identifies novel components required for mitotic spindle integrity in human cells. *Genome Biol* **9**: R44

Rogers SL, Rogers GC, Sharp DJ, Vale RD (2002) Drosophila EB1 is important for proper assembly, dynamics, and positioning of the mitotic spindle. *J Cell Biol* **158**: 873-884

Sambrook J, Russell DW (2001) *Molecular Cloning: A Laboratory Manual.* (Cold Spring Harbor Laboratory Press, Cold Spring Harbor)

Veraksa A, Bauer A, Artavanis-Tsakonas S (2005) Analyzing protein complexes in Drosophila with tandem affinity purification-mass spectrometry. *Dev Dyn* **232**: 827-34

Vernì F, Somma MP, Gunsalus KC, Bonaccorsi S, Belloni G, Goldberg ML, Gatti M (2004) Feo, the Drosophila homolog of PRC1, is required for central-spindle formation and cytokinesis. *Curr Biol* **14**: 1569-75

Vérollet C, Colombié N, Daubon T, Bourbon HM, Wright M, Raynaud-Messina B (2006) Drosophila melanogaster gamma-TuRC is dispensable for targeting gamma-tubulin to the centrosome and microtubule nucleation. *J Cell Biol* **172**: 517-528

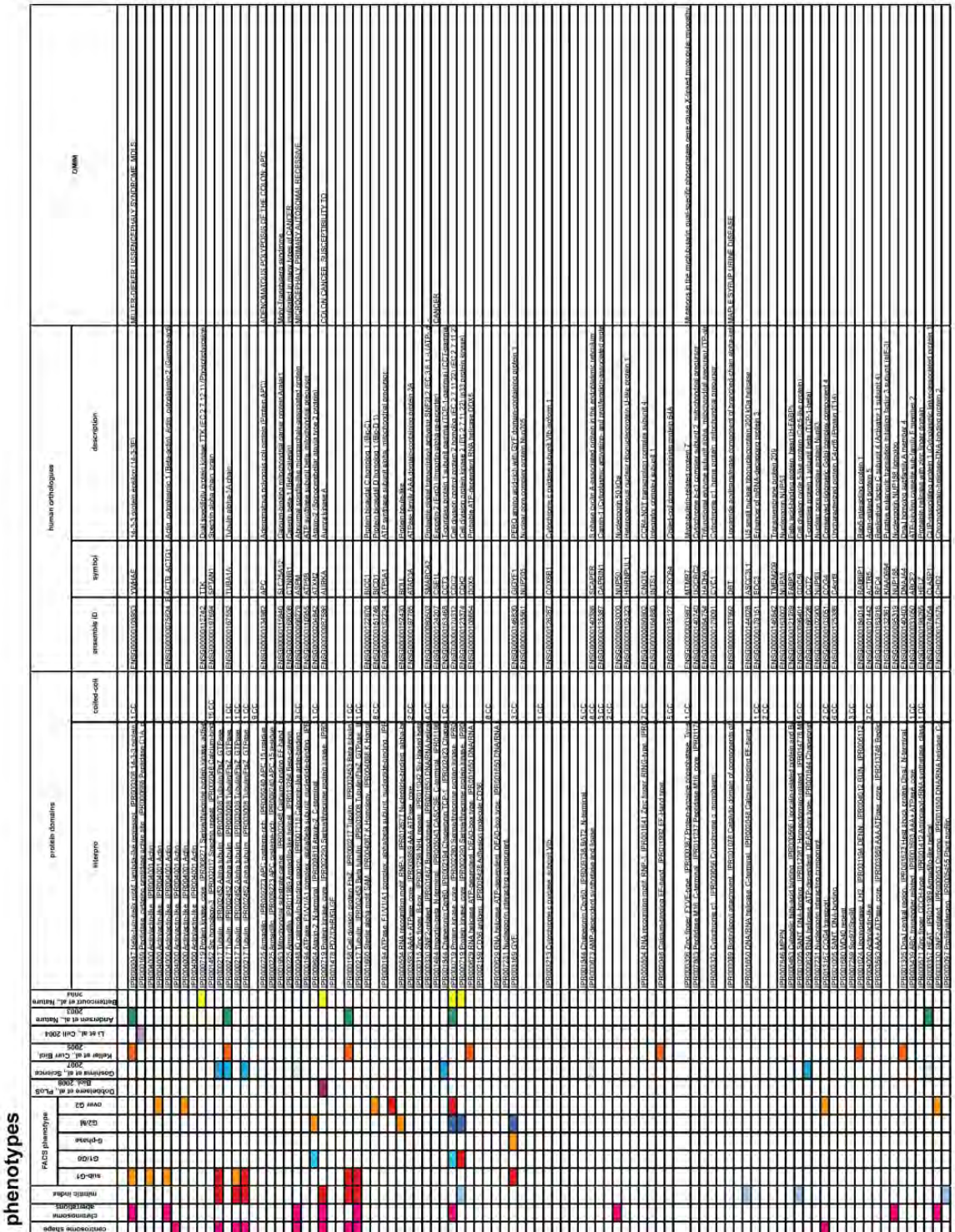
Supplemental Table 1 - SL2 cell phenotypes

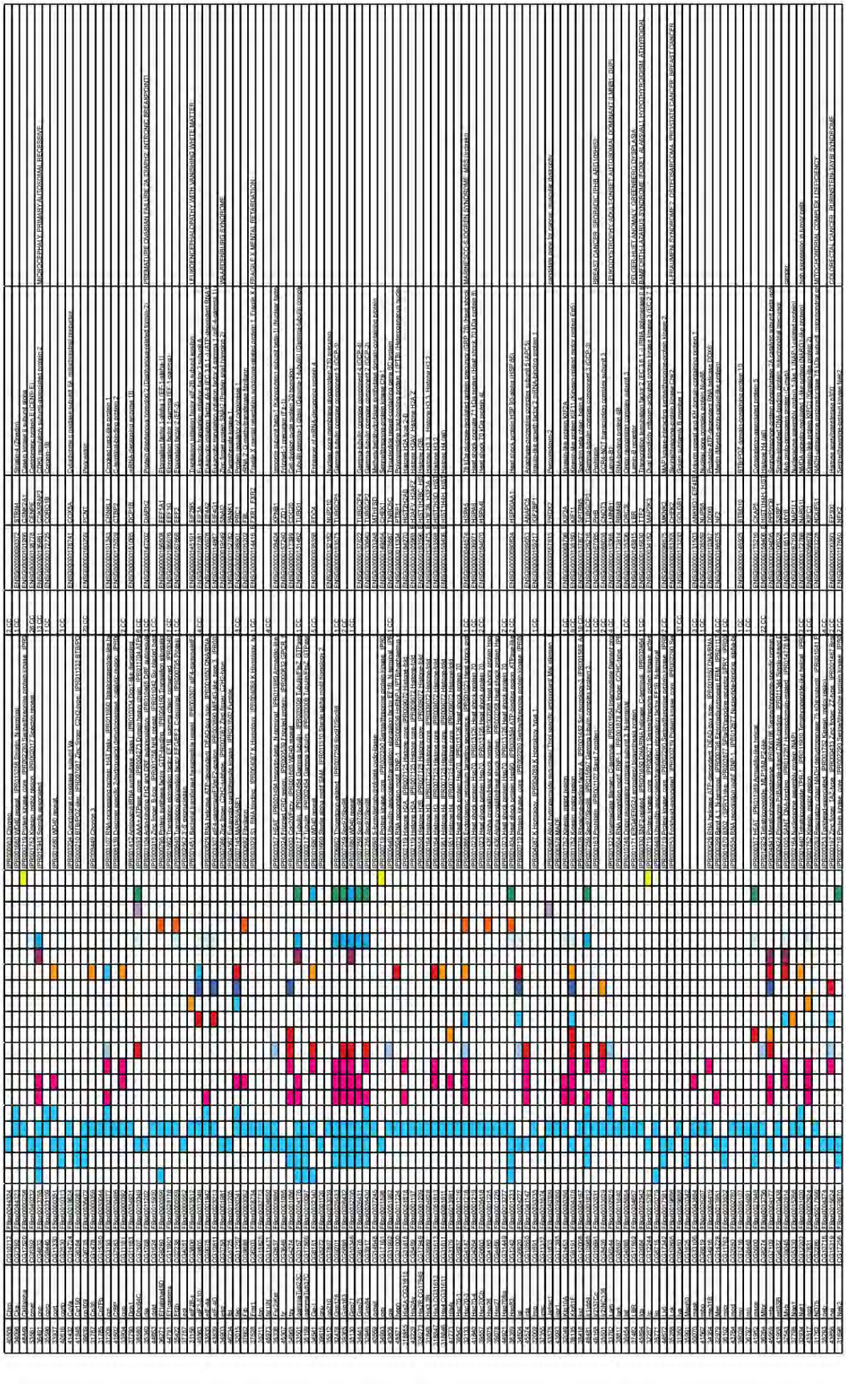

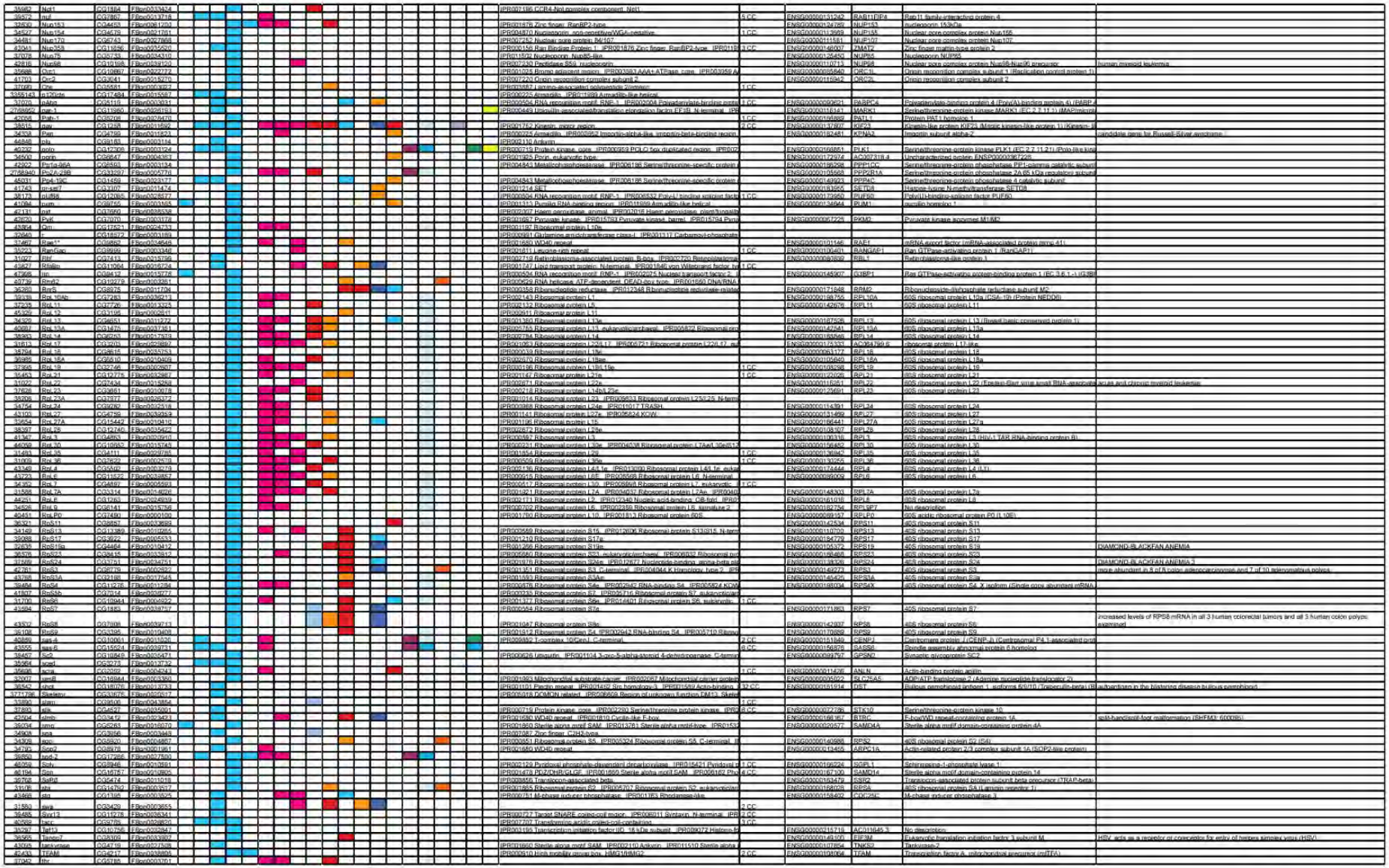

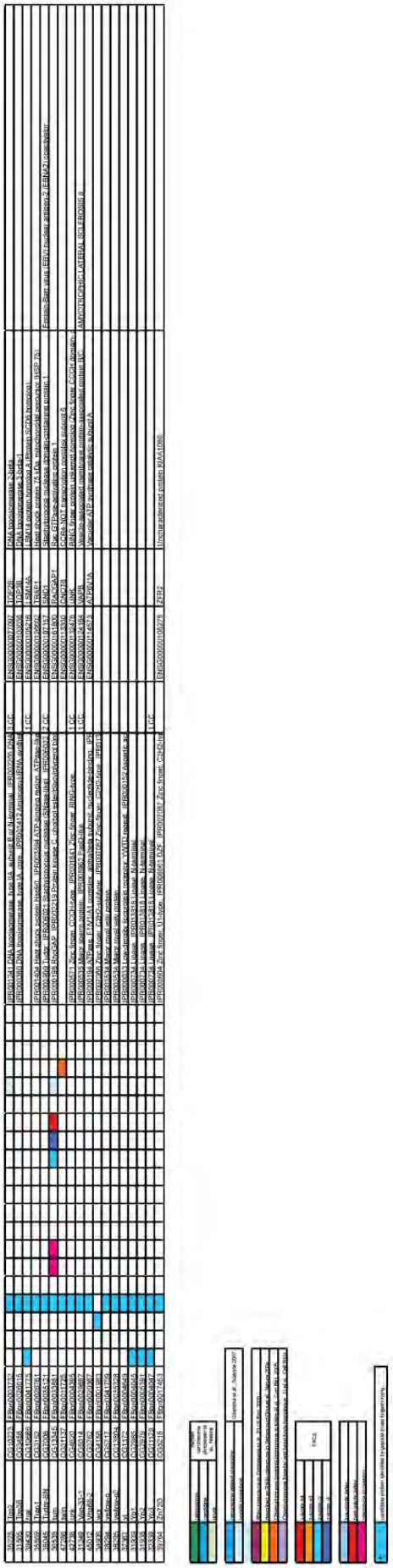

Supplemental Table 1 - HaCaT cell phenotypes

geneID	name	centrosome number	centrosome area	centrosomal γ-tubulin	mitotic index	cell cycle phenotype: sub-G1	G1/G0	S-phase	G2/M	over G2	Mukherji *et al.* 2006	Kittler *et al.* 2007	Rines *et al.* 2008	*Drosophila* orthologue name
27229	76P													Grip75
60	ACTB													Act5C
51433	ANAPC5													ida
54882	ANKHD1													mask
54443	ANLN													scra
324	APC													Apc
10552	ARPC1A													Sop2
259266	ASPM													asp
6790	AURKA													aur
636	BICD1													BicD
8945	BTRC													slmb
10576	CCT2													CG7033
983	CDC2													cdc2
991	CDC20													fzy
995	CDC25C													stg
988	CDC5L													CG6905
1017	CDK2													cdc2c
55755	CDK5RAP2													cnn
1039	CDR2													CG1962
55835	CENPJ													sas-4
1106	CHD2													Chd1
1111	CHEK1													grp
11200	CHEK2													Lok
9793	CKAP5													msps
23332	CLASP1													chb
4849	CNOT3													l(2)NC136
4850	CNOT4													CG31716
25839	COG4													CG7456
51340	CRNKL1													crn
1457	CSNK2A1													CkIIalpha
1656	DDX6													me31B
26173	DKFZP586J0619													CG3173
163786	DKFZP761A078													sas-6
1974	EIF4A2													eIF-4a
2033	EP300													nej
2091	FBL													Fib
645296	hCG_2004593													RpL17
317772	HIST2H2AB													His2A:CG31618
653604	HIST2H3D													His3:CG31613
3309	HSPA5													Hsc70-3
3832	KIF11													Klp61F
3796	KIF2													Klp10A
9493	KIF23													pav
3833	KIFC1													ncd
3838	KPNA2													Pen
3837	KPNB1													Fs(2)Ket
4001	LMNB1													Lam
4602	MYB													Myb
4751	NEK2													Nek2
4771	NF2													Mer
23511	NUP188													CG8771
23165	NUP205													CG11943
10762	NUP50													CG2158
4928	NUP98													Nup98
4998	ORC1L													Orc1
23595	ORC3L													lat
5116	PCNT													cp309
5347	PLK1													polo
5501	PPP1CC													Pp1α-96A
5515	PPP2CA													mts
5518	PPP2R1A													Pp2A-29B
5531	PPP4C													Pp4-19C
9055	PRC1													feo
84440	RAB11-FIP4													nuf
29127	RACGAP1													tum
8480	RAE1													Rae1*
5905	RANGAP1													RanGap
23644	RCD-8													Ge-1
4736	RPL10A													RpL10Ab
6135	RPL11													RpL11
6137	RPL13													RpL13
23521	RPL13A													RpL13A
9045	RPL14													RpL14
6142	RPL18A													RpL18A
6143	RPL19													RpL19
6144	RPL21													RpL21
6146	RPL22													RpL22
9349	RPL23													RpL23
6152	RPL24													RpL24
6155	RPL27													RpL27
6157	RPL27A													RpL27A
6158	RPL28													RpL28
6122	RPL3													RpL3
6133	RPL9													RpL9
6207	RPS13													RpS13
6228	RPS23													RpS23
6191	RPS4X													RpS4
80351	TNKS2													tankyrase
10131	TRAP1													Trap1
7272	TTK													ald
7283	TUBG1													gammaTub23C
10844	TUBGCP2													Grip84
10426	TUBGCP3													l(1)dd4
114791	TUBGCP5													Grip128
7531	YWHAE													14-3-3epsilon

U2OS cell phenotypes

geneID	gene name	phenotype: centrosome number	centrosome morphology	chromosome disorder
60	ACTB			
23165	NUP205			
55125	CEP192			
4850	CNOT4			
1974	EIF4A2			
55835	CENPJ			
4001	LMNB1			
8480	RAE1			
54443	ANLN			
64599	PERQ1			

centrosome number change (select box to see value)
increase in the corresponding phenotypic category
reduction in the corresponding phenotypic category

G1-phase enrichment
G2/M-phase enrichment
following RNAi treatment of U2OS cells, reported in Mukherji *et al.* 2006

high mitotic index
following RNAi treatment of HeLa cells, reported in Rines *et al.* 2007

G1/G0-phase arrest
G2-phase arrest
S-phase arrest
ploidy change
following RNAi treatment of HeLa cells, reported in Kittler *et al.* 2008

Mueller_supp_table1.xls

human HaCaT phenotypes

Supplemental Table 1 - *Drosophila* & human phenotypes comparison

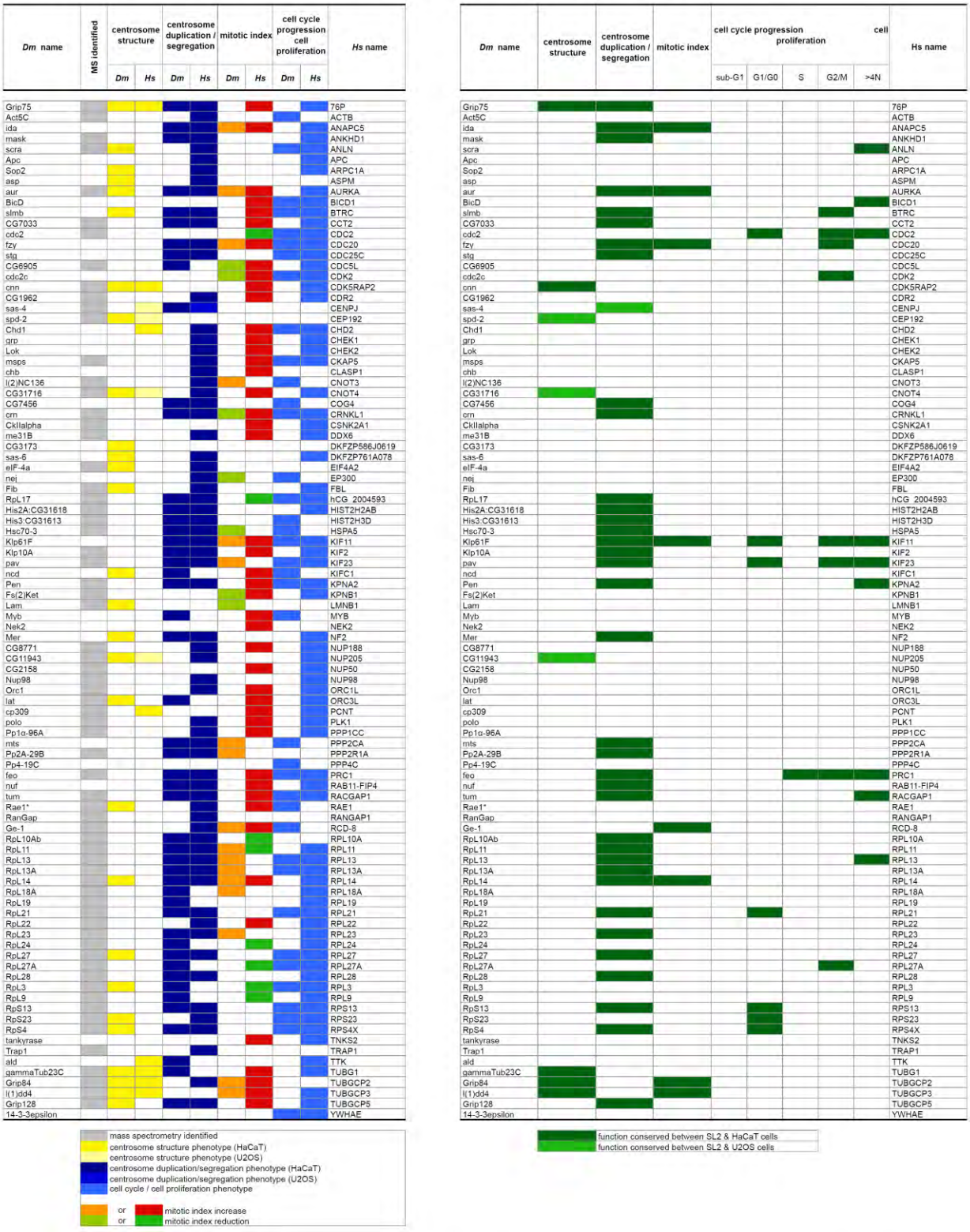

Mueller_supp_table1.xls

phenotypes comparison

Supplemental Table 2 - *Drosophila* RNAi

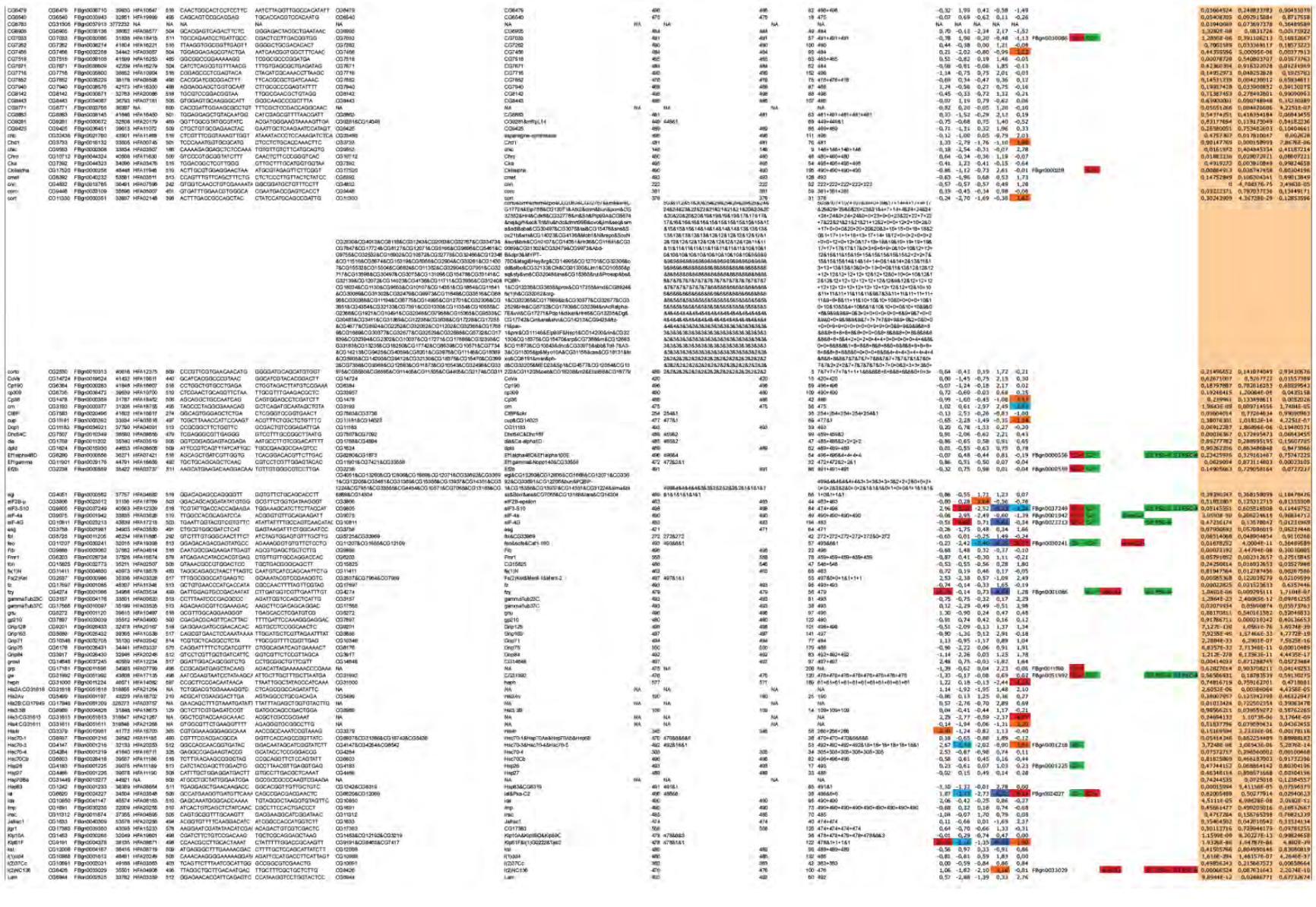

3.3.3 Author contributions

In this study, I performed the RNAi experiments and microscopic phenotype evaluation together with H. Müller, V. Lehmann and B. Lange. I analyzed parts of the data and carried out the Western Blot experiments on isolated centrosomes. Cloning and tagging of genes and transfections were carried out by V. Lehmann and me. Furthermore I wrote minor parts of the manuscript and participated in discussions on the project together with all other authors. Mass spectrometry analysis was done by J. Gobom, K. Mirgorodskaya and N. Gustavson. S. Steinbrink produced dsRNA and performed FACS analysis. Studies in human cells were carried out by D. Schmidt. A. Ploubidou, H. Lehrach, M. Boutros and B. Lange conceived and designed the experiments. B. Lange wrote the manuscript.

MANUSCRIPT 4

Functional analysis of the centrosome phosphoproteome in *Drosophila*

Karin Habermann[1], Johan Gobom[1, 2], Verena Lehmann[1], Hannah Müller[1],

Christoph Erdmann[3], Jens Peter von Kries[3], Bodo M.H. Lange[1, 4]

---

[1] Max Planck Institute for Molecular Genetics, Berlin, Germany

[2] University of Göteborg/Sahlgrenska University Hospital, Mölndal, Sweden (current address)

[3] Leibniz Institute for Molecular Pharmacology, Berlin, Germany

[4] Author of correspondence

Submitted to Journal of Cell Biology

Abstract

The centrosome plays a critical role in many cellular processes besides its main function as the cell's microtubule-organizing center (MTOC). Phosphorylation is one of the key mechanisms that regulate centrosome biogenesis and spindle assembly. However, little is known about centrosome-specific phosphorylation sites and their functional relevance. Here, we analyzed the phosphoproteome of the *Drosophila* centrosome and found previously unknown phosphorylation sites in known and unsuspected centrosome components. We functionally characterized phosphoproteins and integrated them into regulatory signaling networks with the 3 most important mitotic kinases, cdc2, polo, aur, as well as the house keeping kinase CkIIβ. Using a combinatorial RNAi strategy, we demonstrated novel functions for P granule, nuclear envelope (NE) and nuclear proteins in centrosome duplication, maturation and separation. Our dataset comprises the first inventory of *in vivo* centrosome-specific phosphorylation residues in *Drosophila* and thereby provides an important prerequisite for future studies to gain deeper insights into the mechanistic that underlie this organelle's functions throughout the cell cycle.

Introduction

The centrosome is the major organizer of microtubules in higher eukaryotes. In most cells, the centrosome is composed of a pair of centrioles surrounded by an amorphous protein matrix, known as pericentriolar material (PCM). The PCM contains proteins responsible for microtubule nucleation, like γ-Tubulin and γ-Tubulin ring complex components (γ-TuRCs), anchoring proteins that bind to different enzymes and their downstream targets, scaffolding proteins, which form a basic matrix-like structure that other complexes bind to and regulatory proteins like kinases, phosphatases and signaling molecules (Lange, 2002; Bornens, 2002). In proliferating cells, the centrosome is duplicated once per cell cycle such that at the onset of mitosis, a cell has two centrosomes, which serve as poles of the mitotic spindle.

Distinct steps of centrosome biogenesis occur in close coordination with cell cycle progression (Sluder, 2005). In proliferating cells, centrosome duplication is initiated at the G1/S transition and proceeds throughout S-phase in concert with chromosome replication. At the G2/M transition centrosomes recruit additional PCM components required for microtubule nucleation, a process termed maturation (Palazzo et al., 2000), and eventually separate and move to opposite poles to assemble the bipolar mitotic spindle. Protein phosphorylation is one of the key mechanisms that control centrosome functions during the cell cycle. Indeed, several mitotic kinases are known to associate with centrosomes and regulate centrosome cycle events. Four well-studied examples are (a) Cyclin-dependent kinase 1 (CDK1, Dmel\cdc2), which contributes to the separation of centrosomes in late G2 (Blangy et al., 1997; Crasta et al., 2006), (b) Polo-like kinase 1 (PLK1, Dmel\polo), which is known to be involved in recruiting γ-TuRCs and is thus required for centrosome maturation (Lane and Nigg, 1996), (c) SAK/PLK4, another member of the polo kinase family, which is a major regulator of centriole duplication (Habedanck et al., 2005) and (d) Aurora A, which is involved in maturation by targeting several PCM components to the centrosome (Berdnik and Knoblich, 2002). Furthermore Aurora A has been implicated in centrosome duplication and separation pathways (Barr and Gergely, 2007). Another kinase that might be involved in the regulation of centrosome functions is the ubiquitously expressed Casein kinase II (CK2, Dmel\CkII), which is implicated in a variety of cellular processes, including cell cycle progression. It has been shown to colocalize with mitotic spindles and centrosomes in mammalian cells (Faust and Montenarh, 2000) and moreover, an RNAi screen conducted in *Drosophila* cells revealed a possible centrosome-related function as knockdown of CkIIα or its regulatory subunit CkIIβ led to mild centrosome abnormalities (Bettencourt-Dias et al., 2004).

In addition to its main function as MTOC of interphase and mitotic cells, the centrosome is linked to several cellular processes. In many non-dividing cells, centrioles organize the

formation of a cilium or flagellum. Centrosomes also contribute to cell-cycle progression at the G1/s and G2/M transitions and they are required for efficient asymmetric cell division and cytokinesis (reviewed in Bettencourt-Dias and Glover, 2007; Nigg and Raff, 2009). Centrosomes are furthermore involved in stress response pathways, cell-cycle checkpoint control and recent evidence has demonstrated that aberrant centrosome numbers cause genomic instability and consequently tumor formation (Basto et al., 2008). Our knowledge regarding the molecular composition of the centrosome has substantially increased during the past years owing to improved mass spectrometry techniques in combination with the availability of whole genome sequences of a variety of model organisms. Direct proteomic analyses (Wigge et al., 1998; Keller et al., 2005), protein correlation profiling (Andersen et al., 2003), genome-wide RNAi screens (Goshima et al., 2007; Dobbelaere et al., 2008) and comparative genomics (Li et al., 2004) have led to the identification of more than 300 candidate centriole and PCM components, many of which are highly conserved in different species. However, the molecular inventory of the centrosome as well as knowledge of mechanisms controlling its functions still seems far from being complete. Therefore, we now need to explore interactions of centrosomal proteins and the modulation of their function through kinases and phosphatase in order to better understand their function in the context of major cellular signalling events.

Reversible phosphorylation is one of the key regulatory mechanisms controlling most cellular processes, including cell cycle progression, spindle assembly and centrosome biogenesis. Several large scale phosphoproteomic data sets have recently been published. Using *Drosophila* as a model system, Bodenmiller and colleagues (2007) determined the phosphoproteome of Kc167 cells and Zhai et al. (2008) identified phosphorylation sites derived from *Drosophila* embryos in a global fashion. In the present study, we determined the phosphoproteome of a single cell organelle, the centrosome of *Drosophila* embryos. We functionally characterized the identified proteins with respect to their role in centrosome replication and maturation, cell cycle regulatory and chromosome segregation pathways. Using a combinatorial RNAi screening approach, we also identified functional interactions of these proteins with 4 selected kinases (polo, aur, cdc2 and CkIIβ) in order to integrate the centrosome phosphoproteins into signaling networks in a hierarchical manner.

Results

Identification of centrosomal phosphoproteins

We isolated centrosomes from *Drosophila* embryos followed by enrichment of phosphopeptides in order to identify interaction partners of regulatory kinases and phosphatases that are critical for centrosome maturation, duplication and separation pathways. Centrosomes were isolated from preblastoderm embryos (Moritz and Alberts, 1999) and affinity-purified with an anti-cnn antibody. The enrichment of centrosomes in consecutive isolation stages was validated by immunofluorescence microscopy (Fig 1A) and immunoblotting with antibodies against centrosomal proteins Grip84 and γ-Tub (Fig 1B). To minimize dephosphorylation of target proteins during the isolation procedure, all steps were carried out in the presence of phosphatase inhibitors. Immunopurified centrosome samples showed a high abundance of phosphorylated proteins determined by in-gel labeling of proteins containing phospho-serine, phospho-threonine and phospho-tyrosine residues. We detected at least 20 phosphorylated protein bands that were enriched in the immunopurified fraction as compared to the embryo homogenate (Fig 1C). Next we isolated phosphopeptides on titanium dioxide columns following tryptic digestion. The subsequent LC-MALDI MS analysis resulted in the identification of 45 phosphorylation sites in 27 candidate centrosome proteins, shown in Table 1 (Fig 1D). The detailed MS analysis will be published elsewhere. Among the identified proteins we found known centrosome components, like the PCM protein cnn, the gamma-tubulin ring complex proteins Grip71, 75 and 84 and the centriolar protein spd-2 (Goshima et al., 2007). These findings further validated the enrichment of centrosomes in our samples. We also identified a number of proteins associated with the NE (LBR, Ote, Nup98, gp210, Lam, cup) and nuclear proteins (ewg, apt, ball). Ote, Lam and ball have previously been shown to localize to the mitotic spindle and/or function in mitotic spindle organization (Uniprot annotation, Goshima et al., 2007, Cullen et al., 2005). Additionally, we found proteins involved in translational initiation (eIF3-S8), RNA mediated gene silencing (P granule proteins Dcp1 and bel) and stress response (Hsp27), as well as proteins of unknown function (CG15435, CG14309, CG5726, CG15435, CG18190, CG6927). 16 out of the 27 proteins were also MS-identified in our lab in a previous whole proteome analysis of the *Drosophila* centrosome, which will be published elsewhere. This suggests that the 11 new centrosome candidates found in this study have previously escaped identification due to low abundance and/or large complexity of the sample, two drawbacks that were overcome by employing an additional phosphopeptide enrichment step. With the exception of ewg, all proteins identified in this study have previously been shown to be phosphorylated at different residues in two large-scale phosphoproteome studies conducted in *Drosophila* embryos (Zhai et al., 2008) and Kc167

cells (Bodenmiller et al., 2007), respectively. However, we identified 17 previously unknown phosphorylated residues (Fig 1E). For example, we found 9 phosphorylation sites in the centriolar protein spd-2, 5 of which were neither identified in the whole embryo nor the *Drosophila* cell phosphoproteome analysis. We searched our dataset for consensus motifs for the three mitotic kinases Cdk1, Plk1, Aurora-A and binding motifs for the polo box domain (PBD) and found that more than half of the identified sites are predicted to be recognized by these centrosome-associated kinases.

Phosphorylated proteins function in pathways regulating the centrosome cycle, cell division and chromosome segregation

To investigate the function of MS-identified phosphoproteins, we conducted a cell-based RNAi screen followed by automated high-content immunofluorescence microscopy and FACS analysis. We first analyzed the effects on centrosome structure/maturation, centrosome duplication/separation and chromosome segregation as well as cell cycle progression upon downregulation of 25 phosphoproteins and the 4 kinases polo, aur, cdc2 and CkIIβ. Moreover, we developed a combinatorial strategy, in which we incubated SL2 cells with dsRNA targeting one of the 4 kinases in parallel with dsRNA of the phosphoprotein set to reveal functional interdependencies. We chose the 4 cell cycle and centrosome cycle regulatory kinases, based on the assumption that the identified phosphoproteins are probable substrates or functionally interact with them. Phenotypes resulting from RNAi mediated protein depletion were analyzed with respect to the effect on number and size of centrosomes in mitotic cells, mitotic index and mitotic chromosome alignment. By using a microscopy system for automated image capture, processing and analysis, we could efficiently screen large numbers of cells (200 mitotic cells per knockdown from two biological replicates) to score statistically significant phenotypes (Fig 2A). In the initial single knockdown experiments, we found that depletion of 15 out of 29 proteins produced centrosome number and/or size aberrations, depletion of 10 proteins led to a significantly altered number of mitotic cells and depletion of 4 proteins induced chromosome missegregation. The following 6 different centrosome defects were observed and subsequently classified into two main categories: centrosome maturation/structure and centrosome duplication/separation (Fig 2B): (1) An increased proportion of mitotic cells without centrosomes occurred after downregulation of cnn, polo and cdc2, confirming the well-established function of cnn and polo in centrosome maturation and structure maintenance (Lucas and Raff, 2007; Sunkel and Glover, 1988). (2) Downregulation of aur and LBR induced cells with 2 small centrosomes, (3) Dcp1 and apt induced cells with 2 large centrosomes. The latter two centrosome size aberrations were also classified as centrosome maturation defects although we cannot rule out the possibility that large centrosomes are a

consequence of centriole overduplication. While aurora's role in the regulation of maturation has been described before (Berdnik and Knoblich, 2002), it has not previously been shown, that phosphoproteins LBR, Dcp1 and apt are implicated in this process. Inhibition of 8 out of 29 proteins led to an increased number of mitotic cells with only one centrosome, which appeared either (4) normal, (5) large or (6) small in size. The latter three phenotypes indicate a role for the proteins in centrosome duplication and separation, respectively. These results support previous findings for the gamma-tubulin ring complex components Grip 71, 75 and 84 as well as spd-2 and Lam (Goshima et al., 2007). Bel, eIF3-S8 and the kinase CkIIβ had not previously been shown to have functions in centrosome duplication or separation pathways. Knockdown of 10 proteins induced significant deviations in the proportion of mitotic cells indicating a regulatory role for these proteins in progression through the cell cycle (Fig 2D). Low mitotic indices were caused by downregulating Nup98, gp210 and apt, while depletion of Grip71, Grip75, Grip84, polo and aur induced an accumulation of cells in mitosis, which was expected as these proteins are known to regulate mitotic progression (Verollet et al., 2006; Müller et al., 2006; Bettencourt-Dias et al., 2004; Bjorklund et al., 2006). Additionally, a function of phosphoproteins bel and eIF3-S8 in cell cycle regulation was identified, as their inhibition also resulted in an increase of mitotic cells. Defects regarding chromosome segregation were observed after depleting Grip71, Grip84, polo and cdc2, confirming previous results (Müller et al., 2006; Somma et al., 2008; Goshima et al., 2007). To further dissect specific cell cycle stage distributions following dsRNA treatment, we carried out FACS analysis and found that a fraction of the analyzed proteins (10/29) function in cytokinesis as their depletion led to accumulation of cells with more than 2N DNA content (Fig 2 C). As expected, depletion of Grip71 and polo led to an increased proportion of cells with sub-G1 DNA content which indicates that these cells undergo apoptosis as a consequence of chromosomal instability (Castedo et al., 2004). Depletion of the translation initiation factor eIF3-S8 led to an arrest of cells in G1 phase of the cell cycle, consistent with studies conducted in yeast which demonstrated that loss of eIF3 complex subunits causes inhibition of protein synthesis and blocks transition from G1 to S phase (Hanic-Joyce et al., 1987; Evans et al., 1995; Kovarik et al., 1998). Taken together, our RNAi analysis revealed previously unknown functions for the phosphoproteins bel, eIF3-S8, LBR, Dcp1 and apt and the kinase CkIIβ in centrosome cycle regulatory pathways. Bel, eIF3-S8 and apt are additionally required for cell cycle progression, as are nuclear pore proteins Nup98 and gp210. Interestingly, a requirement for efficient cytokinesis was discovered for actin filament organizer qua, CG18190, a protein which is predicted to function in microtubule binding as well as for functionally not annotated proteins CG6927 and CG31326. It has also not been reported before that depletion of the transcriptional regulator ewg causes defects in cell division.

RNAi screening in kinase depleted backgrounds identifies functions of phosphoproteins in relation to polo, aur, cdc2 and CkIIβ

To gain further insight into the hierarchical relationships between kinases and candidate kinase-substrates and to identify functionally redundant genes, we used RNA interference to inhibit two genes simultaneously in 100 combinations. 25 phosphoproteins were downregulated in 4 different kinase-depleted backgrounds and synthetic phenotypes were analyzed again with respect to centrosome number and size, mitotic index and chromosome aberrations. By suppressing gene activity in the 4 sensitized backgrounds we were able to integrate 17 out of 25 analyzed phosphoproteins into signaling networks controlling centrosome duplication or separation while the single knockdown approach identified only 7 proteins as being implicated in these pathways. Moreover, functional roles of 7 phosphoproteins in centrosome maturation or structure maintenance were identified in the combinatorial RNAi screening, 4 of which had also been identified by depleting only the phosphoprotein. Phenotype analysis of double knockdowns revealed functional implications of 23/25 phosphoproteins in pathways regulating progression through the cell cycle, 6 of which were not detectable upon depletion of the phosphoprotein alone. Surprisingly, 18 phosphoproteins were shown to be integrated in chromosome segregation pathways. Most of these were identified in the cdc2 depleted background. In contrast, only two phosphoproteins (Grip71, Grip84) were identified to play a role in chromosome segregation in the single knockdown experiments.

By analyzing synthetic phenotypes with respect to deviations from single knockdown phenotypes of the 4 kinases, we furthermore determined functional relationships of phosphoproteins with aur, cdc2, polo and CkIIβ in 4 signaling networks in a hierarchical fashion. Probable regulatory mechanisms were assigned to each of the 5 types of deviated synthetic phenotypes that we found in this study. (1) For instance, a weaker double knockdown phenotype suggests negative regulation of the phosphoprotein Nup98 downstream of the kinase polo in an independent parallel pathway that is required for the maintenance of centrosome structure. (2) Another example are aur and Dcp1, which differentially regulate centrosome maturation, hence opposite effects on centrosome size were observed in single knockdowns, which compensate each other when both proteins are inhibited simultaneously. (3) ball is redundantly implicated in the regulation of chromosome segregation since silencing in a cdc2 depleted background results in a significantly increased number of cells with chromosome aberrations while single knockdown of ball has no apparent effect on chromosome segregation. (4) A rescue phenotype indicates that kinase and phosphoprotein function in the same pathway in a mutually dependent mechanism. For instance, negative regulation of cup downstream of CkIIβ is required for effective centrosome

duplication/separation. (5) A phosphoprotein is implicated in a certain process independent or upstream of the kinase when the phenotype of the phosphoprotein RNAi is dominant over the kinase RNAi phenotype in the simultaneous knockdown of both. For example, Grip84 is required for centrosome duplication/separation through a mechanism that is independent of aur activity. A summary of all identified phosphoprotein functions arising from combinatorial RNAi screening analysis and functional relations between kinases and phosphoproteins are shown in Figure 3. In conclusion, our data demonstrates that virtually all MS-identified centrosomal phosphoproteins are implicated in signaling pathways related to centrosome biology or cell cycle regulation, either in a direct fashion or through functional interaction with the relevant kinases.

Phosphorylated proteins with centrosome-related functions localize to mitotic spindles and centrosomes in SL2 cells

To determine the subcellular localization of phosphoproteins, we generated SL2 cell lines stably expressing GFP, TAP or FLAG fusion proteins and monitored their expression throughout the cell cycle. We chose one or two proteins, which based on their previously annotated localizations represent 5 different subcellular compartments: centrosome, P granule, nuclear membrane, nucleus and cytosol (see Fig 4). As expected, GFP tagged spd-2 and Grip84 were found to localize to centrosomes throughout the cell cycle, validating the specificity of the tagging and overexpression approach. Phosphoproteins Ote and Lam fused to a FLAG and GFP tag, respectively, were primarily associated with the NE, but also colocalized with centrosomes and the spindle from metaphase until anaphase. FLAG tagged Ote was additionally clearly associated with the midbody in telophase and furthermore found to localize to interphase centrosomes (Fig 5B). Transcriptional regulator ewg fused to a TAP tag localized exclusively to chromatin and neither to spindles nor centrosomes, consistent with our RNAi data that revealed no centrosome related function of this protein in any of the sensitized backgrounds. Another TAP fusion protein, ball, which is a nucleosomal histone kinase (Aihara et al., 2004), localized to chromatin but expression also partially overlapped with the mitotic spindle, supporting previous findings that this kinase is implicated in sister chromatid segregation and mitotic spindle organization (Cullen et al., 2005). Bel and Dcp1, two proteins implicated in RNA mediated gene silencing, localized to cytoplasmic P granules in interphase cells as was expected. Interestingly, in mitosis, GFP tagged bel colocalizes with centrosomes and the mitotic spindle supporting our functional data demonstrating this protein to be required for centrosome duplication/separation. Dcp1, a protein which was identified as a negative regulator of centrosome maturation in our study, also associated with metaphase and anaphase spindles when overexpressed as FLAG fusion protein in SL2 cells. The ninth candidate of the phosphoprotein set whose subcellular localization was examined was

translation initiation factor complex component eIF3-S8. Its expression was restricted to the cytosol in interphase and concentrated adjacent to the nuclear membrane. In mitosis, the peak fraction of the GFP fusion protein was localized to the mitotic spindle. Our overexpression studies confirmed known subcellular localizations of 9 centrosome candidate proteins and revealed previously unknown association with mitotic spindles for 3 proteins (bel, Dcp1 and eIF3-S8) Moreover, we describe for the first time a colocalisation with *Drosophila* centrosomes for the phosphoproteins bel and Ote. These findings are consistent with the functional analysis of the candidate centrosome proteins which identified 8 of the 9 overexpressed fusion proteins to be implicated in centrosome cycle associated signaling pathways. Ewg was the only fusion protein among the nine analyzed candidates that neither associates with centrosomes nor spindles at any cell cycle stage and had no detectable centrosome related function in our RNAi screen.

Dynamic localization of NE phosphoproteins Ote and Lam throughout the cell cycle

To shed more light on the role of NE proteins regarding centrosome and cell cycle regulatory pathways, we analyzed Ote and Lam in more detail. First we used specific antibodies to follow endogenous localization of the two proteins in SL2 at different stages of the cell cycle (Fig. 5A). As expected, interphase cells exhibited prominent staining of the nuclear periphery, but we also observed a weaker cytoplasmic signal in cells labeled with anti-Ote. At the onset of mitosis prior to nuclear envelope breakdown (NEBD), we observed invaginations in the nuclear membrane in close proximity to centrosomes. In mammalian cells it has been shown that such invaginations are generated by dynein-mediated microtubule-dependent forces which create mechanical tension in the nuclear membrane and thereby trigger NEBD (Beaudouin et al., 2002; Salina et al., 2002). In support of this model, the minus-end directed microtubule motor dynein is required for nuclear attachment of centrosomes during mitosis in *Drosophila* (Robinson et al., 1999). However, an interaction partner for dynein at the NE has so far been elusive. Interestingly, Ote has been identified as an in vitro binding partner of dynein light chain Dlc90F in a two hybrid study (Giot et al., 2003), a finding that may provide the missing link for centrosome-NE attachment and tearing of the NE in *Drosophila*. The process of nuclear lamina breakdown in *Drosophila* early embryos has been described as an intermediate form between open and closed mitosis, as complete NE breakdown does not occur until after metaphase (Paddy et al., 1996). Instead Lam persists in an envelope-like structure enclosing the entire mitotic apparatus including centrosomes, condensed chromosomes and spindle microtubules. Ote has also been proposed to be a component of this spindle envelope (Harel et al., 1989). Whether or not this semi-closed mitosis is only a feature of early embryonic divisions or a general mechanism in *Drosophila* continues to be a matter of debate. However, two ultrastructural studies in *Drosophila* cultured cells have

revealed the persistence of nuclear membranes enveloping the mitotic spindle until anaphase (Debec and Marcaillou, 1997; Maiato et al., 2006). In support of these findings, we observed such a structure in fixed SL2 cells when following Lam distribution at prometaphase until metaphase but this was not seen in cells labeled with anti-Ote suggesting that Ote leaves the membrane before complete breakdown, at least in cells derived from later developmental stages. Following NEBD both Lam and Ote are dispersed in the cytoplasm with Ote being rather concentrated at spindle poles. In anaphase, when the NE starts to reassemble, Otefin and Lamin are recruited to chromosomes. Reassembly of the NE involves targeting of lamins and lamin-binding proteins in a temporally and spatially regulated manner. It has been shown that Lam and Ote containing vesicles are among the first that assemble on the chromosomal surface in vitro (Ulitzur et al., 1997). Interestingly we found that, in anaphase, Ote accumulates first at regions adjacent to centrosomes and at peripheral sites of chromosomes but is excluded from the region where mid-spindle microtubules attach. Only later in telophase, Ote forms a continuous rim around chromatin. At the same time the signal becomes stronger in the mid-spindle area. During cytokinesis Ote is again localized to the nuclear periphery, but a minor fraction of the protein remains dispersed in the cytoplasm and is also found at the midbody. A fraction of Lam also localizes to the cytoplasm during telophase and later the signal strongly concentrates in the cleavage furrow of the dividing daughter cells but is absent from the midbody. Despite the colocalization of Ote with spindle poles during metaphase, we also found that a minor portion of the protein localizes to interphase centrosomes as was demonstrated by immunofluorescence microscopy with antibodies detecting the endogenous protein and the overexpressed FLAG fusion protein (Fig 5B). Overexpression of Ote also resulted in the establishment of filamentous structures in the cytoplasm which colocalized with cytoplasmic microtubules (not shown). Labeling at the centrosome was specific and neither a consequence of overexpression nor due to unspecific labeling of rabbit antibodies or secondary antibodies as control cells expressing TAP tagged scra, a nuclear protein, labeled with rabbit serum exhibited no fluorescent signal at interphase centrosomes.

Ote is a component of centrosomes and functionally interacts with aur in maturation

We conducted immunoprecipitation experiments of FLAG:Ote and GFP:Lam with the aim of confirming suspected interaction partners from our RNAi analysis results. We found that γ-Tub copurified in a complex with Ote but not Lam (Fig 5C), supporting the hypothesis that Ote is not only localized to the inner nuclear membrane but indeed a genuine component of *Drosophila* centrosomes. We also confirmed the well established binding of Lam and Ote in these experiments (Goldberg et al., 1998). Furthermore we could show that both Lam and Ote precipitate in a complex with α-Tub. Although it had previously been shown that the

proteins localize to or around the mitotic spindle, we hereby for the first time provide biochemical evidence for an association with microtubules. Lastly, hints to a functional interaction between the centrosome related kinase aur and Ote coming from our RNAi analysis were supported by the fact, that aur was co-purified in Ote and Lam pulldowns. Based on the phenotype analysis of single and double knockdowns of aur and Ote we had discovered that the two proteins cooperate functionally in centrosome maturation as well as cell cycle regulation (Fig 5D). While inhibition of aur induces mitotic cells with small centrosomes, this phenotype is rescued when simultaneously depleting Ote. Similarly, loss of aur function induces accumulation of cells in mitosis, yet additional removal of Ote leads to populations of cells with mitotic indices close to control level. Taken together, these data led us to propose a model in which negative regulation of Ote downstream of aur is required for obtaining mature centrosomes and for progression through mitosis. Another interdependency of a centrosome kinase (polo) and NE component (Lam) was revealed in our functional analysis (Fig 5E). While polo is known to be required for mitotic exit and hence depletion leads to mitotic arrest, a role for Lam in a polo-dependent pathway of mitotic progression is not described. Based on the observation that parallel inhibition of polo and Lam partially rescues the polo induced phenotype while depletion of Lam alone has no significant effect on mitotic progression, we suggest the following mechanism: Negative regulation of Lam in a parallel signaling pathway downstream of polo is required for mitotic exit. These findings are in contrast to yet another NE component, the nuclear pore protein Nup98. Parallel inhibition of Nup98 and polo also significantly weakens the polo induced arrest in mitosis. But other than Lam, Nup98 appears to differentially regulate mitotic progression in a polo-independent manner as single knockdown of the protein induces a low mitotic index suggesting an essential role in the regulation of mitotic entry.

Discussion

We identified 45 phosphorylation sites, of which 17 have not been described before, in 27 proteins applying mass spectrometry analysis with prior organelle purification and phosphopeptide enrichment,. Among the identified proteins are 6 known centrosome components, but the majority of proteins have so far only been linked to non-centrosome associated cellular localizations and processes, including NE assembly, transcriptional and translational regulation and proteolysis. Importantly though, this work revealed redundant and non-redundant functions of phosphoproteins in centrosome maturation, duplication or separation, cell cycle regulation and chromosome segregation and demonstrated their integration into signaling pathways of 4 major protein kinases. For a subset of phosphoproteins, we identified previously unknown centrosome and/or spindle localization via expression of tag fusion proteins in cultured SL2 cells.

Proteomic analysis of Drosophila centrosomes identifies novel centrosome components and phosphorylation sites

Reversible phosphorylation by centrosome-associated kinases and phosphatases is known to play a crucial role in the regulation of intrinsic centrosome functions such as duplication, separation and maturation and it links the organelle to a variety of cellular processes, e.g. stress response, cell cycle progression and tumorigenesis. Therefore a major goal of this study was to determine substrates of these centrosome-associated regulatory enzymes (e.g. cdc2, polo, aur, Nek2, PP1) and in particular centrosome-specific phosphorylation sites. Although a number of high throughput datasets describing the global phosphorylation status of *Drosophila* proteins (Bodenmiller et al., 2007; Zhai et al, 2008) as well as a phosphoproteome analysis of the human mitotic spindle (Nousiainen et al., 2006) have recently become available, our study provides the first inventory of centrosome phosphoproteins and their phosphorylation sites in *Drosophila*. By combining an affinity purification method for the isolation of centrosomes, phosphopeptide enrichment and MS based proteomics, we identified both unknown centrosome components as well as unknown phosphorylation sites. These findings imply that (a) our organelle-based approach is a powerful tool for the identification of novel phosphorylation sites and moreover a novel phosphoprotein (ewg) and that (b) some of the sites identified by this approach are likely to be specific to the subcellular localization of the respective protein. The phosphorylation at these residues may either facilitate the binding of proteins, which are otherwise found at different subcellular sites, to centrosomes at particular stages of the cell cycle, activate a centrosome-associated function of the proteins or both. Interestingly, more than 50% of the identified residues in this study are predicted consensus motifs for the known centrosome-associated kinases polo, aur and cdc2. This result supports the hypothesis that the proteins

stably or transiently localize to centrosomes and are targeted by centrosome kinases. One well-established example of a phosphorylation-dependent localization (and consequently function) applies to the nucleolar protein nucleophosmin, which dissociates from the centrosome upon phosphorylation by Cdk2/cyclinE thereby initiating duplication (Okuda et al., 2002). However, most centrosome-related regulatory mechanisms remain enigmatic.

Cell-cycle-dependent localization and function of phosphoproteins

We used two complementary approaches to confirm an association with centrosomes for the proteins that were not predicted to be centrosomal on the basis of their previously described function. (1) We cloned 9 candidate genes, expressed them in *Drosophila* SL2 cells and examined their subcellular localization in interphase and mitosis. In addition to the 2 known centrosome components spd-2 and Grip84, which served as positive control in this experiment, we could show colocalisation with spindles and/or centrosomes for 6 other candidate proteins in mitosis. As eukaryotic cells undergo extreme remodeling of their structure during cell division, for instance by dissolving the nuclear membrane, many proteins relocate to different cellular compartments and perform functions which are distinct from their fate in interphase cells. In the case of symmetric cell division, these proteins need to be equally distributed to the progeny cells, a process that also employs the mitotic spindle. In addition, previous reports have demonstrated that components of the translation machinery associate with spindle microtubules to regulate translation of mRNAs that are required for mitotic progression and spindle assembly (Suprenant, 1993, Liska et al., 2004, Blower et al., 2007, Eliscovich et al., 2008). In support of this model, 3 proteins involved in RNA processing/translation initiation (bel, Dcp1and eIF3-S8) were shown to be localized at mitotic spindles in our study. It has long been proposed that the structure of the mitotic spindle apparatus might be stabilized by a so-called spindle matrix, a macromolecular complex constituted by several nuclear components in *Drosophila* (Qi et al., 2004). Lamin B was reported to be a structural component of this matrix in *Xenopus* and humans (Tsai et al., 2006), consistent with our findings that Lam colocalizes with spindles and moreover it was purified in a complex with α-Tubulin in our study.

(2) In a second approach aimed at identifying relevant centrosome components, we conducted a cell-based functional RNAi analysis and screened for phenotypes affecting centrosome biogenesis, cell cycle progression and chromosome segregation. Remarkably, we found that out of the 25 analyzed proteins, 21 appear to be involved in regulating the centrosome cycle, 23 play a role in cell cycle progression and 18 in chromosome segregation pathways. It is important to note, that most of the functions became apparent only by analyzing synthetic phenotypes, in which a phosphoprotein and one of the four centrosome-associated kinases were downregulated concomitantly. While silencing of one gene may be

sufficient to identify it as an essential component of a signaling network, such an approach often fails to detect redundant protein functions, most likely due to the existence of alternative pathways which compensate for the loss of activity of only one component of the respective signaling network. Identification of redundant regulators of a certain biological process therefore requires removal of a second element in the respective pathway. In addition to revealing many unsuspected new functions, our combinatorial RNAi approach also allowed us to identify functional interdependencies between kinases and phosphoproteins in the 4 examined signaling networks. Hence, this strategy proved very informative for unraveling previously unknown regulatory mechanisms controlling centrosome and cell cycle events.

The centrosome and NE components

Following the identification of the centrosome phosphoproteome in *Drosophila*, one of the most striking observations was that 6 out of the 27 MS identified candidate proteins (22%) were components of the NE. Our subsequent functional and localization analysis suggested that these were not simply contaminants of the centrosome preparations since we identified centrosome cycle related functions for all of them, either directly or in the kinase depleted backgrounds. Localization studies of FLAG/GFP tagged Ote and Lam in SL2 cells encouraged the assumption that these proteins have cell cycle dependent functions for the centrosome and spindle despite their main role in assembling the nuclear membrane. There is accumulating evidence for an interaction between centrosomal and NE components from various studies. For example, it has been shown that nuclear pore sub-complexes relocate to kinetochores upon NEBD, where they interact with the γ-TuRC and promote mitotic spindle assembly (Mishra et al., 2010). Furthermore, the nuclear membrane protein Emerin has been shown to be associated with microtubules and thereby linking the centrosome to the NE in metazoan cells (Salpingidou et al., 2007). Similarly, *C. elegans* ZYG-12 localizes to both centrosomes and the NE and is essential for their attachment (Malone et al., 2003). Centrin 2, a core component of the centriole, also associates with nuclear pore complexes in *Xenopus* and human cells (Resendes et al., 2008). In this study, several lines of evidence indicate that the nuclear inner membrane protein Ote is also a genuine component of interphase centrosomes. It binds to Lam and is found in a complex with both γ- and α-Tubulin suggesting that it may facilitate bridging of the centrosome to the NE in interphase via microtubules. Ote was also shown to be involved in centrosome maturation downstream of aur. Whether or not Ote is a direct target of aur remains to be elucidated. Another large scale phosphoproteomic study identified T63 as a phosphorylated residue of Ote (Bodenmiller et al., 2007). This site is a predicted consensus motif for Aurora-A kinase and therefore it is tempting to speculate that direct phosphorylation of Ote by aur at T63 is one required

signaling event that ensures proper maturation of centrosomes as well as progression through mitosis. A functional interdependency was also observed between Nup98 and polo. While depletion of polo leads to severe centrosome aberrations, a simultaneous knockdown of Nup98 significantly weakened the polo induced phenotype indicating that Nup98 is a downstream target in a pathway that maintains centrosome structure. Yet another pore complex component, gp210, was found to play a role in centrosome duplication since simultaneous inhibition with aur led to cells with more than 2 centrosomes (see Fig. 3 and S1). Single knockdown of these proteins does not induce aberrations in centrosome number which indicates, that gp210 is a component of a pathway that blocks overduplication but loss of its function can be compensated by aur activity. Loss of gp210 activity also prevents cells from entering mitosis which might be the result of activation of a checkpoint that controls centrosome integrity at the G2/M transition.

In conclusion, the findings of the present study support the notion that the centrosome functions as a signaling platform (Doxsey et al., 2005) and is integrated into a number of major cellular signaling pathways (Lange, 2002). Many components transiently associate with the centrosome to fulfill unsuspected tasks that differ from their established functions in other cellular compartments (Kalt and Schliwa, 1993). As posttranslational modifications such as phosphorylation can affect a protein’s function, localization and interaction with other proteins, our description of the in vivo phosphorylation status of centrosome-associated proteins provides a basis for future research aimed at understanding the molecular mechanisms controlling centrosome and cell cycle regulatory pathways.

Materials and Methods

Preparation of centrosome samples

Centrosomes were isolated from *Drosophila melanogaster* preblastoderm stage embryos through two sucrose gradient centrifugations and subsequently affinity-purified on magnetic beads (Dynabeads® Protein G, Invitrogen) as described by Lehman et al. (2005) with following modifications: All purification steps were carried out in buffers containing phosphatase inhibitors (1 mM sodium fluoride, 2mM sodium orthovanadate, 25mM β-glycerophosphate) in order to avoid dephosphorylation of centrosomal proteins during the procedure.

The enrichment of centrosome proteins during consecutive isolation steps was monitored by western blotting with mouse monoclonal anti-γ-Tubulin antibody GTU88 (Sigma) and rabbit polyclonal Anti-dGrip 84 WD (Y. Zheng, Carnegie Institution of Washington, Washington DC, USA). In parallel immunofluorescence microscopy of centrosomes from all isolation steps using anti-γ-Tubulin antibody was performed as described before (Lehmann *et al.*, 2005).

Immunopurified centrosomes were eluted from magnetic beads by treating the samples with 0,1% RapiGest™SF Protein Solubilization Reagent (Waters) for 30 min at 9°C while shaking at 800rpm in a thermomixer. The elution buffer was prepared as follows. One vial of RapiGest (1 mg) was dissolved in 100 µl of 50 mM ammonium hydrogen carbonate, producing a 1% stock solution to which 900 µl of a 20 mM Hepes buffer, pH 7,5 containing 100 mM $NaCl_2$, 10 mM EGTA and 2 µM β-mercaptoethanol was added (final concentration of 0.1% RapiGest). The supernatant containing the RapiGest eluted proteins was further processed for enrichment by titanium dioxide and subsequently analyzed by mass spectrometry. Magnetic beads cross-linked with rabbit preimmune serum and incubated with centrosomes were treated as described above and served as a negative control in all experiments.

Phosphopeptide enrichment and MS analysis

Following tryptic digestions of the ALS-eluted centrosome samples, phosphopeptides were enriched using a method based on TiO_2 affinity (Thingholm et al., 2006). LC-MALDI MS was performed on a 1100 Series Nanoflow LC system (Agilent Technologies) as described previously (Mirgorodskaya et al., 2005). Proteins were identified by searching the MS/MS data against the FlyBase sequence database (http://flybase.bio.indiana.edu/) using the Mascot software (Matrixscience). A total of 45 utilized phosphorylation sites in 27 different proteins were identified (detailed MS analysis will be published elsewhere) and these are shown in Fig. 1.

In-gel detection of phosphorylated proteins

Embryo homogenate (EH), centrosomes enriched fraction (CEF) and immunopurified centrosomes (IPC) were incubated in SDS loading buffer for 10 min at 95°C. Protein samples were separated by sodium dodecyl-sulfate polyacrylamide gel electrophoresis (SDS-PAGE) and stained with Pro-Q Diamond Phosphoprotein Gel Stain (Invitrogen), which recognizes phosphate groups attached to serine, threonine and tyrosine residues, followed by SYPRO Ruby protein gel stain (Invitrogen), according to the manufacturer's instructions. Pro-Q Diamond and SYPRO Ruby stained proteins were detected at excitation wavelength 532 nm (green filter) and 473 nm (blue filter) respectively, through the Fuji FLA-5100 laser scanner. The images were further processed with the AIDA image analyzer software and subsequently annotated with Adobe Photoshop and Adobe Illustrator.

RNA interference

Long dsRNA for RNAi experiments was generated by PCR-amplifying ~500bp long fragments using genomic DNA as template. The amplicons contained T7 promoter sites and were amplified using primers designed with the E-RNAi tool from DKFZ (http://rnai.dkfz.de). In-vitro transcription was performed using T7 RiboMAX Express Large Scale RNA Production System (Promega) according to the manufacturer's instructions, followed by DNaseI digestion and ethanol precipitation to purify the RNA. Both PCR-amplified DNA and precipitated dsRNA were subjected to gel electrophoresis and photometric measurements for quality control and quantification. Primer and amplicon sequence information are shown in Table S2.

SL2 cells were cultured in Schneider's *Drosophila* Medium (Invitrogen) with 10% FBS (Fetal bovine serum, Invitrogen) at 25°C. dsRNA treatment was performed essentially according to Clemens et al. (2000) with the following modifications: $1x10^6$ cells were incubated with 10 µg dsRNA for 1 hour at room temperature in serum-free medium. After 72 hours a second dsRNA treatment was carried out to ensure optimal depletion of protein levels. In the case of simultaneous knockdowns, 10 µg of dsRNA targeting a kinase and 10 µg of dsRNA targeting a phosphoprotein were added to $1x10^6$ cells and this treatment was repeated after 72 h. All knockdowns were carried out in biological replicates. After 4 days cells were harvested and analyzed via automated immunofluorescence microscopy and FACS.

Automated immunofluorescence microscopy high content screening

Following RNAi treatment cells were transferred to Concanavalin A-coated (Sigma) glass-bottom 96-well plates (Greiner) and allowed to adhere for 1.5 h before fixation in 4% paraformaldehyde (Applichem). Cells were incubated with rabbit polyclonal anti-cnn (Pineda)

and mouse monoclonal anti-phospho histone H3 (Abcam) followed by labeling with secondary antibodies and HCS CellMask Blue cytoplasmic/nuclear stain (Invitrogen). Plates were automatically imaged with the ArrayScan VTI HCS Reader (Thermo Scientific), using a 40x, 0.75 NA PlanNeoFluar objective lens to obtain high resolution images. Images were acquired in 3 channels (Hoechst, FITC, Texas Red) until 100 mitotic cells per well were obtained (depending on the mitotic index of the sample approximately 500 fields/well). High content analysis was performed using the Morphology Explorer Bioapplication. Cells were identified by segmenting the Hoechst channel based on size, shape, and fluorescence intensity of objects. Mitotic cells were selected in the FITC channel based on the intensity of nuclear anti-phospho H3 staining. An average of n=20000 cells per knockdown was imaged to determine the mitotic index. Amount and size of centrosomes were determined within each mitotic cell based on the anti-cnn fluorescent signal in the Texas Red channel. Algorithm parameters for object segmentation, object selection (gating) and segmentation of intracellular objects (spots) were manually optimized for each individual plate using control cells. Following scan completion all relevant reported data, including percent of selected objects/well (mitotic index), spot count and mean spot area per selected object (number and size of centrosomes per mitotic cell) were exported to an Excel® spreadsheet using the Cellomics vHCS View software and analyzed statistically.

Data analysis

Mitotic indices in each well were automatically determined as the ratio of total number of cells segmented in the DAPI channel to the number of phosphorylated histone H3 positive cells selected in the FITC channel. An average of n=20000 cells per knockdown was analyzed. Mean values and standard deviations were computed for biological replicates of all knockdowns. If the sum of the mean and two times the standard deviation of a sample was smaller than the difference of mean and two times standard deviation of the control, the mitotic index of the sample was considered significantly decreased. If the difference of the mean and two times the standard deviation of the sample was greater than the sum of mean and two times standard deviation of the control, the mitotic index of the sample was considered significantly increased. Significant phenotypes regarding centrosome number and size were scored as follows: An average of n=200 mitotic cells per knockdown was analyzed and each cell was assigned to one of four different categories: 0, 1, 2 or >2 spot counts/object (centrosomes/mitotic cell). The resulting distributions of the two independent experiments were averaged and compared to the average distribution of the control by means of a non-parametric two-tailed chi square test. A significant deviation from the control distribution was assigned for significance levels $p<0.0001$. Knockdowns causing significantly altered distributions were then assigned a centrosome number phenotype depending on

which category of cells was most increased compared to the control. To score phenotypes regarding centrosome size, we first computed the mean spot area and standard deviation over all control cells and three size categories were set using the control values: large (spot area is bigger than the sum of mean area and standard deviation), small (spot area is smaller than the difference of mean area and standard deviation) and normal (spot area is within the range of positive and negative standard deviation). Each sample mitotic cell was then assigned to one of the categories. Average distributions of samples were compared to control distributions as described above and knockdowns causing a significantly altered distribution were assigned to large or small centrosome phenotypes. For the identification of chromosome segregation defects n=100 mitotic cells were visually inspected and the distribution of normal and misaligned chromosomes was determined for each knockdown. Significant phenotypes were resolved as described above, except that $p<0.001$ was set as cutoff. In the case of double knockdowns, significant phenotype alterations were not only determined in relation to the egfp controls but also in relation to single knockdown of the respective kinase. This step was used to identify enhanced or reduced penetrance of phenotypes. Table S1 lists all phenotypes identified in single and double knockdowns.

Cell cycle analysis

For FACS analysis, SL2 cells were fixed in 70% icecold ethanol and stained with propidium iodide [50 µg/ml pancreatic RNaseA (Sigma) and 50 µg/ml propidium iodide (Calbiochem) in PBS] for 1.5 h at 37°C. The DNA content of an average n=20000 cells per knockdown was quantified on a flow cytometer (FACSCalibur, BD) and analyzed using FlowJo software (Tree star). The cell populations were gated and quantified within the different cell cycle phases. The average of two replicates was calculated and the z-scores were assessed for each sample. Z-scores represent the ratio of the sample value minus the mean of the control divided by the standard deviation of the control. Phenotypes were considered to be statistically significant when the z-score was found to be ≥ 3.8.

Generation of SL2 cell lines stably expressing fusion proteins

For localization studies and immunoprecipitation experiments, we generated SL2 cell lines stably expressing proteins fused to a GFP, FLAG or TAP tag. FLAG and TAP vectors carrying target genes Ote, ball and Dcp1 were obtained from the BDGP Expression clone collection. All other expression vectors used in this study were generated by PCR amplifying the target genes using DGRC clones as templates. The Gateway cloning technology (Invitrogen) was applied to shuttle genes into EGFP expression vectors pAGW and pAWG, which were obtained from the DGRC *Drosophila* Gateway vector collection, and into the TAP expression vectors pDEST NTAP and pDEST CTAP as described in Müller et al.(2010).

Cells were co-transfected with vectors carrying the tagged target genes and pCoBlast (Invitrogen), a vector carrying a Blasticidin resistance gene, by calcium phosphate transfection (Invitrogen) according to the manufacturer's instructions. After three weeks of selection for Blasticidin-resistant cells, stable expression of target genes was confirmed by immunofluorescence microscopy and Western blotting with the corresponding tag specific antibodies.

Immunofluorescence microscopy of fixed SL2 cells

SL2 cells were allowed to settle on Con A-coated coverslips and fixed with methanol for at least 5 min at -20°C. TAP fusion proteins were labeled with rabbit polyclonal anti-calmodulin binding site (CBS) (Eurogentec), FLAG fusion proteins with mouse monoclonal anti-FLAG M2 (Sigma) and EGFP fusion proteins with rabbit polyclonal anti-GFP antibody (Clontech). Lam and Ote were visualized with mouse monoclonal anti-ADL67.10 Lamin Dm0 (Hybridoma Bank) and rabbit anti-Otefin (D. Chen, Beijing), respectively. Centrosomes were visualized with either mouse monoclonal anti-γ-Tubulin GTU-88 (Sigma) or rabbit anti-cnn. Microtubules were labeled with mouse monoclonal anti α-Tubulin (Sigma).Following primary antibody labeling, cells were incubated with the appropriate fluorescence-conjugated secondary antibodies (Invitrogen) and DNA was labeled with DAPI. For image acquisition, we used an Axio Imager Z1 fluorescence microscope (Zeiss) with MRM CCD camera and AxioVision software. Image processing and annotation was done using the Adobe Photoshop and Adobe Illustrator software.

Co-immunoprecipitation of FLAG and GFP fusion proteins

FLAG fusion proteins were immunoprecipitated from SL2 cell lysates using EZview Red ANTI-FLAG M2 Affinity Gel (Sigma-Aldrich). For GFP-IP's, magnetic beads (Dynabeads® Protein G, Invitrogen) were cross-linked with anti-GFP antibody and incubated with cell lysate. Beads with bound protein were washed 5 times for 10 min and elution was performed at 50°C with SDS PAGE sample buffer lacking β-mercaptoethanol to avoid elution of the antibody. Immunoprecipitated complexes were resolved by SDS-PAGE followed by Western blotting and probed with antibodies against bait protein (anti-FLAG/GFP) and potential complex partners (anti γ-Tub, α-Tub, aur [rabbit anti Aurora A (DM), Knoblich] and Lam). Cell lysates from untransfected SL2 cells served as negative control for FLAG-IP's and lysates from cells stably transfected with the empty GFP vector served as control for the GFP-IP's.

Acknowledgements

We are very grateful to Dahua Chen, Yixian Zheng and Jürgen A. Knoblich for providing antibodies that were used in this study. We thank Martin Neuenschwander for technical assistance and Thomas Kessler and Seon-Hi Jang for helpful discussions and critical reading of the manuscript.

K. Habermann and B. Lange conceived and designed the experiments. J. Gobom performed phosphopeptide enrichment and MS analysis. K. Habermann, V. Lehmann and H. Müller performed the experiments. C. Erdmann and J. von Kries provided reagents, materials, analysis tools and technical support for high content screening. K. Habermann analyzed the data, generated the figures and wrote the manuscript.

We thank Mike Cooper from Thermofisher Scientific (former Cellomics Inc.) for excellent support in High-Content-Imaging with the ArrayScan and the Technologiestiftung Berlin for funding the automated microscopes (ESFRI). This work was supported by NGFN Plus Mutanom, IG Cell, IG Neuronet, GABI Centroplanta.

Abbreviations list

CBS, calmodulin binding site

γ-TuRC, γ-Tubulin ring complex

NE, nuclear envelope

NEBD, nuclear envelope breakdown

PCM, pericentriolar matrix

TAP, tandem affinity purification

References

Aihara, H., T. Nakagawa, K. Yasui, T. Ohta, S. Hirose, N. Dhomae, K. Takio, M. Kaneko, Y. Takeshima, M. Muramatsu, and T. Ito. 2004. Nucleosomal histone kinase-1 phosphorylates H2A Thr 119 during mitosis in the early *Drosophila* embryo. *Genes Dev*. 18:877-88.

Andersen, J.S., C.J. Wilkinson, T. Mayor, P. Mortensen, E.A. Nigg, and M. Mann. 2003. Proteomic characterization of the human centrosome by protein correlation profiling. *Nature*. 426:570-4.

Barr, A.R., and F. Gergely. 2007. Aurora-A: the maker and breaker of spindle poles. *J Cell Sci*. 120:2987-96.

Basto, R., K. Brunk, T. Vinadogrova, N. Peel, A. Franz, A. Khodjakov, and J.W. Raff. 2008. Centrosome amplification can initiate tumorigenesis in flies. *Cell*. 133:1032-42.

Beaudouin, J., D. Gerlich, N. Daigle, R. Eils, and J. Ellenberg. 2002. Nuclear envelope breakdown proceeds by microtubule-induced tearing of the lamina. *Cell*. 108:83-96.

Berdnik, D., and J.A. Knoblich. 2002. *Drosophila* Aurora-A is required for centrosome maturation and actin-dependent asymmetric protein localization during mitosis. *Curr Biol*. 12:640-7.

Bettencourt-Dias, M., R. Giet, R. Sinka, A. Mazumdar, W.G. Lock, F. Balloux, P.J. Zafiropoulos, S. Yamaguchi, S. Winter, R.W. Carthew, M. Cooper, D. Jones, L. Frenz, and D.M. Glover. 2004. Genome-wide survey of protein kinases required for cell cycle progression. *Nature*. 432:980-7.

Bettencourt-Dias, M., and D.M. Glover. 2007. Centrosome biogenesis and function: centrosomics brings new understanding. *Nat Rev Mol Cell Biol*. 8:451-63.

Bjorklund, M., M. Taipale, M. Varjosalo, J. Saharinen, J. Lahdenpera, and J. Taipale. 2006. Identification of pathways regulating cell size and cell-cycle progression by RNAi. *Nature*. 439:1009-13.

Blangy, A., L. Arnaud, and E.A. Nigg. 1997. Phosphorylation by p34cdc2 protein kinase regulates binding of the kinesin-related motor HsEg5 to the dynactin subunit p150. *J Biol Chem*. 272:19418-24.

Blower, M.D., E. Feric, K. Weis, and R. Heald. 2007. Genome-wide analysis demonstrates conserved localization of messenger RNAs to mitotic microtubules. *J Cell Biol*. 179:1365-73.

Bodenmiller, B., J. Malmstrom, B. Gerrits, D. Campbell, H. Lam, A. Schmidt, O. Rinner, L.N. Mueller, P.T. Shannon, P.G. Pedrioli, C. Panse, H.K. Lee, R. Schlapbach, and R. Aebersold. 2007. PhosphoPep--a phosphoproteome resource for systems biology research in *Drosophila* Kc167 cells. *Mol Syst Biol*. 3:139.

Bornens, M. 2002. Centrosome composition and microtubule anchoring mechanisms. *Curr Opin Cell Biol*. 14:25-34.

Castedo, M., J.L. Perfettini, T. Roumier, A. Valent, H. Raslova, K. Yakushijin, D. Horne, J. Feunteun, G. Lenoir, R. Medema, W. Vainchenker, and G. Kroemer. 2004. Mitotic catastrophe constitutes a special case of apoptosis whose suppression entails aneuploidy. *Oncogene*. 23:4362-70.

Clemens, J.C., C.A. Worby, N. Simonson-Leff, M. Muda, T. Maehama, B.A. Hemmings, and J.E. Dixon. 2000. Use of double-stranded RNA interference in *Drosophila* cell lines to dissect signal transduction pathways. *Proc Natl Acad Sci U S A*. 97:6499-503.

Crasta, K., P. Huang, G. Morgan, M. Winey, and U. Surana. 2006. Cdk1 regulates centrosome separation by restraining proteolysis of microtubule-associated proteins. *EMBO J*. 25:2551-63.

Cullen, C.F., A.L. Brittle, T. Ito, and H. Ohkura. 2005. The conserved kinase NHK-1 is essential for mitotic progression and unifying acentrosomal meiotic spindles in *Drosophila* melanogaster. *J Cell Biol*. 171:593-602.

Debec, A., and C. Marcaillou. 1997. Structural alterations of the mitotic apparatus induced by the heat shock response in *Drosophila* cells. *Biol Cell*. 89:67-78.

Dobbelaere, J., F. Josue, S. Suijkerbuijk, B. Baum, N. Tapon, and J. Raff. 2008. A genome-wide RNAi screen to dissect centriole duplication and centrosome maturation in Drosophila. *PLoS Biol*. 6:e224.

Doxsey, S., W. Zimmerman, and K. Mikule. 2005. Centrosome control of the cell cycle. *Trends Cell Biol*. 15:303-11.

Eliscovich, C., I. Peset, I. Vernos, and R. Mendez. 2008. Spindle-localized CPE-mediated translation controls meiotic chromosome segregation. *Nat Cell Biol*. 10:858-65.

Evans, D.R., C. Rasmussen, P.J. Hanic-Joyce, G.C. Johnston, R.A. Singer, and C.A. Barnes. 1995. Mutational analysis of the Prt1 protein subunit of yeast translation initiation factor 3. *Mol Cell Biol*. 15:4525-35.

Faust, M., and M. Montenarh. 2000. Subcellular localization of protein kinase CK2. A key to its function? *Cell Tissue Res*. 301:329-40.

Giot, L., J.S. Bader, C. Brouwer, A. Chaudhuri, B. Kuang, Y. Li, Y.L. Hao, C.E. Ooi, B. Godwin, E. Vitols, G. Vijayadamodar, P. Pochart, H. Machineni, M. Welsh, Y. Kong, B. Zerhusen, R. Malcolm, Z. Varrone, A. Collis, M. Minto, S. Burgess, L. McDaniel, E. Stimpson, F. Spriggs, J. Williams, K. Neurath, N. Ioime, M. Agee, E. Voss, K. Furtak, R. Renzulli, N. Aanensen, S. Carrolla, E. Bickelhaupt, Y. Lazovatsky, A. DaSilva, J. Zhong, C.A. Stanyon, R.L. Finley, Jr., K.P. White, M. Braverman, T. Jarvie, S. Gold, M. Leach, J. Knight, R.A. Shimkets, M.P. McKenna, J. Chant, and J.M. Rothberg. 2003. A protein interaction map of Drosophila melanogaster. *Science*. 302:1727-36.

Goldberg, M., H. Lu, N. Stuurman, R. Ashery-Padan, A.M. Weiss, J. Yu, D. Bhattacharyya, P.A. Fisher, Y. Gruenbaum, and M.F. Wolfner. 1998. Interactions among Drosophila nuclear envelope proteins lamin, otefin, and YA. *Mol Cell Biol*. 18:4315-23.

Goshima, G., R. Wollman, S.S. Goodwin, N. Zhang, J.M. Scholey, R.D. Vale, and N. Stuurman. 2007. Genes required for mitotic spindle assembly in Drosophila S2 cells. *Science*. 316:417-21.

Habedanck, R., Y.D. Stierhof, C.J. Wilkinson, and E.A. Nigg. 2005. The Polo kinase Plk4 functions in centriole duplication. *Nat Cell Biol*. 7:1140-6.

Hanic-Joyce, P.J., R.A. Singer, and G.C. Johnston. 1987. Molecular characterization of the yeast PRT1 gene in which mutations affect translation initiation and regulation of cell proliferation. *J Biol Chem*. 262:2845-51.

Harel, A., E. Zlotkin, S. Nainudel-Epszteyn, N. Feinstein, P.A. Fisher, and Y. Gruenbaum. 1989. Persistence of major nuclear envelope antigens in an envelope-like structure during mitosis in Drosophila melanogaster embryos. *J Cell Sci*. 94 (Pt 3):463-70.

Kalt, A., and M. Schliwa. 1993. Molecular components of the centrosome. *Trends Cell Biol*. 3:118-28.

Keller, L.C., E.P. Romijn, I. Zamora, J.R. Yates, 3rd, and W.F. Marshall. 2005. Proteomic analysis of isolated chlamydomonas centrioles reveals orthologs of ciliary-disease genes. *Curr Biol*. 15:1090-8.

Kovarik, P., J. Hasek, L. Valasek, and H. Ruis. 1998. RPG1: an essential gene of saccharomyces cerevisiae encoding a 110-kDa protein required for passage through the G1 phase. *Curr Genet*. 33:100-9.

Lane, H.A., and E.A. Nigg. 1996. Antibody microinjection reveals an essential role for human polo-like kinase 1 (Plk1) in the functional maturation of mitotic centrosomes. *J Cell Biol*. 135:1701-13.

Lange, B.M. 2002. Integration of the centrosome in cell cycle control, stress response and signal transduction pathways. *Curr Opin Cell Biol*. 14:35-43.

Lehmann, V., H. Müller, and B.M. Lange. 2006. Immunoisolation of centrosomes from Drosophila melanogaster. *Curr Protoc Cell Biol*. Chapter 3:Unit 3 17.

Li, J.B., J.M. Gerdes, C.J. Haycraft, Y. Fan, T.M. Teslovich, H. May-Simera, H. Li, O.E. Blacque, L. Li, C.C. Leitch, R.A. Lewis, J.S. Green, P.S. Parfrey, M.R. Leroux, W.S. Davidson, P.L. Beales, L.M. Guay-Woodford, B.K. Yoder, G.D. Stormo, N. Katsanis, and S.K. Dutcher. 2004. Comparative genomics identifies a flagellar and basal body proteome that includes the BBS5 human disease gene. *Cell*. 117:541-52.

Liska, A.J., A.V. Popov, S. Sunyaev, P. Coughlin, B. Habermann, A. Shevchenko, P. Bork, and E. Karsenti. 2004. Homology-based functional proteomics by mass spectrometry: application to the Xenopus microtubule-associated proteome. *Proteomics*. 4:2707-21.

Lucas, E.P., and J.W. Raff. 2007. Maintaining the proper connection between the centrioles and the pericentriolar matrix requires Drosophila centrosomin. *J Cell Biol*. 178:725-32.

Maiato, H., P.J. Hergert, S. Moutinho-Pereira, Y. Dong, K.J. Vandenbeldt, C.L. Rieder, and B.F. McEwen. 2006. The ultrastructure of the kinetochore and kinetochore fiber in Drosophila somatic cells. *Chromosoma*. 115:469-80.

Malone, C.J., L. Misner, N. Le Bot, M.C. Tsai, J.M. Campbell, J. Ahringer, and J.G. White. 2003. The C. elegans hook protein, ZYG-12, mediates the essential attachment between the centrosome and nucleus. *Cell*. 115:825-36.

Mirgorodskaya, E., C. Braeuer, P. Fucini, H. Lehrach, and J. Gobom. 2005. Nanoflow liquid chromatography coupled to matrix-assisted laser desorption/ionization mass spectrometry: sample preparation, data analysis, and application to the analysis of complex peptide mixtures. *Proteomics*. 5:399-408.

Mishra, R.K., P. Chakraborty, A. Arnaoutov, B.M. Fontoura, and M. Dasso. 2010. The Nup107-160 complex and gamma-TuRC regulate microtubule polymerization at kinetochores. *Nat Cell Biol*. 12:164-9.

Moritz, M., and B.M. Alberts. 1999. Isolation of centrosomes from Drosophila embryos. *Methods Cell Biol*. 61:1-12.

Müller, H., M.L. Fogeron, V. Lehmann, H. Lehrach, and B.M. Lange. 2006. A centrosome-independent role for gamma-TuRC proteins in the spindle assembly checkpoint. *Science*. 314:654-7.

Nousiainen, M., H.H. Sillje, G. Sauer, E.A. Nigg, and R. Korner. 2006. Phosphoproteome analysis of the human mitotic spindle. *Proc Natl Acad Sci U S A*. 103:5391-6.

Okuda, M. 2002. The role of nucleophosmin in centrosome duplication. *Oncogene*. 21:6170-4.

Paddy, M.R., H. Saumweber, D.A. Agard, and J.W. Sedat. 1996. Time-resolved, in vivo studies of mitotic spindle formation and nuclear lamina breakdown in Drosophila early embryos. *J Cell Sci*. 109 (Pt 3):591-607.

Palazzo, R.E., J.M. Vogel, B.J. Schnackenberg, D.R. Hull, and X. Wu. 2000. Centrosome maturation. *Curr Top Dev Biol*. 49:449-70.

Qi, H., U. Rath, D. Wang, Y.Z. Xu, Y. Ding, W. Zhang, M.J. Blacketer, M.R. Paddy, J. Girton, J. Johansen, and K.M. Johansen. 2004. Megator, an essential coiled-coil protein that localizes to the putative spindle matrix during mitosis in Drosophila. *Mol Biol Cell*. 15:4854-65.

Resendes, K.K., B.A. Rasala, and D.J. Forbes. 2008. Centrin 2 localizes to the vertebrate nuclear pore and plays a role in mRNA and protein export. *Mol Cell Biol*. 28:1755-69.

Robinson, J.T., E.J. Wojcik, M.A. Sanders, M. McGrail, and T.S. Hays. 1999. Cytoplasmic dynein is required for the nuclear attachment and migration of centrosomes during mitosis in Drosophila. *J Cell Biol*. 146:597-608.

Salina, D., K. Bodoor, D.M. Eckley, T.A. Schroer, J.B. Rattner, and B. Burke. 2002. Cytoplasmic dynein as a facilitator of nuclear envelope breakdown. *Cell*. 108:97-107.

Salpingidou, G., A. Smertenko, I. Hausmanowa-Petrucewicz, P.J. Hussey, and C.J. Hutchison. 2007. A novel role for the nuclear membrane protein emerin in association of the centrosome to the outer nuclear membrane. *J Cell Biol*. 178:897-904.

Sluder, G. 2005. Two-way traffic: centrosomes and the cell cycle. *Nat Rev Mol Cell Biol*. 6:743-8.

Somma, M.P., F. Ceprani, E. Bucciarelli, V. Naim, V. De Arcangelis, R. Piergentili, A. Palena, L. Ciapponi, M.G. Giansanti, C. Pellacani, R. Petrucci, G. Cenci, F. Verni, B. Fasulo, M.L. Goldberg, F. Di Cunto, and M. Gatti. 2008. Identification of Drosophila mitotic genes by combining co-expression analysis and RNA interference. *PLoS Genet*. 4:e1000126.

Sunkel, C.E., and D.M. Glover. 1988. polo, a mitotic mutant of Drosophila displaying abnormal spindle poles. *J Cell Sci*. 89 (Pt 1):25-38.

Suprenant, K.A. 1993. Microtubules, ribosomes, and RNA: evidence for cytoplasmic localization and translational regulation. *Cell Motil Cytoskeleton*. 25:1-9.

Thingholm, T.E., T.J. Jorgensen, O.N. Jensen, and M.R. Larsen. 2006. Highly selective enrichment of phosphorylated peptides using titanium dioxide. *Nat Protoc*. 1:1929-35.

Tsai, M.Y., S. Wang, J.M. Heidinger, D.K. Shumaker, S.A. Adam, R.D. Goldman, and Y. Zheng. 2006. A mitotic lamin B matrix induced by RanGTP required for spindle assembly. *Science*. 311:1887-93.

Ulitzur, N., A. Harel, M. Goldberg, N. Feinstein, and Y. Gruenbaum. 1997. Nuclear membrane vesicle targeting to chromatin in a Drosophila embryo cell-free system. *Mol Biol Cell*. 8:1439-48.

Verollet, C., N. Colombie, T. Daubon, H.M. Bourbon, M. Wright, and B. Raynaud-Messina. 2006. Drosophila melanogaster gamma-TuRC is dispensable for targeting gamma-tubulin to the centrosome and microtubule nucleation. *J Cell Biol*. 172:517-28.

Wigge, P.A., O.N. Jensen, S. Holmes, S. Soues, M. Mann, and J.V. Kilmartin. 1998. Analysis of the Saccharomyces spindle pole by matrix-assisted laser desorption/ionization (MALDI) mass spectrometry. *J Cell Biol*. 141:967-77.

Zhai, B., J. Villen, S.A. Beausoleil, J. Mintseris, and S.P. Gygi. 2008. Phosphoproteome analysis of Drosophila melanogaster embryos. *J Proteome Res*. 7:1675-82.

Figure legends

Figure 1. **Phosphoproteome analysis of the *Drosophila* embryo centrosome**

Centrosomes for subsequent phosphoproteome analysis were enriched from *Drosophila melanogaster* embryos through sucrose gradient centrifugation followed by immunoisolation. **(A)** Immunofluorescence microscopy with anti-cnn antibody shows enrichment of centrosomes (white) at different isolation stages: embryo homogenate (EH), centrosome enriched fraction (CEF) after velocity sedimentation and immunopurified centrosomes (red, IPC) bound to magnetic beads (green). Scale bar, 10 µm. **(B)** Western blotting with antibodies against centrosomal proteins γ-Tubulin and Grip84 confirms the enrichment of centrosomes throughout the isolation procedure. **(C)** To detect the abundance of phosphoproteins in our centrosome preparations, samples from different isolation steps, a negative control (mock) and two molecular weight standards, which contain two (M1) and one (M2) phosphorylated protein bands, respectively, were separated on a 10% polyacrylamide gel and stained with ProQ-Diamond phosphoprotein gel stain and SYPRO Ruby total protein gel stain. The total protein as well as the phosphoprotein patterns observed in the embryo homogenate significantly differed from the ones seen after centrosome enrichment and affinity-purification. An enrichment of at least 20 phosphorylated protein bands (arrows) was observed in the immunopurified sample, with the most prominent band at around 130 kD. **(D)** Table 1 lists 45 phosphorylation sites and their respective consensus kinase motifs identified in 27 proteins from immunopurified *Drosophila* centrosomes using enrichment of trypsin-digested phosphopeptides on titanium dioxide columns followed by MS analysis. A comparison with two whole phosphoproteome analyses in *Drosophila* Kc167 cells (Bodenmiller et al., 2007) and *Drosophila* early embryos (Zhai et al., 2008) is given in column 5 and 6● indicates that a site was identified and ○ indicates that a site was not identified in the respective study. **(E)** The Venn diagram illustrates the overlap of the 45 phosphorylation sites identified with our approach and the two whole phosphoproteome studies conducted in *Drosophila*. The total number of identified phosphorylation sites in each study is given in parenthesis.

Figure 2. **Functional characterization of phosphoproteins and regulatory kinases applying RNAi, automated immunofluorescence microscopy imaging and FACS**

(A) Representative fluorescence microscopy images illustrate the image processing and segmentation approach, which was applied to assign identified phosphoproteins and kinases to regulatory pathways. RNAi treated SL2 cells were analysed with respect to the effect on number and size of mitotic centrosomes (labeled with anti-cnn, green) using an algorithm

that reports amount and morphology of intracellular objects. Cell cycle effects were monitored via calculating the ratio of total number of cells (labeled with cytoplasmic stain, blue) segmented in channel 1 to the number of mitotic cells (labeled with phospho-histone-H3 antibody, red) selected in channel 2. **(B)** Examples of mitotic cells (centrosomes in green and chromosomes in red) reflecting the 6 aberrant centrosome phenotypes that were observed after RNAi mediated gene silencing: no centrosome (structure maintenance), one, one small or one large centrosome (duplication/separation), small and large centrosomes (maturation). Knockdown of *egfp* served as a negative control. The corresponding RNAi target proteins are indicated within each image. **(C)** FACS analysis of SL2 cells incubated with dsRNA reveals genes involved in the regulation of cell cycle progression. Three types of aberrant cell cycle distribution profiles were identified: increased subG1 DNA content, increased number of polyploid cells and accumulation of cells in G0/G1 phase of the cell cycle. Each profile shown contains a control histogram (grey, cells treated with dsRNA targeting egfp) and aberrant histogram representative for its phenotypic class (red line, names of all target genes exhibiting similar profiles upon depletion are given in the corresponding panel). **(D)** Two fluorescence microscopy images (superimposition of DAPI, blue and mitotic chromosomes, red) representative of cells displaying low or high mitotic indices after dsRNA treatment are shown. Proteins whose depletion induced an aberrant proportion of mitotic cells are given on the right of the corresponding image. **(E)** Cells were manually scored for chromosome segregation defects after depletion of target proteins. A control cell depleted of egfp with normal chromosome (red) alignment in metaphase and an example of abnormally distributed mitotic chromosomes is shown. The proteins inducing this phenotype are given on the right side of the panel.

Figure 3. **Integration of phosphoproteins in pathways regulating the centrome cycle, cell cycle and chromosome segregation**

Functional implications of 25 phosphoproteins and 4 kinases (bottom rows) in signaling pathways controlling centrosome duplication/segregation, centrosome maturation/structure as well as cell cycle progression and chromosome segregation were identified by RNAi phenotype scoring in SL2 cells. Protein functions identified in single knockdown experiments are depicted in olive panels. Protein functions identified by the occurrence of synthetic phenotypes resulting from simultaneous downregulation of a phosphoprotein and either of the 4 kinases are color coded as follows: polo in purple, aur in orange, cdc2 in blue and CkIIβ in red. ↑ and ↓ indicate that simultaneous depletion of the phosphoprotein leads to increased or decreased strength of the kinase RNAi phenotype. ± indicates that the phenotype observed after kinase inhibition is reverted when additionally depleting a phosphoprotein. ±

indicates a mixed phenotype after simultaneous knockdown as compared to single knockdown phenotypes of the corresponding phosphoprotein and kinase≠ ind icates that a phenotype is induced only by simultaneous downregulation of phosphoprotein and kinase while depletion of one component does not lead to aberrations in the respective category.→ indicates a dominant phosphoprotein RNAi phenotype.

Figure 4. **Expression of MS-identified phosphoproteins in SL2 cells confirms known localizations and identifies new spindle and centrosome localizations**

Immunofluorescence microscopy of SL2 cells expressing GFP/FLAG/TAP fusion proteins labeled with anti-GFP/FLAG/CBS (green), a centrosome marker (anti-gamma-tubulin or anti-cnn, red) and DAPI (blue) confirms known localization to the centrosome (spd-2 and Grip84), the nuclear membrane (Ote and Lam), the nucleus/chromatin (ewg and ball), P granules (bel and Dcp1) and the cytosol (eIF3-S8). GFP-control cells show uniform distribution of the tag. Localization was monitored throughout the cell cycle and representative images for interphase and mitotic localization of each fusion protein are shown. Previously unknown localization to the anaphase spindle was identified for Ote, Lam and Dcp1. eIF3-S8 and bel localize to the metaphase spindle and additionally, bel and Ote co-localize with centrosomes.

Figure 5. **Nuclear membrane protein Ote localizes to interphase centrosomes and functions downstream of aur in centrosome maturation**

(A) Localization of endogenous NE proteins Ote and Lam is shown throughout the cell cycle. SL2 cells were labeled with anti-Ote (red) and anti-α-Tub (green) or anti-Lam (red) and anti-cnn antibodies (green). Superimposition with DAPI in blue. **(B)** Endogenous Ote and overexpressed FLAG tagged Ote localize to centrosomes in interphase. Fluorescence microscopy image of a SL2 cell labeled with rabbit anti-Ote (green) and anti-γ-Tub (red) is shown in the left panel. Cells stably expressing Ote fused to a FLAG tag were labeled with rabbit anti-FLAG (green) and anti-γ-Tub (red) (middle panel). The right panel shows a cell expressing TAP tagged nuclear protein scra as a negative control, in which the tag was labeled with rabbit immunoglobulin (IgG, green) and the centrosome with anti-γ-Tub (red). Superimpositions of both channels are shown in the bottom row and magnifications of the area around the interphase centrosomes are given in each image. Fluorescent images in the right panel serve as a control for the specificity of the anti-Ote antibody as well as the specificity of fusion protein localization. Brightness and contrast of endogenous Ote staining was enhanced three-fold in the magnified section to clarify localization of a minor portion of

the protein to the centrosome while the majority of the protein localizes to the nuclear membrane. **(C)** Extracts from SL2 cells expressing FLAG tagged Ote and GFP tagged Lam were analyzed by immunoprecipitation with anti-FLAG and anti-GFP, respectively. Interacting proteins were determined by Western blotting with specific antibodies targeting α-Tub, γ-Tub, aur and Lam. The known interaction of Lam and Ote was verified and additionally α-Tub, γ-Tub and aur were found to copurify with FLAG:Ote while the purified GFP:Lam complex is lacking γ-Tub. SL2 cells expressing the GFP tag (pAWG) and untransfected cells (control) served as controls for GFP- and FLAG-IP, respectively. **(D)** Ote functionally interacts with aur. Phenotypes of single and double knockdowns regarding centrosome size and mitotic index are shown in the graphs. egfp RNAi served as control. The schematic illustrates the possible regulatory mechanism. ---| indicates negative regulation of the phosphoprotein Ote by the kinase aur. **(E)** The graph shows effects on mitotic index upon downregulation of NE proteins Lam and Nup98 and polo kinase as well as synthetic phenotypes observed after depletion in polo depleted background. The schematic illustrates the pathway model.

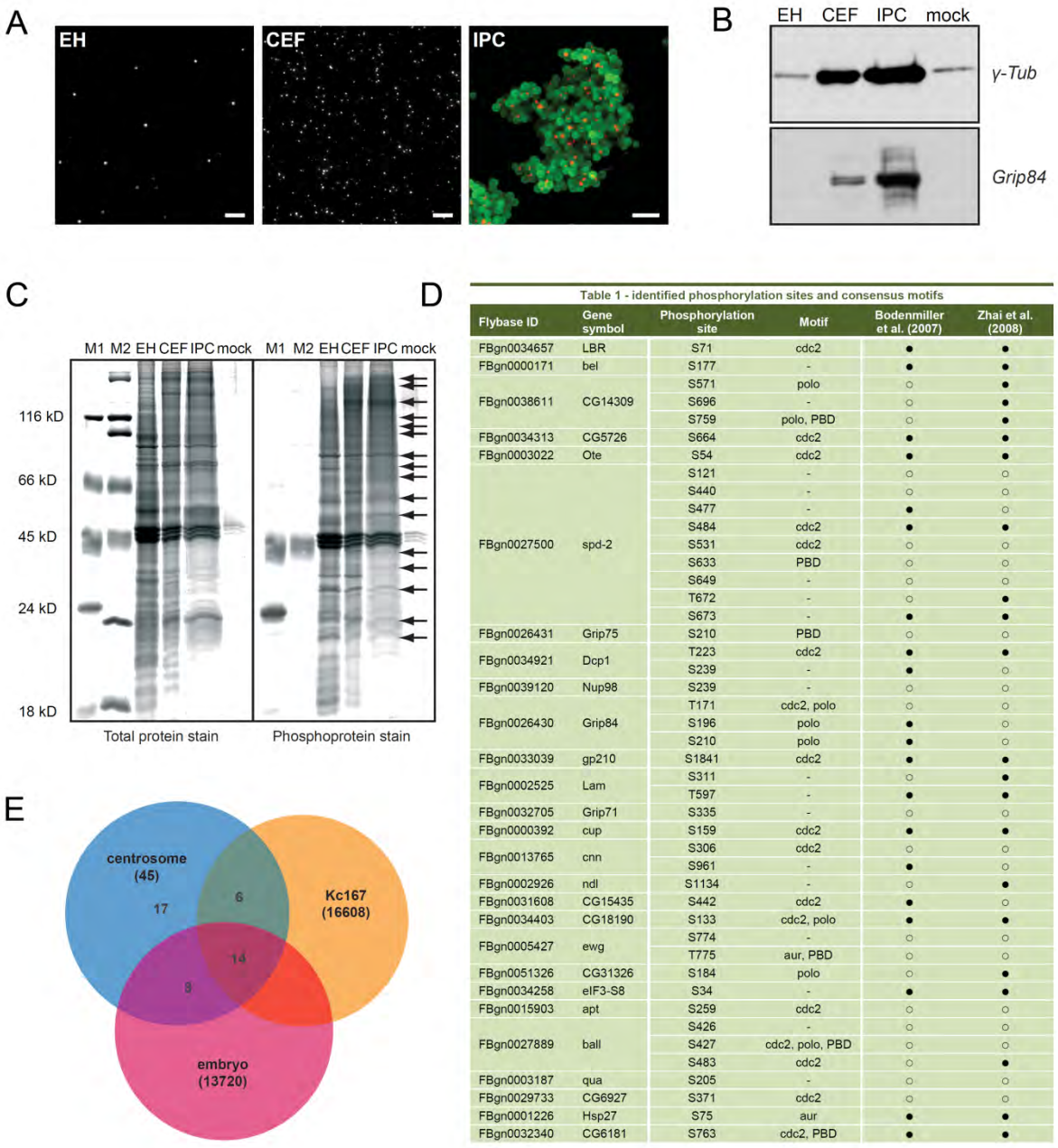

Table 1 - identified phosphorylation sites and consensus motifs

Flybase ID	Gene symbol	Phosphorylation site	Motif	Bodenmiller et al. (2007)	Zhai et al. (2008)
FBgn0034657	LBR	S71	cdc2	●	●
FBgn0000171	bel	S177	-	●	●
FBgn0038611	CG14309	S571	polo	○	●
		S696	-	○	●
		S759	polo, PBD	○	●
FBgn0034313	CG5726	S664	cdc2	●	●
FBgn0003022	Ote	S54	cdc2	●	●
FBgn0027500	spd-2	S121	-	○	○
		S440	-	○	○
		S477	-	●	○
		S484	cdc2	●	●
		S531	cdc2	○	○
		S633	PBD	○	○
		S649	-	○	○
		T672	-	○	●
		S673	-	●	●
FBgn0026431	Grip75	S210	PBD	○	○
FBgn0034921	Dcp1	T223	cdc2	●	●
		S239	-	●	○
FBgn0039120	Nup98	S239	-	○	○
FBgn0026430	Grip84	T171	cdc2, polo	○	○
		S196	polo	●	○
		S210	polo	●	○
FBgn0033039	gp210	S1841	cdc2	●	●
FBgn0002525	Lam	S311	-	○	●
		T597	-	●	●
FBgn0032705	Grip71	S335	-	○	○
FBgn0000392	cup	S159	cdc2	●	●
FBgn0013765	cnn	S306	cdc2	○	○
		S961	-	●	○
FBgn0002926	ndl	S1134	-	○	●
FBgn0031608	CG15435	S442	cdc2	●	○
FBgn0034403	CG18190	S133	cdc2, polo	●	●
FBgn0005427	ewg	S774	-	○	○
		T775	aur, PBD	○	○
FBgn0051326	CG31326	S184	polo	○	●
FBgn0034258	eIF3-S8	S34	-	●	●
FBgn0015903	apt	S259	cdc2	○	○
FBgn0027889	ball	S426	-	○	○
		S427	cdc2, polo, PBD	○	○
		S483	cdc2	○	●
FBgn0003187	qua	S205	-	○	○
FBgn0029733	CG6927	S371	cdc2	○	○
FBgn0001226	Hsp27	S75	aur	●	●
FBgn0032340	CG6181	S763	cdc2, PBD	●	●

Figure 1
Habermann et al.

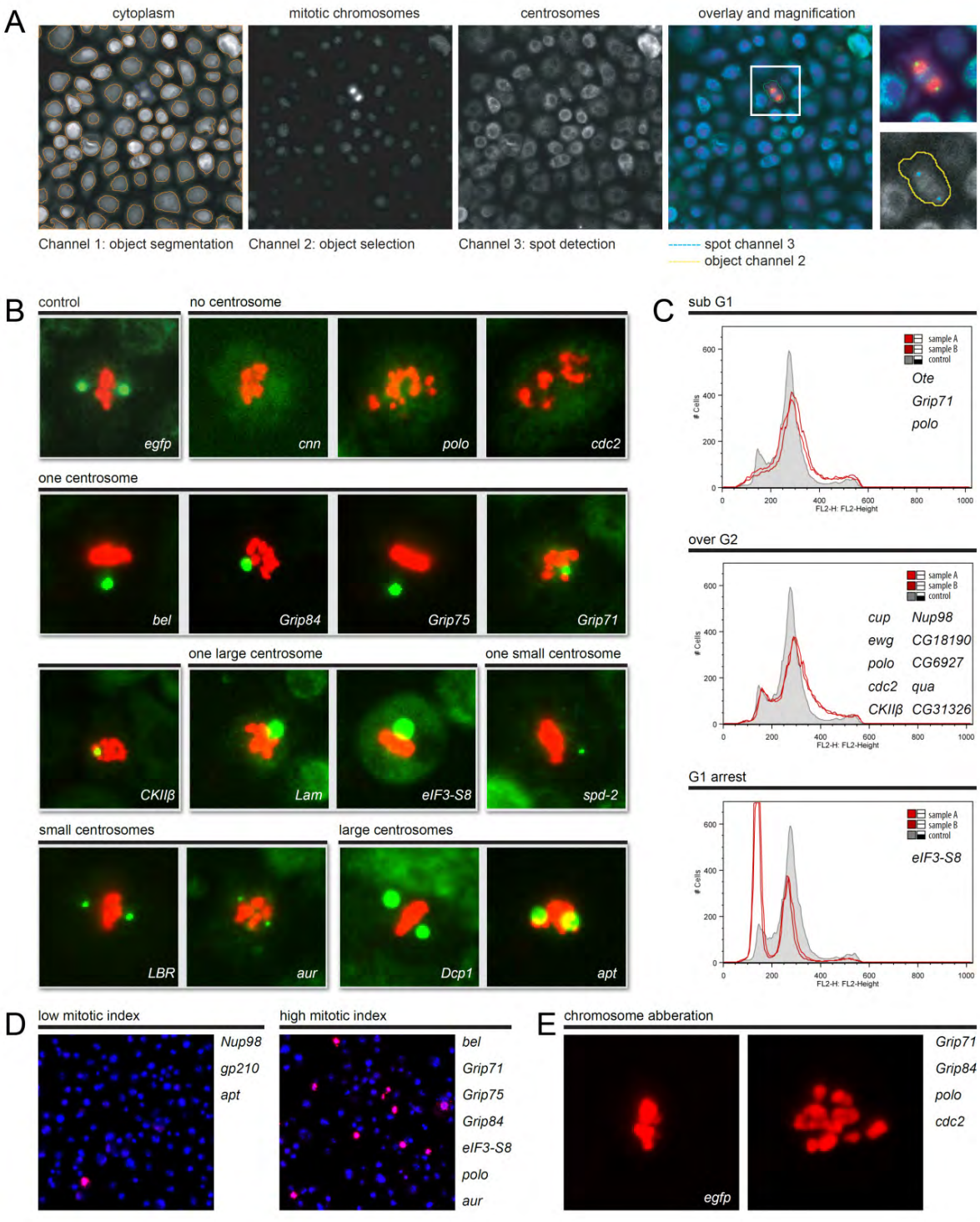

Figure 2
Habermann et al.

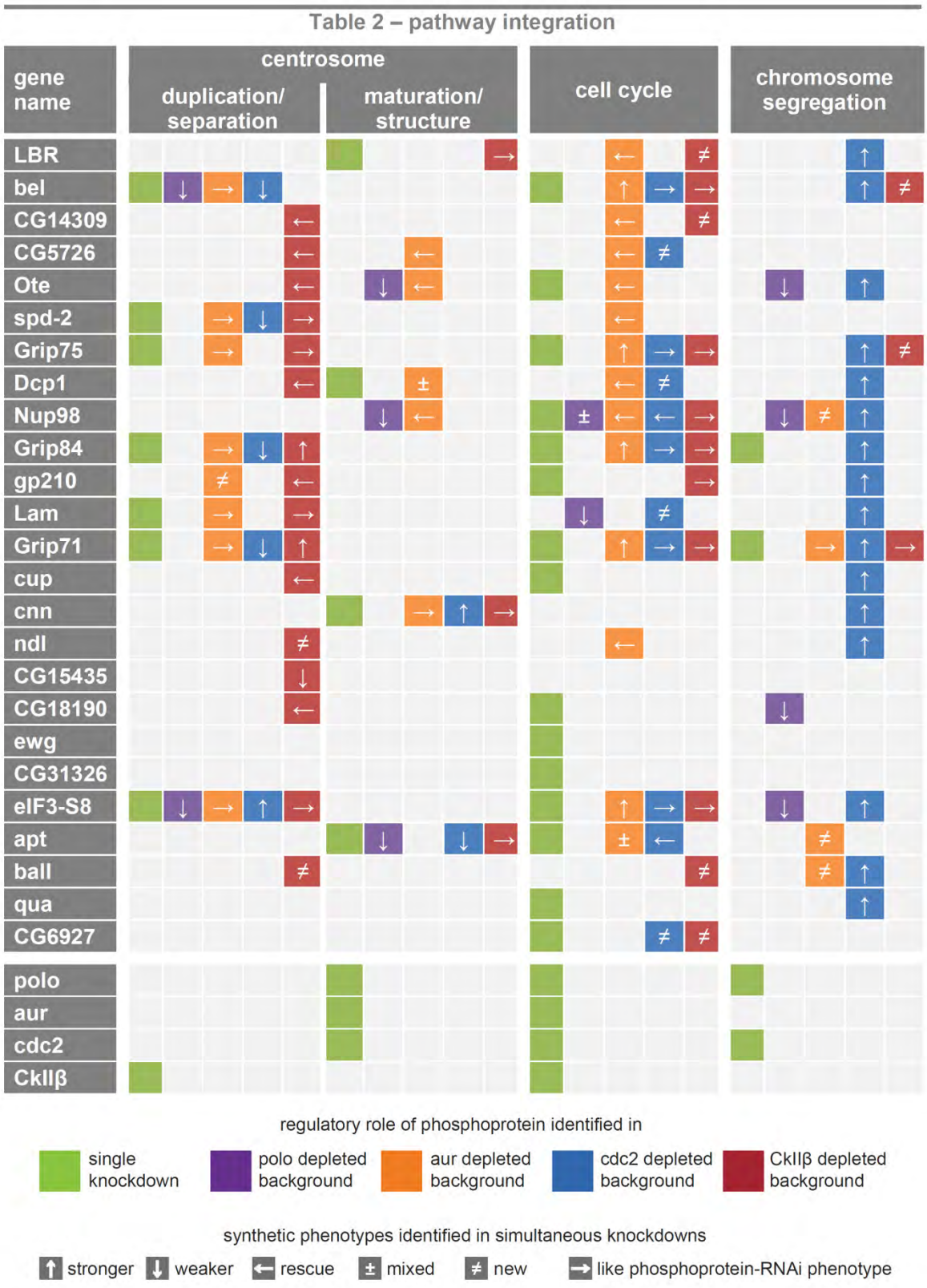

Figure 3
Habermann et al.

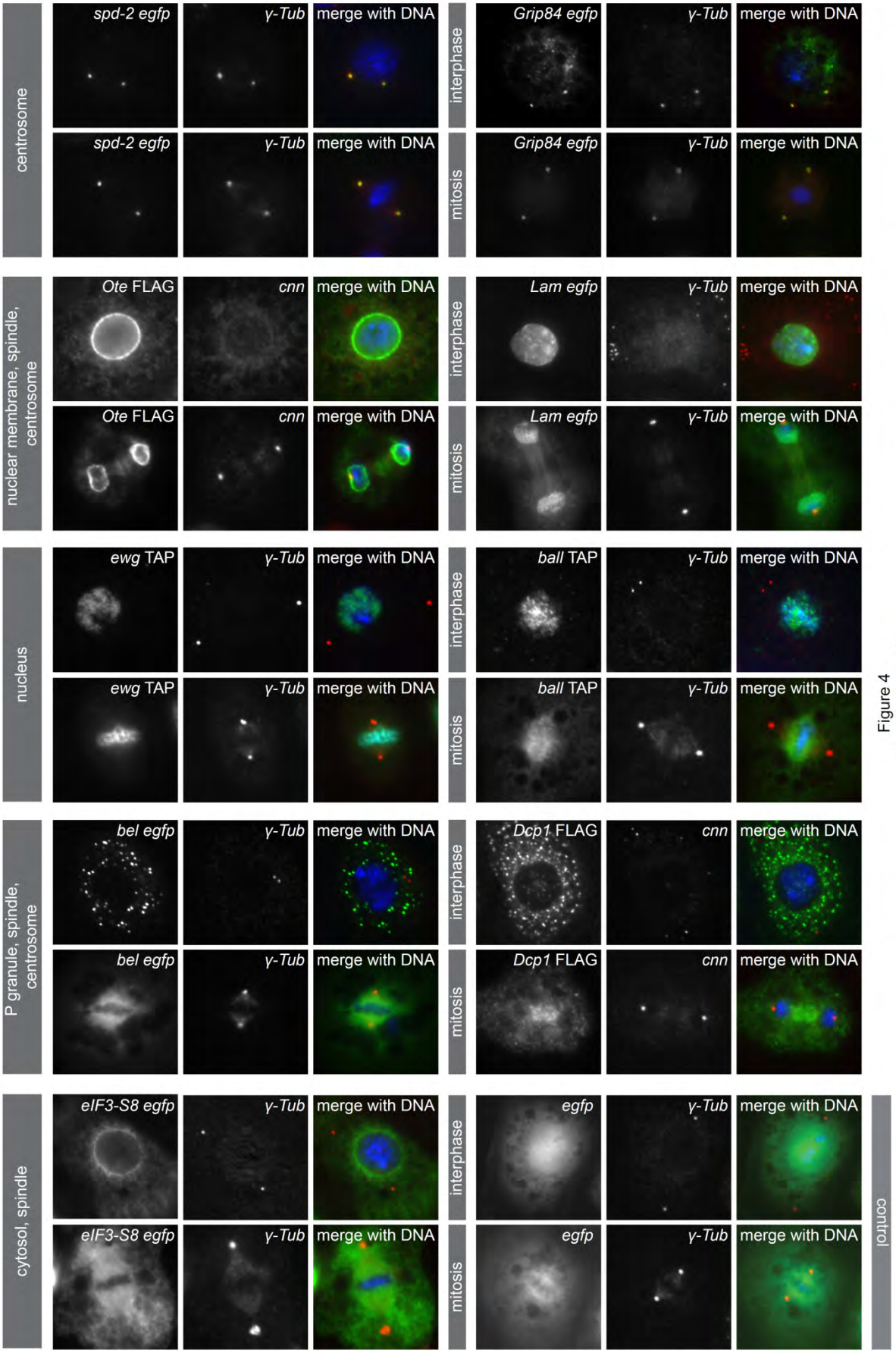

Figure 4
Habermann *et al.*

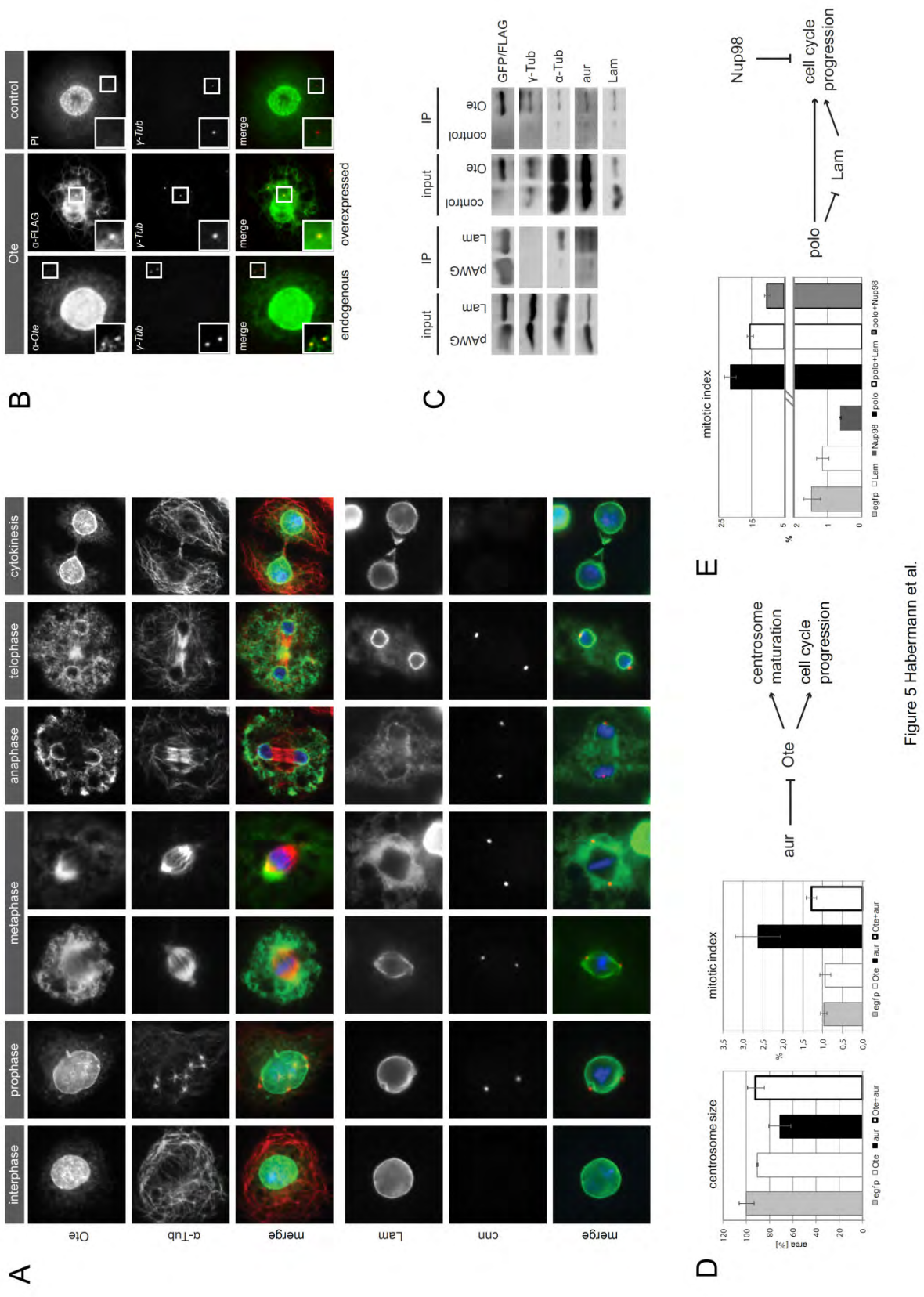

Figure 5 Habermann et al.

Online supplemental material

Table S1. **RNAi phenotypes of phosphoproteins in SL2 cells assigned from single knockdowns and in a background of 4 simultaneously depleted kinases**

Significant phenotypes regarding centrosome duplication/segregation, centrosome morphology, cell cycle progression and chromosome segregation upon depletion of 25 MS-identified phosphoproteins and 4 kinases are listed in the left olive panel and highlighted in a dark shade. egfp RNAi served as a control (bottom row). Additionally, synergistic effects were analyzed by simultaneous knockdowns of phosphoproteins with each of the 4 kinases. Light and dark shades indicate a weaker and stronger phenotype, respectively compared to the single knockdown of polo (purple panel), aur (orange panel), cdc2 (blue panel) or CkIIβ (red panel). Panels shaded like the control bottom row indicate that no significant phenotype was observed in the category. • indicate that the number of cells with abnormal chromosomes was significantly increased compared to control cells.

Table S2. **Oligos, plasmids, z-scores, p-values, GO terms**

Sequences of all RNAi and cloning primers as well as plasmids used in this study are listed. Furthermore, we show z-scores for FACS analysis and p-values for single knockdown analysis. Consistency of our results with relevant high throughput datasets and gene ontology annotation from Uniprot is also indicated.

Table S1 - RNAi phenotypes

Gene symbol	Human homologue	single knockdown					double knockdown with polo				double knockdown with aur				double knockdown with cdc2				double knockdown with CkIIβ			
		centrosome number	centrosome size	mitotic index	chromosome aberration	FACS	centrosome number	centrosome size	mitotic index	chromosome aberration	centrosome number	centrosome size	mitotic index	chromosome aberration	centrosome number	centrosome size	mitotic index	chromosome aberration	centrosome number	centrosome size	mitotic index	chromosome aberration
LBR	LBR		small				0	small	high	•		small			0	n/a		•		small	low	
bel	DDX3X	1		high			0	small	high	•	1	large	high		0	n/a	high	•	1		high	•
CG14309	-						0	small	high	•		small			0	n/a		•			low	
CG5726	-						0	small	high	•					0	n/a	high	•				
Ote	-					< G1	0	small	high	•					0	n/a		•				
spd-2	CEP192	1	small				0	small	high	•	0/1	small			0	n/a		•	0/1	small		
Grip75	TUBGCP4	1		high			0	small	high	•	1		high		0	n/a	high	•	0/1		high	•
Dcp1	DCP1B		large				0	small	high	•					0	n/a	high	•				
Nup98	NUP98			low		> G2	0	small	high	•				•	0	n/a		•	1		low	
Grip84	TUBGCP2	1		high	•		0	small	high	•	1	small	high		0	n/a	high	•	1		high	
gp210	NUP210			low			0	small	high	•	>2	small	high		0	n/a		•			low	
Lam	LMNB2	0/1	large				0	small	high	•	0		high		0	n/a	high	•	0/1	large		
Grip71	NEDD1	1		high	•	< G1	0	small	high	•	1		high	•	0	n/a	high	•	1		high	•
cup	-					> G2	0	small	high	•		small	high		0	n/a		•				
cnn	CDK5RAP2	0	small				0	small	high	•	0	small	high		0	n/a		•	0	small		
ndl	-						0	small	high	•		small			0	n/a		•	1	large		
CG15435	-						0	small	high	•		small	high		0	n/a		•	1			
CG18190	-					> G2	0	small	high	•		small	high		0	n/a		•				
ewg	NRF1					> G2	0	small	high	•		small	high		0	n/a		•	1			
CG31326	-					> G2	0	small	high	•		small	high		0	n/a		•	1			
eIF3-S8	EIF3S8	0/1	large	high		G1/G0	0	small	high	•	0/1	large	high		0	n/a	high		0/1	large	high	
apt	-		large	low			0	small	high	•		small		•	0	n/a		•		large		
ball	VRK1						0	small	high	•		small	high	•	0	n/a		•	1	large	high	
qua	-					> G2	0	small	high	•		small	high		0	n/a		•	1			
CG6927	-					> G2	0	small	high	•		small	high		0	n/a	high	•	1		high	
polo	PLK1	0	small	high	•	< G1/ > G2	0	small	high	•		small	high		0	n/a		•	1			
aur	AURKA		small	high																		
cdc2	CDC2	0			•	> G2																
CkIIβ	CSNK2B	1				> G2																
egfp																						

Supplementary Table 2 - oligos, plasmids, z-scores, p-values, GO terms

gene symbol	annotation symbol	Flybase ID	human homologue	RNAi primer		amplicon length (b)	cloning primer				amplicon length (b)	stable SL2 cell line		
							N-terminal		C-terminal					
				3' T7	5' T7		3' attB	5' attB	3' attB	5' attB		GFP expression vector	TAP expression vector (clone ID)	FLAG expression vector (clone ID)
LBR	CG17952	FBgn0034657	LBR	GCCAGTCCTGCCATAATCA	AGTTGAAGGCTCCTAGAGAA	543								
bel	CG9748	FBgn0000171	DDX3X	GGTTGGCGGCATGTTTAG	CACCGGTGCAGAAGCAC	540	GGGGACCACTTTGTACAAGAAAGCTGGGTCTCATTGAGC CCACCAGTCGG	GGGGACAAGTTTGTACAAAAAAGCAGGCTTCAGTAATG CTATTAACCAAAA	-	-	2460	pAGW	pDEST NTAP	
CG14309	CG14309	FBgn0038611	-	AGTCGAAAAGGGGCTTATTC	CTGCCCGATGTCAATCTG	551								
CG5726	CG5726	FBgn0034313	-	CTATGCTGGCTGGTTGTTG	GCTGACCGCTAAGGTGAA	537								
Ote	CG5581	FBgn0003022	-	CCTTGGGCTGCAGTACG	TCCGAGGAGCCCGTTG	546							pMK33 C-TAP (MXO52604)	pMK33 C-FLAG-HA (FMO02634)
spd-2	CG17286	FBgn0027500	-	CATCCGCAAATCACCATCA	GTGGAACTGGCCTCACTAC	512	TTAAAATTTAAAACTAATCGGGACA	CAACGACAGTAGCAGTGGAAGCCAA	-	-		pAGW	pDEST CTAP, NTAP	
Grip75	CG6176	FBgn0026431	TUBGCP4	CAGGATTTTTCTCCATCGTTT	CTGGCAGATCAGTGAAAACT	570								
Dcp1	CG11183	FBgn0034921	DCP1B	GCGCCGTTAAATTCACAAAT	CACATCGGTCTTTTCCCACT	216								pMK33 C-FLAG-HA (FMO04886)
Nup98	CG10198	FBgn0039120	NUP98	CAGGCGGTGCTTGGAG	CAGAGGGAACGTGCAGTT	614								
Grip84	CG3917	FBgn0026430	TUBGCP2	GTCCTCGTTGGTGATCATTC	GGTCGTTCTCCGTTAGCA	512	-	-	GGGGACCACTTTGTACAAGAAAGCTGGGTCGCCAATGG CATCCTCTACAC	GGGGACAAGTTTGTACAAAAAAGCAGGCTACCATGGGTTACG CACTGCTGGTGTT	2522	pAWG	pDEST CTAP	
gp210	CG7897	FBgn0033039	NUP210	TTTTGATTCCAAAGGGAGGAC	CGAGACGCAGTTCACTTAC	540								
Lam	CG6944	FBgn0002525	LMNB2	CCATAAGGTCCTGGTACTCC	GGAGAACACCATTCAGAGTC	552	GGGGACCACTTTGTACAAGAAAGCTGGGTCTTACATAAT GGCGCACTTCT	GGGGACAAGTTTGTACAAAAAAGCAGGCTTCTCGAGCA AATCCCGACGTGC	GGGGACCACTTTGTACAAGAAAGCTGGGTCCATAATGG CGCACTTCTCGT	GGGGACAAGTTTGTACAAAAAAGCAGGCTACCATGGGTTCGA GCAAATCCCGACGTGC	1931	pAWG , pAGW	pDEST CTAP, NTAP	
Grip71	CG10346	FBgn0032705	NEDD1	TCGTGCTCAGGCCTCTA	TTGCGGTTTTCGGTTGAG	514								
Eyp	CG11181	FBgn0000392	-	CAGGTCCAAGGAGAGCTTTG	TTGGAATGGTTTAAGCGACC	321								
cnn	CG4832	FBgn0013765	CDK5RAP2	GTGGTCAACCTGTCGAAAATA	GGCGGATGCTGTTTCCTT	242								
ndl	CG10129	FBgn0002926	-	TTTTCCTCGCTCTCCTTCA	TCCCATGCGCCAGGTTA	553								
CG15435	CG15435	FBgn0031608	-	GGCCAGAAGCGAGTCTAT	AGTACTTAAACGTGCTGTTCA	555								
CG18190	CG18190	FBgn0034403	-	CCATCTATCGTTTTGTAGAGC	CAGATGATGGAGATGATCTTTC	555								
ewg	CG3114	FBgn0005427	NRF1	TCTGTTTGTCATCCTCTGAAC	TAAAAAGCGAAAGAGACCCC	559	GGGGACCACTTTGTACAAGAAAGCTGGGTCCTACCCCAA GTGCTCCAGTT	GGGGACAAGTTTGTACAAAAAAGCAGGCTTCCTGGAAG AGGATATCCAGAG	GGGGACCACTTTGTACAAGAAAGCTGGGTCCCCCAAGT GCTCCAGTTTAA	GGGGACAAGTTTGTACAAAAAAGCAGGCTACCATGggtCTGGA AGAGGATATCCA	2320	pAGW	pDEST CTAP, NTAP	
CG31326	CG31326	FBgn0051326	-	GAGTGAATGGCCAAAGTATTTC	GTCAACCCAGACTAGAGGATA	548								
eIF3-S8	CG4954	FBgn0034258	EIF3S8	GATGTGCGCCAGGATGG	GCCCATGAAGCTAGAACAC	548	GGGGACCACTTTGTACAAGAAAGCTGGGTCCTACTCCTC GTCGATCGTTT	GGGGACAAGTTTGTACAAAAAAGCAGGCTTCTCGCGTT TCTTTGCCAACGG	GGGGACCACTTTGTACAAGAAAGCTGGGTCCTCCTCGT CGATCGTTTGGA	GGGGACAAGTTTGTACAAAAAAGCAGGCTACCATGggtTCGCG TTTCTTTGCCAA	2790	pAWG , pAGW	pDEST CTAP, NTAP	
apt	CG5393	FBgn0015903	-	CTGCCCAACATGCTACCA	ACACCGCCGCAGGAAC	546								
ball	CG6386	FBgn0027889	VRK1	TTTTTTCGTCCAGTGATGAGT	ACCCCAAGAAGATGCATAATG	541							pMK33 C-TAP (MXO03728)	pMK33 C-FLAG-HA (FMO02828)
que	CG6433	FBgn0003187	-	GCACGCTGTACTTGACCA	TGCAATCAACGGGGAAGG	554								
CG6927	CG6927	FBgn0029733	-	CGAGGCCAGGGTAATGAA	CGGAGAAGGACATCCTCAC	534								
polo	CG12306	FBgn0003124	PLK1	TTCCGTTGATAAGATTAGTGAG	TCCTTCGAGGTGGACATCT	544								
aur	CG3068	FBgn0000147	AURKA	TGTCATGCGCATGGAGTT	CCCAGAAGCCGAAGAAGA	549								
cdc2	CG5363	FBgn0004106	CDC2	GAATAGCGGCTTTCTCGTTG	GCTGCCAGTTGATAAGCACA	374								
CkIβ	CG15224	FBgn0000259	CSNK2B	GGCTGACTTTCACAGTAGAC	AGCTCGAGGACAATCCAC	212								

Supplementary Table 2 - oligos, plasmids, z-scores, p-values, GO terms

gene symbol	phenotype analysis						FACS analysis								GO annotation	
	p values - single knockdowns 0.0001 significance: <			centrosome/spindle defects - other studies			z scores - this study significance: > 3.8 / < -3.8				Bjorklund et al.		Müller et al.		cellular component	biological process
	centrosome number	centrosome size	chromosome abberation	Dobbelaere et al.	Goshima et al.	Müller et al.	sub-G1	G1/G0	G2/M	over G2						
LBR	6,29E-03	4,11E-09	6,81E-01				-0,2	0,9	-1,4	1,7					nuclear inner membrane	nucleus organization
bel	1,41E-07	1,34E-03	7,63E-01				0,1	-0,2	0,5	-0,4	G1				P granule	RNA mediated gene silencing
CG14309	9,83E-01	4,85E-01	4,05E-01				-0,5	0,6	-1,3	0,1					lipid particle	-
CG5726	6,87E-01	2,08E-02	5,82E-02				-0,5	-0,2	-1,5	1,4					lipid particle	-
Ote	5,93E-01	1,23E-02	1,93E-03				3,8	1,6	-4,5	-0,9			subG1		nuclear inner membrane, spindle, cytoplasm, cytoskeleton, nucleus	NE reassembly
spd-2	3,47E-16	1,93E-17	1,20E-02				1,0	2,6	-3,6	-1,4					centriole	mitotic spindle organisation
Grip75	6,61E-80	1,66E-02	6,98E-03				2,1	-0,7	-1,0	3,4					centrosome, γ-TURC, MT	mitotic spindle organization, MT nucleation, mitosis
Dcp1	1,18E-01	6,20E-04	2,62E-01				1,6	0,7	-1,9	0,1					P granule	gene silencing by miRNA, mRNA catabolic process
Nup98	2,24E-02	5,58E-03	7,47E-01				1,6	-1,7	-0,9	4,0					nuclear pore	transport, phagocytosis
Grip84	2,25E-75	6,01E-01	2,01E-06				1,4	-0,4	-1,3	0,8					centrosome, γ-TUSC, MT	mitotic spindle + centrosome organization, MT nucleation, mitosis, cell cycle regulation
gp210	2,28E-03	2,98E-01	1,79E-02				2,6	3,3	-3,6	-0,7					-	olfactory learning
Lam	4,71E-08	2,42E-04	6,48E-02				1,5	-1,1	-1,8	-0,7					nuclear lamina, lipid particle	NE reassembly, chromatin silencing, nuclear migration
Grip71	1,17E-89	5,88E-02	7,60E-06				5,3	0,2	-2,6	2,2					γ-TURC	mitosis, mitotic spindle organization, cell cycle regulation
cup	8,08E-01	5,70E-03	8,92E-01				-0,3	0,0	-2,7	4,1			over G2		cytoplasm, nuclear envelope lumen	chromosome organization, transcription regulation, mRNA localization
cnn	0,00E+00	1,08E-25	1,59E-01				3,5	3,2	-3,4	-0,1					centrosome, PCM	centrosome cycle, cell cycle, mitotic spindle organization, cell division
ndl	3,23E-01	2,67E-01	1,43E-02			N	0,3	0,4	-2,8	0,7			N		extracellular matrix	Proteolysis, Toll signaling pathway
CG15435	9,06E-01	2,93E-01	6,04E-01			N	1,3	2,1	-3,2	0,7			N		nucleus	-
CG18190	3,12E-04	2,21E-01	7,76E-01			N	0,1	-1,0	-2,2	6,7			N		-	- (function: MT binding)
ewg	1,89E-01	8,67E-02	8,92E-01			N	-1,5	-0,6	-2,3	6,2			N		nucleus	transcription regulation
CG31326	1,03E-02	9,49E-02	5,61E-01			N	-0,6	0,1	-2,2	4,8			N		-	proteolysis
eIF3-S8	2,11E-17	2,36E-08	4,68E-03			N	13,0	23,6	17,0	-3,6			N		cytoplasm	translational initiation
apt	4,51E-04	9,47E-06	1,53E-01			N	0,6	-0,2	-1,2	2,3			N		nucleus	positive regulation of transcription from RNA polymerase II promoter
ball	9,17E-03	8,39E-01	1,18E-02			N	1,1	1,0	-2,1	0,7			N		nucleus, chromatin	histone phosphorylation, mitotic sister chromatid segregation, mitotic spindle organization, cell division
qua	3,92E-01	8,89E-01	4,07E-01			N	-0,6	0,0	-2,3	4,3			N		-	Actin filament organization
CG6927	2,75E-01	6,77E-01	9,91E-01			N	-0,8	-1,8	-1,7	5,5			N		membrane, cell junction	ion transport
polo	0,00E+00	4,69E-148	4,75E-51				4,2	-3,1	-1,2	5,3	subG1	over G2			centrosome, spindle, kinetochore, midbody	mitotic spindle organization, mitosis, cell cycle, cytokinesis, pronuclear fusion
aur	1,90E-04	1,97E-07	2,38E-01				-0,5	-0,9	-0,6	1,2					centrosome	centrosome cycle, centrosome separation, asymmetric protein localization, establishment of spindle orientation
cdc2	2,83E-25	5,55E-03	5,75E-05				-0,6	-5,1	-5,7	25,1	subG1	G1	G1/G2	over G2	nucleus	G2/M transition of mitotic cell cycle, asymmetric neuroblast division
CkIIβ	5,24E-07	8,05E-01	2,99E-02			N	1,0	-3,0	-2,2	7,6	G2		N		nucleus, cytoplasm	Wnt signaling pathway

significant deviation

increase

decrease

N not tested

References:

Dobbelaere, J., F. Josue, S. Suijkerbuijk, B. Baum, N. Tapon, and J. Raff. 2008. A genome-wide RNAi screen to dissect centriole duplication and centrosome maturation in Drosophila. PLoS Biol. 6:e224.

Goshima, G., R. Wollman, S.S. Goodwin, N. Zhang, J.M. Scholey, R.D. Vale, and N. Stuurman. 2007. Genes required for mitotic spindle assembly in Drosophila S2 cells. Science. 316:417-21.

Müller H., Mirgorodskaya E., Steinbrink S., Schmidt D., Lehmann V., Habermann K., Gustavsson N., Kessler T., Ploubidou A., Lehrach H., Gobom J., Boutros M., Lange B.M.H. (2010) Proteomic and functional analysis of the mitotic Drosophila centrosome. Embo J. in revision

Bjorklund, M., M. Taipale, M. Varjosalo, J. Saharinen, J. Lahdenpera, and J. Taipale. 2006. Identification of pathways regulating cell size and cell-cycle progression by RNAi. Nature. 439:1009-13.

3.4.3 Author contributions

B. Lange and me conceived and designed the experiments for this study. J. Gobom performed phosphopeptide enrichment and mass spectrometry analysis. RNAi experiments were carried out with the help of V. Lehmann and H. Müller. I carried out the automated microscopy analysis, IP experiments, cloning and tagging of genes, establishment of stable cell lines and localization studies. C. Erdmann and J. von Kries provided reagents, materials, analysis tools and technical support for high content screening. I analyzed the data, generated the figures and wrote the manuscript.

4 Discussion

Significant advances have been made in the past two decades regarding the identification of centrosome-associated proteins, mainly owing to improved isolation methods and more sensitive mass spectrometry techniques in combination with the availability of complete genome sequences of an increasing number of model organisms. Research on the biology of the centrosome has revealed many aspects of its functional, structural and biochemical properties. However, the molecular make-up of this large protein complex is still not known in its entirety and the exact molecular mechanisms underlying this organelle's biogenesis and the centrosome's implication in se veral cellular processes, like cilia formation, cell cycle regulation, stress response and cancer remain to be uncovered (Bettencourt-Dias and Glover, 2007).

In order to reveal the biophysical properties of the centrosome and to better understand its integration into cellular signaling pathways, we isolated centrosomes from *Drosophila* embryos, subsequently determined their electrical nature, identified the centrosomal proteome, analyzed the functions of all identified candidate centrosome components and the role of protein phosphorylation for centrosome biology. In the following sections, the results obtained in the three projects that comprise this PhD thesis will be discussed in relation to previously published studies.

4.1 Electric charge and hydrodynamic behavior of the centrosome

Local electric fields inferred from charged structures, such as membranes and microtubules, are ubiquitously present in the cell and electric phenomena have important functions in cellular processes, e.g. cell division (Vassilev and Kanazirska, 1985; Zhao et al., 1999; Stracke et al., 2002; McCaig et al., 2005). Knowing the electrical nature of supramolecular complexes, such as the centrosome, is critical to understand their structural organization, interactions, diffusion and function inside the cell. In principle, the charge and isoelectric region of supramolecular assemblies can be predicted through direct examination of its individual components. However, the precise composition of the centrosome is not known and moreover, the high level of organization of this large protein complex, which influences charge distribution, makes it difficult to precisely predict its biophysical properties. Therefore, in the first study (Hormeño et al., 2009), laser-based optical trapping and manipulation of individual *Drosophila* embryo centrosomes in between two microelectrodes was used to reveal the electric charge and hydrodynamic behavior of this organelle under physiological conditions. Such a single organelle methodology has the advantage that it provides unambiguous signals that are not confused by the simultaneous presence of other specimens or stochastic dynamics from crowding effects. This work provided the first

evidence that the centrosome is a negatively charged organelle. Isoelectricity of the *Drosophila* centrosome was marked in the region of pH3.1. Interestingly, when comparing our data with previous electrophoresis experiments on microtubules (Stracke et al., 2002; van den Heuvel et al., 2007), we found that the effective charge of the centrosome is significantly smaller than that of microtubules, although both exhibit a net negative charge. These findings may help explain how the growth of microtubule dimers with radial directionality from the centrosome is achieved in vivo.

The centrosome is a highly dynamic structure. It lacks a membrane that delimits its extent and has no definite size or shape. The molecular lattice surrounding the centriolar core contributes to the morphology and activity changes of the centrosome during the cell cycle. To gain deeper insights into the structural dynamics of the centrosome we also investigated the hydrodynamic behavior under various environmental conditions. We found that the physiological size measured in aqueous solution is significantly larger than the electron microscopy diameter determined in previous studies (Moritz et al., 1995a; Lange et al., 2005). Based on these findings and the known diffusive nature of the PCM, we discriminated between two hydrodynamic centrosome domains: (a) the PCM neighborhood, which comprises proteinacious fibrils in the outer extent of the PCM and (b) the denser centriole core which is constituted by centrioles and proximal pericentriolar material. The PCM neighborhood is not present under the dehydrating conditions used in electron microscopy studies, which explains the larger diameters measured in this analysis. It has long been known, that centrosome structure is influenced by divalent cations (Baron et al., 1994). Ca^{2+} was reported to contract the structure of centrosomes, specifically it decreases the intercentriolar distance (Paintrand et al., 1992). Consistent with these findings, we measured a decreased centrosome diameter in the presence of Ca^{2+}. Moreover, we demonstrate that the contracting effect was stronger on the centriole core domain, validating the specificity of this approach. Importantly, we also demonstrated that the electric charge of the centrosome, which is modulated by the environmental pH, has influence over its own structure. The minimum size was determined near the pH where the centrosome is neutral, while the dimension of centrosomes increased gradually below and above the isoelectric pH. This pH-dependent self-modulating structural effect might also contribute to the structural dynamics of centrosomes in vivo, as variations in intracellular pH are known to occur with progression of the cell cycle.

In the future, the laser-based manipulation of individual centrosomes provides a valuable tool to study the sensitivity of this organelle to different environmental conditions, to follow the progression of the centrosome cycle or to investigate the effect of posttranslational modifications on the electric and hydrodynamic behavior of the centrosome.

4.2 Centrosome proteome analysis

The number of centrosomal proteins has been difficult to determine due to the fact that true components may be lost and contaminants are included during the isolation procedure, respectively (Schatten, 2008). Furthermore, many proteins only transiently associate with centrosomes and less abundant proteins may escape identification due to the limited sensitivity of mass spectrometry techniques. Nevertheless, the list of newly identified centrosome proteins continuously grows. Centrosome:db, a database for the human centrosome, contains a total of 383 genes encoding proteins that either stably or transiently localize to the centrosome (Nogales-Cadenas et al., 2008). Genes were added on the basis of different kinds of evidences, including high-throughput proteomics datasets and Gene Ontology annotation in public databases. Andersen and colleagues contributed a large fraction of centrosomal proteins (108) to this collection by analyzing the interphase centrosome of human KE-37 cells. Their initial MS analysis resulted in the identification of roughly 500 proteins. In order to discriminate between contaminants and true centrosome components, they used protein correlation profiling and validated a subset of novel candidates via GFP tagging and localization studies (Andersen et al., 2003). Proteomics analyses of isolated centrosomes or related structures have also been applied in other model organisms, such as the *Saccharomyces* spindle pole body (Wigge et al., 1998), the *Dictyostelium* centrosome (Reinders et al., 2006) and the *Chlamydomonas* basal body (Keller et al., 2005). Remarkably, a comprehensive analysis of the centrosome proteome in *Drosophila* has until know been missing, although genome-wide RNAi studies have identified a series of centrosomal components (Goshima et al., 2007; Dobbelaere et al., 2008). The centrosome has been estimated to consist of several hundred proteins (Bettencourt-Dias and Glover, 2007), however, FLYBASE currently only lists 35 proteins as components of the *Drosophila* centrosome, centriole or spindle pole based on their Gene Ontology annotation.

In this work, we used a direct biochemical approach in combination with mass spectrometry to determine the proteome of the early *Drosophila* embryo centrosome (Müller et al., in revision). In contrast to mammalian centrosomes that are primarily derived from interphase cells, the highly mitotic syncytial embryos contain centrosomes with large amounts of PCM allowing the identification of additional proteins, which may not localize to the interphase centrosome. To improve the purity of our preparations we used immunoisolation with a centrosome specific-antibody following enrichment of centrosomes via sucrose-gradient centrifugation. Proteomic studies of centrosomes in other organisms were so far only based on isolation protocols lacking the immunoisolation step, leading to preparations that contained large amounts of unspecific proteins (Andersen et al., 2003). The MS analysis of immunoisolated *Drosophila* centrosomes identified 260 proteins, including 20 of the 35

known centrosomal proteins. Through GFP-tagging and expression of fusion proteins in *Drosophila* SL2 cells, we demonstrated centrosome (8) and spindle (4) localization for 12 novel candidate proteins validating the robustness of our approach.

4.3 Functional characterization of centrosomal proteins

Following the MS analysis, RNAi in *Drosophila* SL2 cells was employed in order to determine the function of the identified proteins in centrosome structure, duplication and cell cycle progression. In total, our RNAi phenotype scoring revealed previously unknown centrosome-related functions for 27 proteins. One major functional group was comprised of proteins, which upon depletion led to centrosome loss (11) or induced morphologically abnormal centrosomes (13) implying a role of these proteins in centrosome structure maintenance. Downregulation of the centriolar protein spd-2 and the PCM components cnn, Grip84 and l(1)dd4, which had previously been shown to be required for maintaining centrosome structure (Dix and Raff, 2007; Megraw et al., 1999; Colombie et al., 2006; Barbosa et al., 2000) resulted in a ‘’0 centrosome’’ phenotype, demonstrating the specificity of our RNAi analysis. Surprisingly, proteins involved in RNA binding (e.g. Rae1, CG31716), translational control (e.g. eIF-4a, cup) and components of the actin cytoskeleton (Act57B, Act79B) were also shown to be important for centrosome structure in our analysis. The second functional group (56/260) consisted of proteins whose depletion induced centrosome duplication or separation defects. This group included proteins that were known to be implicated in the regulation of the centrosome cycle, such as α-/β-Tubulins, γ-TuRC components, Tum and the motor protein Klp10A (Zavortink et al., 2005; Goshima et al., 2007). In addition, we found proteins that were previously described to be involved in RNA processing (e.g. crn), DNA-replication (e.g. lat) and translation (ribosomal proteins) to function in centrosome duplication and separation pathways, respectively. It has been proposed before that the translation of centrosomal proteins and their regulation occurs in close association with the centrosome based on the finding that components of the transcription/translation machinery as well as mRNAs localize to centrosomes and the mitotic spindle (Lécuyer et al., 2007; Blower et al., 2005). Our results provide further evidence for a link between transcriptional and translational control and the control of centrosome duplication and separation as well as structure maintenance.

To elucidate possible links of centrosomal proteins to cell proliferation pathways, we performed FACS analysis and determined the mitotic indices of cells upon downregulation of all MS-identified proteins. Depletion of 26/260 proteins led to accumulation of cells with sub-G1-phase DNA content indicating decreased viability. Downregulation of 20 proteins led to defects in cytokinesis and inhibition of 25 proteins led cells to arrest in mitosis. The majority of proteins that caused mitotic arrest also blocked centrosome duplication/separation (e.g.

members of the γ-TuRC) and hence impaired the assembly of a normal bipolar spindle. Mitotic arrest was therefore most probably induced through activation of the spindle assembly checkpoint. This finding supports the previously reported importance of the centrosome for mitotic progression (Doxsey et al., 2005a). Errors in cytokinesis frequently occur upon depletion of centrosome components and also as a consequence of experimentally induced centrosome ablation (Hinchcliffe et al., 2001; Khodjakov and Rieder, 2001). Here we identified proteins that were known to affect cell division (e.g. cdc2 and Pav) as well as proteins whose implication into cytokinesis was unexpected (Heph), thereby revealing new molecular evidence for the well-established requirement of the centrosome in cytokinesis (Fabbro et al., 2005). Many known centrosomal proteins, e.g. Fzy, Klp61F, Pav, Msps and the uncharacterized centrosome associated protein CG11148, were shown to be required for cell viability. Again, most members of this group were correlated with a function in centrosome duplication/separation suggesting that both cell survival and cell cycle progression depend on the correct execution of the centrosome cycle.

In addition to the identification and functional analysis of *Drosophila* centrosomal proteins, we also investigated whether the identified centrosome-associated functions are conserved in human cells by siRNA mediated depletion of homologous proteins in HaCaT cells. We found that the most prominent functional conservation occurs in the group of proteins involved in centrosome duplication and segregation (75%) while less (29%) had a conserved function in maintaining centrosome structure. These results were in agreement with previous reports demonstrating a high level of interspecies conservation of core centrosome proteins, e.g. the γ-TuRC components (Moritz et al., 1995b; Zheng et al., 1995).

In conclusion, this work provides the first comprehensive molecular inventory of the *Drosophila* centrosome as well as a functional description of its components. Importantly, we revealed centrosome-related functions for numerous proteins that were previously annotated to function in diverse cellular processes, like nuclear transport, RNA processing, transcription, translation, DNA replication and so forth. It will be interesting to learn, how the multi-functionality of these proteins is achieved, what their interaction partners are and how shuttling of these proteins between the centrosome and other cellular compartments is regulated. The high level of functional conservation between *Drosophila* centrosome proteins and their human orthologues make *Drosophila* a favorable model organism to study the molecular mechanisms underlying the processes of centrosome duplication and separation.

4.4 Centrosome phosphoproteome analysis

Among other posttranslational modifications, reversible phosphorylation is one of the key regulatory mechanisms controlling most cellular processes, including cell cycle progression,

spindle assembly and centrosome biogenesis. As outlined in the introduction, many regulatory kinases have been shown to localize to the centrosome. However, little is known about their centrosomal targets and the role of phosphorylation events regarding centrosome functions. Therefore the main goal of my PhD project was the identification of centrosomal kinase substrates and the functional characterization of phosphoproteins (Habermann et al., submitted). The MS-analysis of immunoisolated centrosomes resulted in the identification of 27 phosphorylated proteins, of which 11 had not been identified in the previous whole proteome analysis. This may be due to the additional phosphopeptide enrichment step that preceded the MS-analysis in this study and possibly enabled the identification of less abundant proteins that were missed in the whole proteome analysis of isolated centrosomes (Müller et al., in revision). Several large scale phosphoproteomic data sets using *Drosophila* as a model system have recently been published. Aebersold and colleagues determined the phosphoproteome of Kc167 cells and Zhai et al. identified phosphorylation sites derived from *Drosophila* embryos in a global fashion (Bodenmiller et al., 2007, Zhai et al., 2008). Our organelle isolation and phosphopeptide enrichment approach identified 45 phosphorylation sites. Comparison of our data with the two large-scale studies conducted in *Drosophila* cells and embryos, respectively, revealed 17 novel phosphorylation sites and one protein (ewg) that had not been shown to be phosphorylated before. Furthermore, most of the identified sites in our study display recognition motifs for the centrosome-associated kinases Cdk1, Aurora-A and Plk1. These findings indicate that the majority of phosphorylation sites identified in this study might be specific to the centrosomal localization of the respective protein. As many of the MS-identified proteins are known to localize to non-centrosomal cellular compartments, such as the nucleus, nuclear membrane and P granules, we speculate that their transient association with the centrosome could occur in a phosphorylation-dependent manner. Such a phosphorylation-dependent shuttling between the centrosome and other cellular sites has been shown before, e.g. for the nucleolar protein nucleophosmin (Okuda, 2002). Further experiments will be required to test the hypothesis that the here identified phosphorylation sites affect centrosomal localization of these proteins.

4.5 Functional characterization of centrosomal phosphoproteins

To determine the functions of MS-identified phosphoproteins with respect to their role in centrosome replication, cell cycle regulatory and chromosome segregation pathways, we conducted a cell-based RNAi screen in combination with automated high-content immunofluorescence microscopy and FACS analysis. Among the analyzed proteins were 6 known centrosome components but the majority of the MS-identified proteins have so far only been linked to non-centrosome associated cellular localizations and processes, including nuclear envelope assembly, transcriptional and translational regulation and

proteolysis. Consistent with the findings of previously published genome-wide RNAi studies in *Drosophila* (Goshima et al., 2007; Dobbelaere et al., 2008) we demonstrated that the γ-TuRC components grip 71, 75 and 84 as well as centriolar protein spd-2 and Lam are involved in centrosome duplication and separation. Surprisingly, our study also revealed unknown functions for the phosphoproteins bel, eIF3-S8, LBR, Dcp1 and apt and the kinase CkIIβ in centrosome cycle regulatory pathways. Additionally, bel, eIF3-S8 and apt were shown to be required for cell cycle progression, as are nuclear pore proteins Nup98 and gp210. Interestingly, a requirement for efficient cytokinesis was discovered for actin filament organizer qua, CG18190, a protein which is predicted to function in microtubule binding (FLYBASE) as well as for functionally not annotated proteins CG6927 and CG31326. It has also not been shown before that depletion of the transcriptional regulator ewg causes defects in cellular division.

It has been reported before that single knockdown approaches often fail to detect redundant protein functions, most likely due to the existence of alternative pathways which compensate for the loss of activity of only one component of the respective signaling network. As has been shown in other functional screens, identification of redundant regulators of a certain biological process often requires removal of a second element in the pathway (Bakal et al., 2008). In addition to the single knockdown analysis of phosphoproteins we therefore also applied a combinatorial RNAi screening approach, in which we simultaneously depleted phosphoproteins and 4 selected kinases (polo, aur, cdc2 and CkIIβ). The kinases were chosen because the 25 analyzed phosphoproteins represent likely targets of these regulatory enzymes. By using this strategy, we were able to integrate the centrosome phosphoproteins into signaling networks in a hierarchical manner and to reveal unsuspected functions in centrosome maturation, duplication or separation pathways for 21 of the analyzed phosphoproteins, many of which had not been detected following the single-knockdown analysis. Moreover, we demonstrated involvement in cell cycle regulation for 23 and chromosome segregation for 18 of the 25 analyzed phosphoproteins. Our combinatorial RNAi approach also allowed us to identify functional interdependencies between kinases and phosphoproteins. For instance, the nuclear inner membrane protein Ote was shown to be involved in centrosome maturation through negative regulation downstream of the kinase aurora. Consistent with this finding, we could show Ote to be localized to the interphase centrosome in *Drosophila* SL2 cells and moreover it was found in a complex with γ-Tubulin.

In conclusion, our data demonstrated that virtually all MS-identified centrosomal phosphoproteins are implicated in signaling pathways related to centrosome biology or cell cycle regulation, either in a direct fashion or through functional interaction with the relevant kinases. These results further support the notion that many signaling components transiently

associate with centrosomes to fulfill unsuspected tasks that differ from their annotated functions in other cellular compartments. As posttranslational modifications such as phosphorylation can affect a protein's function, localization and interaction with other proteins, the description of the in vivo phosphorylation status of centrosome-associated proteins provides a useful basis for future research aimed at gaining a deeper understanding of the molecular mechanisms controlling centrosome and cell cycle regulatory pathways.

5 References

Andersen, J.S., Wilkinson, C.J., Mayor, T., Mortensen, P., Nigg, E.A., and Mann, M. (2003). Proteomic characterization of the human centrosome by protein correlation profiling. Nature *426*, 570-574.

Badano, J.L., Mitsuma, N., Beales, P.L., and Katsanis, N. (2006). The ciliopathies: an emerging class of human genetic disorders. Annu Rev Genomics Hum Genet *7*, 125-148.

Badano, J.L., Teslovich, T.M., and Katsanis, N. (2005). The centrosome in human genetic disease. Nat Rev Genet *6*, 194-205.

Bahe, S., Stierhof, Y.D., Wilkinson, C.J., Leiss, F., and Nigg, E.A. (2005). Rootletin forms centriole-associated filaments and functions in centrosome cohesion. J Cell Biol *171*, 27-33.

Bakal, C., Linding, R., Llense, F., Heffern, E., Martin-Blanco, E., Pawson, T., and Perrimon, N. (2008). Phosphorylation networks regulating JNK activity in diverse genetic backgrounds. Science *322*, 453-456.

Bakhoum, S.F., and Compton, D.A. (2009). Cancer: CINful centrosomes. Curr Biol *19*, R642-645.

Barbosa, V., Yamamoto, R.R., Henderson, D.S., and Glover, D.M. (2000). Mutation of a Drosophila gamma tubulin ring complex subunit encoded by discs degenerate-4 differentially disrupts centrosomal protein localization. Genes Dev *14*, 3126-3139.

Baron, A.T., Suman, V.J., Nemeth, E., and Salisbury, J.L. (1994). The pericentriolar lattice of PtK2 cells exhibits temperature and calcium-modulated behavior. J Cell Sci *107 (Pt 11)*, 2993-3003.

Barros, T.P., Kinoshita, K., Hyman, A.A., and Raff, J.W. (2005). Aurora A activates D-TACC-Msps complexes exclusively at centrosomes to stabilize centrosomal microtubules. J Cell Biol *170*, 1039-1046.

Basto, R., Brunk, K., Vinadogrova, T., Peel, N., Franz, A., Khodjakov, A., and Raff, J.W. (2008). Centrosome amplification can initiate tumorigenesis in flies. Cell *133*, 1032-1042.

Basto, R., Lau, J., Vinogradova, T., Gardiol, A., Woods, C.G., Khodjakov, A., and Raff, J.W. (2006). Flies without centrioles. Cell *125*, 1375-1386.

Berdnik, D., and Knoblich, J.A. (2002). Drosophila Aurora-A is required for centrosome maturation and actin-dependent asymmetric protein localization during mitosis. Curr Biol *12*, 640-647.

Bettencourt-Dias, M., and Glover, D.M. (2007). Centrosome biogenesis and function: centrosomics brings new understanding. Nat Rev Mol Cell Biol *8*, 451-463.

Bettencourt-Dias, M., Rodrigues-Martins, A., Carpenter, L., Riparbelli, M., Lehmann, L., Gatt, M.K., Carmo, N., Balloux, F., Callaini, G., and Glover, D.M. (2005). SAK/PLK4 is required for centriole duplication and flagella development. Curr Biol *15*, 2199-2207.

Blagden, S.P., and Glover, D.M. (2003). Polar expeditions--provisioning the centrosome for mitosis. Nat Cell Biol *5*, 505-511.

Blangy, A., Arnaud, L., and Nigg, E.A. (1997). Phosphorylation by p34cdc2 protein kinase regulates binding of the kinesin-related motor HsEg5 to the dynactin subunit p150. J Biol Chem *272*, 19418-19424.

Blower, M.D., Nachury, M., Heald, R., and Weis, K. (2005). A Rae1-containing ribonucleoprotein complex is required for mitotic spindle assembly. Cell *121*, 223-234.

Bodenmiller, B., Malmstrom, J., Gerrits, B., Campbell, D., Lam, H., Schmidt, A., Rinner, O., Mueller, L.N., Shannon, P.T., Pedrioli, P.G.*, et al.* (2007). PhosphoPep--a phosphoproteome resource for systems biology research in Drosophila Kc167 cells. Mol Syst Biol *3*, 139.

Bornens, M. (2002). Centrosome composition and microtubule anchoring mechanisms. Curr Opin Cell Biol *14*, 25-34.

Boveri, T. (1901). Über die Natur der Centrosomen. In Z Med Naturw (Jena), pp. 1-220.

Boveri, T. (2008). Concerning the origin of malignant tumours by Theodor Boveri. Translated and annotated by Henry Harris. J Cell Sci *121 Suppl 1*, 1-84.

Castedo, M., Perfettini, J.L., Roumier, T., Valent, A., Raslova, H., Yakushijin, K., Horne, D., Feunteun, J., Lenoir, G., Medema, R.*, et al.* (2004a). Mitotic catastrophe constitutes a special case of apoptosis whose suppression entails aneuploidy. Oncogene *23*, 4362-4370.

Castedo, M., Perfettini, J.L., Roumier, T., Yakushijin, K., Horne, D., Medema, R., and Kroemer, G. (2004b). The cell cycle checkpoint kinase Chk2 is a negative regulator of mitotic catastrophe. Oncogene *23*, 4353-4361.

Castellanos, E., Dominguez, P., and Gonzalez, C. (2008). Centrosome dysfunction in Drosophila neural stem cells causes tumors that are not due to genome instability. Curr Biol *18*, 1209-1214.

Cheng, K.C., and Loeb, L.A. (1997). Genomic stability and instability: a working paradigm. Curr Top Microbiol Immunol *221*, 5-18.

Colombie, N., Verollet, C., Sampaio, P., Moisand, A., Sunkel, C., Bourbon, H.M., Wright, M., and Raynaud-Messina, B. (2006). The Drosophila gamma-tubulin small complex subunit Dgrip84 is required for structural and functional integrity of the spindle apparatus. Mol Biol Cell *17*, 272-282.

Crosio, C., Fimia, G.M., Loury, R., Kimura, M., Okano, Y., Zhou, H., Sen, S., Allis, C.D., and Sassone-Corsi, P. (2002). Mitotic phosphorylation of histone H3: spatio-temporal regulation by mammalian Aurora kinases. Mol Cell Biol *22*, 874-885.

Debec, A., and Marcaillou, C. (1997). Structural alterations of the mitotic apparatus induced by the heat shock response in Drosophila cells. Biol Cell *89*, 67-78.

Delattre, M., Canard, C., and Gonczy, P. (2006). Sequential protein recruitment in C. elegans centriole formation. Curr Biol *16*, 1844-1849.

Dirksen, E.R. (1991). Centriole and basal body formation during ciliogenesis revisited. Biol Cell *72*, 31-38.

Diviani, D., Langeberg, L.K., Doxsey, S.J., and Scott, J.D. (2000). Pericentrin anchors protein kinase A at the centrosome through a newly identified RII-binding domain. Curr Biol *10*, 417-420.

Diviani, D., and Scott, J.D. (2001). AKAP signaling complexes at the cytoskeleton. J Cell Sci *114*, 1431-1437.

Dix, C.I., and Raff, J.W. (2007). Drosophila Spd-2 recruits PCM to the sperm centriole, but is dispensable for centriole duplication. Curr Biol *17*, 1759-1764.

do Carmo Avides, M., Tavares, A., and Glover, D.M. (2001). Polo kinase and Asp are needed to promote the mitotic organizing activity of centrosomes. Nat Cell Biol *3*, 421-424.

Dobbelaere, J., Josue, F., Suijkerbuijk, S., Baum, B., Tapon, N., and Raff, J. (2008). A genome-wide RNAi screen to dissect centriole duplication and centrosome maturation in Drosophila. PLoS Biol *6*, e224.

Doxsey, S. (2001). Re-evaluating centrosome function. Nat Rev Mol Cell Biol *2*, 688-698.

Doxsey, S., McCollum, D., and Theurkauf, W. (2005a). Centrosomes in cellular regulation. Annu Rev Cell Dev Biol *21*, 411-434.

Doxsey, S., Zimmerman, W., and Mikule, K. (2005b). Centrosome control of the cell cycle. Trends Cell Biol *15*, 303-311.

Dutcher, S.K. (2003). Elucidation of basal body and centriole functions in Chlamydomonas reinhardtii. Traffic *4*, 443-451.

Dutertre, S., Cazales, M., Quaranta, M., Froment, C., Trabut, V., Dozier, C., Mirey, G., Bouche, J.P., Theis-Febvre, N., Schmitt, E.*, et al.* (2004). Phosphorylation of CDC25B by Aurora-A at the centrosome contributes to the G2-M transition. J Cell Sci *117*, 2523-2531.

Elia, A.E., Rellos, P., Haire, L.F., Chao, J.W., Ivins, F.J., Hoepker, K., Mohammad, D., Cantley, L.C., Smerdon, S.J., and Yaffe, M.B. (2003). The molecular basis for phosphodependent substrate targeting and regulation of Plks by the Polo-box domain. Cell *115*, 83-95.

Fabbro, M., Zhou, B.B., Takahashi, M., Sarcevic, B., Lal, P., Graham, M.E., Gabrielli, B.G., Robinson, P.J., Nigg, E.A., Ono, Y.*, et al.* (2005). Cdk1/Erk2- and Plk1-dependent phosphorylation of a centrosome protein, Cep55, is required for its recruitment to midbody and cytokinesis. Dev Cell *9*, 477-488.

Fry, A.M. (2002). The Nek2 protein kinase: a novel regulator of centrosome structure. Oncogene *21*, 6184-6194.

Fry, A.M., Mayor, T., and Nigg, E.A. (2000). Regulating centrosomes by protein phosphorylation. Curr Top Dev Biol *49*, 291-312.

Ganem, N.J., Godinho, S.A., and Pellman, D. (2009). A mechanism linking extra centrosomes to chromosomal instability. Nature *460*, 278-282.

Giet, R., McLean, D., Descamps, S., Lee, M.J., Raff, J.W., Prigent, C., and Glover, D.M. (2002). Drosophila Aurora A kinase is required to localize D-TACC to centrosomes and to regulate astral microtubules. J Cell Biol *156*, 437-451.

Giet, R., Uzbekov, R., Cubizolles, F., Le Guellec, K., and Prigent, C. (1999). The Xenopus laevis aurora-related protein kinase pEg2 associates with and phosphorylates the kinesin-related protein XlEg5. J Biol Chem *274*, 15005-15013.

Gillingham, A.K., and Munro, S. (2000). The PACT domain, a conserved centrosomal targeting motif in the coiled-coil proteins AKAP450 and pericentrin. EMBO Rep *1*, 524-529.

Glover, D.M. (2005). Polo kinase and progression through M phase in Drosophila: a perspective from the spindle poles. Oncogene *24*, 230-237.

Glover, D.M., Leibowitz, M.H., McLean, D.A., and Parry, H. (1995). Mutations in aurora prevent centrosome separation leading to the formation of monopolar spindles. Cell *81*, 95-105.

Golsteyn, R.M., Mundt, K.E., Fry, A.M., and Nigg, E.A. (1995). Cell cycle regulation of the activity and subcellular localization of Plk1, a human protein kinase implicated in mitotic spindle function. J Cell Biol *129*, 1617-1628.

Gonczy, P. (2008). Mechanisms of asymmetric cell division: flies and worms pave the way. Nat Rev Mol Cell Biol *9*, 355-366.

Gonzalez, C., Tavosanis, G., and Mollinari, C. (1998). Centrosomes and microtubule organisation during Drosophila development. J Cell Sci *111 (Pt 18)*, 2697-2706.

Goshima, G., Wollman, R., Goodwin, S.S., Zhang, N., Scholey, J.M., Vale, R.D., and Stuurman, N. (2007). Genes required for mitotic spindle assembly in Drosophila S2 cells. Science *316*, 417-421.

Habedanck, R., Stierhof, Y.D., Wilkinson, C.J., and Nigg, E.A. (2005). The Polo kinase Plk4 functions in centriole duplication. Nat Cell Biol *7*, 1140-1146.

Habermann, K., and Lange, B.M.H. (2010). Centrosomes: Methods for Preparation. In Encyclopedia of Life Sciences (ELS) (Chichester, John Wiley & Sons, Ltd).

Hansen, D.V., Loktev, A.V., Ban, K.H., and Jackson, P.K. (2004). Plk1 regulates activation of the anaphase promoting complex by phosphorylating and triggering SCFbetaTrCP-dependent destruction of the APC Inhibitor Emi1. Mol Biol Cell *15*, 5623-5634.

Helps, N.R., Luo, X., Barker, H.M., and Cohen, P.T. (2000). NIMA-related kinase 2 (Nek2), a cell-cycle-regulated protein kinase localized to centrosomes, is complexed to protein phosphatase 1. Biochem J *349*, 509-518.

Hinchcliffe, E.H., Miller, F.J., Cham, M., Khodjakov, A., and Sluder, G. (2001). Requirement of a centrosomal activity for cell cycle progression through G1 into S phase. Science *291*, 1547-1550.

Hinchcliffe, E.H., and Sluder, G. (2001). "It takes two to tango": understanding how centrosome duplication is regulated throughout the cell cycle. Genes Dev *15*, 1167-1181.

Hormeño, S., Ibarra, B., Chichón, F.J., Habermann, K., Lange, B.M., Valpuesta, J.M., Carrascosa, J.L., and Arias-Gonzalez, J.R. (2009). Single centrosome manipulation reveals its electric charge and associated dynamic structure. Biophys J *97*, 1022-1030.

Hut, H.M., Lemstra, W., Blaauw, E.H., Van Cappellen, G.W., Kampinga, H.H., and Sibon, O.C. (2003). Centrosomes split in the presence of impaired DNA integrity during mitosis. Mol Biol Cell *14*, 1993-2004.

Jackman, M., Lindon, C., Nigg, E.A., and Pines, J. (2003). Active cyclin B1-Cdk1 first appears on centrosomes in prophase. Nat Cell Biol *5*, 143-148.

Jaspersen, S.L., and Winey, M. (2004). The budding yeast spindle pole body: structure, duplication, and function. Annu Rev Cell Dev Biol *20*, 1-28.

Kalt, A., and Schliwa, M. (1993). Molecular components of the centrosome. Trends Cell Biol *3*, 118-128.

Keller, L.C., Geimer, S., Romijn, E., Yates, J., 3rd, Zamora, I., and Marshall, W.F. (2009). Molecular architecture of the centriole proteome: the conserved WD40 domain protein POC1 is required for centriole duplication and length control. Mol Biol Cell *20*, 1150-1166.

Keller, L.C., Romijn, E.P., Zamora, I., Yates, J.R., 3rd, and Marshall, W.F. (2005). Proteomic analysis of isolated chlamydomonas centrioles reveals orthologs of ciliary-disease genes. Curr Biol *15*, 1090-1098.

Khodjakov, A., and Rieder, C.L. (2001). Centrosomes enhance the fidelity of cytokinesis in vertebrates and are required for cell cycle progression. J Cell Biol *153*, 237-242.

Khodjakov, A., Rieder, C.L., Sluder, G., Cassels, G., Sibon, O., and Wang, C.L. (2002). De novo formation of centrosomes in vertebrate cells arrested during S phase. J Cell Biol *158*, 1171-1181.

Kimura, K., Hirano, M., Kobayashi, R., and Hirano, T. (1998). Phosphorylation and activation of 13S condensin by Cdc2 in vitro. Science *282*, 487-490.

Kleylein-Sohn, J., Westendorf, J., Le Clech, M., Habedanck, R., Stierhof, Y.D., and Nigg, E.A. (2007). Plk4-induced centriole biogenesis in human cells. Dev Cell *13*, 190-202.

Kohlmaier, G., Loncarek, J., Meng, X., McEwen, B.F., Mogensen, M.M., Spektor, A., Dynlacht, B.D., Khodjakov, A., and Gonczy, P. (2009). Overly long centrioles and defective cell division upon excess of the SAS-4-related protein CPAP. Curr Biol *19*, 1012-1018.

Kraft, C., Herzog, F., Gieffers, C., Mechtler, K., Hagting, A., Pines, J., and Peters, J.M. (2003). Mitotic regulation of the human anaphase-promoting complex by phosphorylation. EMBO J *22*, 6598-6609.

Kramer, A., Mailand, N., Lukas, C., Syljuasen, R.G., Wilkinson, C.J., Nigg, E.A., Bartek, J., and Lukas, J. (2004). Centrosome-associated Chk1 prevents premature activation of cyclin-B-Cdk1 kinase. Nat Cell Biol *6*, 884-891.

Kramer, E.R., Scheuringer, N., Podtelejnikov, A.V., Mann, M., and Peters, J.M. (2000). Mitotic regulation of the APC activator proteins CDC20 and CDH1. Mol Biol Cell *11*, 1555-1569.

Kumagai, A., and Dunphy, W.G. (1996). Purification and molecular cloning of Plx1, a Cdc25-regulatory kinase from Xenopus egg extracts. Science *273*, 1377-1380.

Kwon, M., Godinho, S.A., Chandhok, N.S., Ganem, N.J., Azioune, A., Thery, M., and Pellman, D. (2008). Mechanisms to suppress multipolar divisions in cancer cells with extra centrosomes. Genes Dev *22*, 2189-2203.

Lane, H.A., and Nigg, E.A. (1996). Antibody microinjection reveals an essential role for human polo-like kinase 1 (Plk1) in the functional maturation of mitotic centrosomes. J Cell Biol *135*, 1701-1713.

Lange, B.M. (2002). Integration of the centrosome in cell cycle control, stress response and signal transduction pathways. Curr Opin Cell Biol *14*, 35-43.

Lange, B.M., Bachi, A., Wilm, M., and Gonzalez, C. (2000). Hsp90 is a core centrosomal component and is required at different stages of the centrosome cycle in Drosophila and vertebrates. EMBO J *19*, 1252-1262.

Lange, B.M., Kirfel, G., Gestmann, I., Herzog, V., and Gonzalez, C. (2005). Structure and microtubule-nucleation activity of isolated Drosophila embryo centrosomes characterized by whole mount scanning and transmission electron microscopy. Histochem Cell Biol *124*, 325-334.

Lecuyer, E., Yoshida, H., Parthasarathy, N., Alm, C., Babak, T., Cerovina, T., Hughes, T.R., Tomancak, P., and Krause, H.M. (2007). Global analysis of mRNA localization reveals a prominent role in organizing cellular architecture and function. Cell *131*, 174-187.

Lee, K.S., Grenfell, T.Z., Yarm, F.R., and Erikson, R.L. (1998). Mutation of the polo-box disrupts localization and mitotic functions of the mammalian polo kinase Plk. Proc Natl Acad Sci U S A *95*, 9301-9306.

Leidel, S., Delattre, M., Cerutti, L., Baumer, K., and Gonczy, P. (2005). SAS-6 defines a protein family required for centrosome duplication in C. elegans and in human cells. Nat Cell Biol *7*, 115-125.

Leidel, S., and Gonczy, P. (2005). Centrosome duplication and nematodes: recent insights from an old relationship. Dev Cell *9*, 317-325.

Li, J.B., Gerdes, J.M., Haycraft, C.J., Fan, Y., Teslovich, T.M., May-Simera, H., Li, H., Blacque, O.E., Li, L., Leitch, C.C.*, et al.* (2004). Comparative genomics identifies a flagellar and basal body proteome that includes the BBS5 human disease gene. Cell *117*, 541-552.

Marshall, W.F., Vucica, Y., and Rosenbaum, J.L. (2001). Kinetics and regulation of de novo centriole assembly. Implications for the mechanism of centriole duplication. Curr Biol *11*, 308-317.

McCaig, C.D., Rajnicek, A.M., Song, B., and Zhao, M. (2005). Controlling cell behavior electrically: current views and future potential. Physiol Rev *85*, 943-978.

Megraw, T.L., Li, K., Kao, L.R., and Kaufman, T.C. (1999). The centrosomin protein is required for centrosome assembly and function during cleavage in Drosophila. Development *126*, 2829-2839.

Meraldi, P., Honda, R., and Nigg, E.A. (2002). Aurora-A overexpression reveals tetraploidization as a major route to centrosome amplification in p53-/- cells. EMBO J *21*, 483-492.

Meraldi, P., and Nigg, E.A. (2002). The centrosome cycle. FEBS Lett *521*, 9-13.

Mikule, K., Delaval, B., Kaldis, P., Jurcyzk, A., Hergert, P., and Doxsey, S. (2007). Loss of centrosome integrity induces p38-p53-p21-dependent G1-S arrest. Nat Cell Biol *9*, 160-170.

Mishra, R.K., Chakraborty, P., Arnaoutov, A., Fontoura, B.M., and Dasso, M. (2010). The Nup107-160 complex and gamma-TuRC regulate microtubule polymerization at kinetochores. Nat Cell Biol *12*, 164-169.

Moritz, M., Braunfeld, M.B., Fung, J.C., Sedat, J.W., Alberts, B.M., and Agard, D.A. (1995a). Three-dimensional structural characterization of centrosomes from early Drosophila embryos. J Cell Biol *130*, 1149-1159.

Moritz, M., Braunfeld, M.B., Guenebaut, V., Heuser, J., and Agard, D.A. (2000). Structure of the gamma-tubulin ring complex: a template for microtubule nucleation. Nat Cell Biol *2*, 365-370.

Moritz, M., Braunfeld, M.B., Sedat, J.W., Alberts, B., and Agard, D.A. (1995b). Microtubule nucleation by gamma-tubulin-containing rings in the centrosome. Nature *378*, 638-640.

Moritz, M., Zheng, Y., Alberts, B.M., and Oegema, K. (1998). Recruitment of the gamma-tubulin ring complex to Drosophila salt-stripped centrosome scaffolds. J Cell Biol *142*, 775-786.

Mueller, P.R., Coleman, T.R., and Dunphy, W.G. (1995a). Cell cycle regulation of a Xenopus Wee1-like kinase. Mol Biol Cell *6*, 119-134.

Mueller, P.R., Coleman, T.R., Kumagai, A., and Dunphy, W.G. (1995b). Myt1: a membrane-associated inhibitory kinase that phosphorylates Cdc2 on both threonine-14 and tyrosine-15. Science *270*, 86-90.

Muller, H., Fogeron, M.L., Lehmann, V., Lehrach, H., and Lange, B.M. (2006). A centrosome-independent role for gamma-TuRC proteins in the spindle assembly checkpoint. Science *314*, 654-657.

Nigg, E.A. (2001). Mitotic kinases as regulators of cell division and its checkpoints. Nat Rev Mol Cell Biol *2*, 21-32.

Nigg, E.A. (2002). Centrosome aberrations: cause or consequence of cancer progression? Nat Rev Cancer *2*, 815-825.

Nigg, E.A., and Raff, J.W. (2009). Centrioles, centrosomes, and cilia in health and disease. Cell *139*, 663-678.

Nogales-Cadenas, R., Abascal, F., Diez-Perez, J., Carazo, J.M., and Pascual-Montano, A. (2009). CentrosomeDB: a human centrosomal proteins database. Nucleic Acids Res *37*, D175-180.

Nonaka, S., Tanaka, Y., Okada, Y., Takeda, S., Harada, A., Kanai, Y., Kido, M., and Hirokawa, N. (1998). Randomization of left-right asymmetry due to loss of nodal cilia generating leftward flow of extraembryonic fluid in mice lacking KIF3B motor protein. Cell *95*, 829-837.

O'Toole, E.T., McDonald, K.L., Mantler, J., McIntosh, J.R., Hyman, A.A., and Muller-Reichert, T. (2003). Morphologically distinct microtubule ends in the mitotic centrosome of Caenorhabditis elegans. J Cell Biol *163*, 451-456.

Okuda, M. (2002). The role of nucleophosmin in centrosome duplication. Oncogene *21*, 6170-6174.

Ostrowski, L.E., Blackburn, K., Radde, K.M., Moyer, M.B., Schlatzer, D.M., Moseley, A., and Boucher, R.C. (2002). A proteomic analysis of human cilia: identification of novel components. Mol Cell Proteomics *1*, 451-465.

Paintrand, M., Moudjou, M., Delacroix, H., and Bornens, M. (1992). Centrosome organization and centriole architecture: their sensitivity to divalent cations. J Struct Biol *108*, 107-128.

Palazzo, R.E., Vogel, J.M., Schnackenberg, B.J., Hull, D.R., and Wu, X. (2000). Centrosome maturation. Curr Top Dev Biol *49*, 449-470.

Parker, L.L., Atherton-Fessler, S., and Piwnica-Worms, H. (1992). p107wee1 is a dual-specificity kinase that phosphorylates p34cdc2 on tyrosine 15. Proc Natl Acad Sci U S A *89*, 2917-2921.

Peel, N., Stevens, N.R., Basto, R., and Raff, J.W. (2007). Overexpressing centriole-replication proteins in vivo induces centriole overduplication and de novo formation. Curr Biol *17*, 834-843.

Pelletier, L., O'Toole, E., Schwager, A., Hyman, A.A., and Muller-Reichert, T. (2006). Centriole assembly in Caenorhabditis elegans. Nature *444*, 619-623.

Peter, M., Nakagawa, J., Doree, M., Labbe, J.C., and Nigg, E.A. (1990). In vitro disassembly of the nuclear lamina and M phase-specific phosphorylation of lamins by cdc2 kinase. Cell *61*, 591-602.

Petronczki, M., Lenart, P., and Peters, J.M. (2008). Polo on the Rise-from Mitotic Entry to Cytokinesis with Plk1. Dev Cell *14*, 646-659.

Piel, M., Meyer, P., Khodjakov, A., Rieder, C.L., and Bornens, M. (2000). The respective contributions of the mother and daughter centrioles to centrosome activity and behavior in vertebrate cells. J Cell Biol *149*, 317-330.

Piel, M., Nordberg, J., Euteneuer, U., and Bornens, M. (2001). Centrosome-dependent exit of cytokinesis in animal cells. Science *291*, 1550-1553.

Pines, J. (2006). Mitosis: a matter of getting rid of the right protein at the right time. Trends Cell Biol *16*, 55-63.

Portier, N., Audhya, A., Maddox, P.S., Green, R.A., Dammermann, A., Desai, A., and Oegema, K. (2007). A microtubule-independent role for centrosomes and aurora a in nuclear envelope breakdown. Dev Cell *12*, 515-529.

Prigent, C., Glover, D.M., and Giet, R. (2005). Drosophila Nek2 protein kinase knockdown leads to centrosome maturation defects while overexpression causes centrosome fragmentation and cytokinesis failure. Exp Cell Res *303*, 1-13.

Prigozhina, N.L., Oakley, C.E., Lewis, A.M., Nayak, T., Osmani, S.A., and Oakley, B.R. (2004). gamma-tubulin plays an essential role in the coordination of mitotic events. Mol Biol Cell *15*, 1374-1386.

Quintyne, N.J., Reing, J.E., Hoffelder, D.R., Gollin, S.M., and Saunders, W.S. (2005). Spindle multipolarity is prevented by centrosomal clustering. Science *307*, 127-129.

Rajagopalan, S., Bimbo, A., Balasubramanian, M.K., and Oliferenko, S. (2004). A potential tension-sensing mechanism that ensures timely anaphase onset upon metaphase spindle orientation. Curr Biol *14*, 69-74.

Reinders, Y., Schulz, I., Graf, R., and Sickmann, A. (2006). Identification of novel centrosomal proteins in Dictyostelium discoideum by comparative proteomic approaches. J Proteome Res *5*, 589-598.

Reinton, N., Collas, P., Haugen, T.B., Skalhegg, B.S., Hansson, V., Jahnsen, T., and Tasken, K. (2000). Localization of a novel human A-kinase-anchoring protein, hAKAP220, during spermatogenesis. Dev Biol *223*, 194-204.

Roghi, C., Giet, R., Uzbekov, R., Morin, N., Chartrain, I., Le Guellec, R., Couturier, A., Doree, M., Philippe, M., and Prigent, C. (1998). The Xenopus protein kinase pEg2 associates with the centrosome in a cell cycle-dependent manner, binds to the spindle microtubules and is involved in bipolar mitotic spindle assembly. J Cell Sci *111 (Pt 5)*, 557-572.

Roninson, I.B., Broude, E.V., and Chang, B.D. (2001). If not apoptosis, then what? Treatment-induced senescence and mitotic catastrophe in tumor cells. Drug Resist Updat *4*, 303-313.

Rout, M.P., and Kilmartin, J.V. (1990). Components of the yeast spindle and spindle pole body. J Cell Biol *111*, 1913-1927.

Satir, P., and Christensen, S.T. (2007). Overview of structure and function of mammalian cilia. Annu Rev Physiol *69*, 377-400.

Schatten, H. (2008). The mammalian centrosome and its functional significance. Histochem Cell Biol *129*, 667-686.

Schmidt, T.I., Kleylein-Sohn, J., Westendorf, J., Le Clech, M., Lavoie, S.B., Stierhof, Y.D., and Nigg, E.A. (2009). Control of centriole length by CPAP and CP110. Curr Biol *19*, 1005-1011.

Schmit, A.C. (2002). Acentrosomal microtubule nucleation in higher plants. Int Rev Cytol *220*, 257-289.

Schnackenberg, B.J., Khodjakov, A., Rieder, C.L., and Palazzo, R.E. (1998). The disassembly and reassembly of functional centrosomes in vitro. Proc Natl Acad Sci U S A *95*, 9295-9300.

Sibon, O.C., Kelkar, A., Lemstra, W., and Theurkauf, W.E. (2000). DNA-replication/DNA-damage-dependent centrosome inactivation in Drosophila embryos. Nat Cell Biol *2*, 90-95.

Silkworth, W.T., Nardi, I.K., Scholl, L.M., and Cimini, D. (2009). Multipolar spindle pole coalescence is a major source of kinetochore mis-attachment and chromosome mis-segregation in cancer cells. PLoS One *4*, e6564.

Singla, V., and Reiter, J.F. (2006). The primary cilium as the cell's antenna: signaling at a sensory organelle. Science *313*, 629-633.

Sluder, G. (2005). Two-way traffic: centrosomes and the cell cycle. Nat Rev Mol Cell Biol *6*, 743-748.

Srsen, V., Gnadt, N., Dammermann, A., and Merdes, A. (2006). Inhibition of centrosome protein assembly leads to p53-dependent exit from the cell cycle. J Cell Biol *174*, 625-630.

Stracke, R., Bohm, K.J., Wollweber, L., Tuszynski, J.A., and Unger, E. (2002). Analysis of the migration behaviour of single microtubules in electric fields. Biochem Biophys Res Commun *293*, 602-609.

Sunkel, C.E., and Glover, D.M. (1988). polo, a mitotic mutant of Drosophila displaying abnormal spindle poles. J Cell Sci *89 (Pt 1)*, 25-38.

Takada, S., Kelkar, A., and Theurkauf, W.E. (2003). Drosophila checkpoint kinase 2 couples centrosome function and spindle assembly to genomic integrity. Cell *113*, 87-99.

Theurkauf, W.E., and Hawley, R.S. (1992). Meiotic spindle assembly in Drosophila females: behavior of nonexchange chromosomes and the effects of mutations in the nod kinesin-like protein. J Cell Biol *116*, 1167-1180.

Tsou, M.F., and Stearns, T. (2006). Mechanism limiting centrosome duplication to once per cell cycle. Nature *442*, 947-951.

Tsou, M.F., Wang, W.J., George, K.A., Uryu, K., Stearns, T., and Jallepalli, P.V. (2009). Polo kinase and separase regulate the mitotic licensing of centriole duplication in human cells. Dev Cell *17*, 344-354.

Uetake, Y., Loncarek, J., Nordberg, J.J., English, C.N., La Terra, S., Khodjakov, A., and Sluder, G. (2007). Cell cycle progression and de novo centriole assembly after centrosomal removal in untransformed human cells. J Cell Biol *176*, 173-182.

van den Heuvel, M.G., de Graaff, M.P., Lemay, S.G., and Dekker, C. (2007). Electrophoresis of individual microtubules in microchannels. Proc Natl Acad Sci U S A *104*, 7770-7775.

Vassilev, P., and Kanazirska, M. (1985). The role of cytoskeleton in the mechanisms of electric field effects and information transfer in cellular systems. Med Hypotheses *16*, 93-96.

Wadsworth, P., and Khodjakov, A. (2004). E pluribus unum: towards a universal mechanism for spindle assembly. Trends Cell Biol *14*, 413-419.

Wakefield, J.G., Huang, J.Y., and Raff, J.W. (2000). Centrosomes have a role in regulating the destruction of cyclin B in early Drosophila embryos. Curr Biol *10*, 1367-1370.

Wigge, P.A., Jensen, O.N., Holmes, S., Soues, S., Mann, M., and Kilmartin, J.V. (1998). Analysis of the Saccharomyces spindle pole by matrix-assisted laser desorption/ionization (MALDI) mass spectrometry. J Cell Biol *141*, 967-977.

Wong, C., and Stearns, T. (2003). Centrosome number is controlled by a centrosome-intrinsic block to reduplication. Nat Cell Biol *5*, 539-544.

Yamashita, Y.M., Jones, D.L., and Fuller, M.T. (2003). Orientation of asymmetric stem cell division by the APC tumor suppressor and centrosome. Science *301*, 1547-1550.

Yang, J., Adamian, M., and Li, T. (2006). Rootletin interacts with C-Nap1 and may function as a physical linker between the pair of centrioles/basal bodies in cells. Mol Biol Cell *17*, 1033-1040.

Yang, Z., Loncarek, J., Khodjakov, A., and Rieder, C.L. (2008). Extra centrosomes and/or chromosomes prolong mitosis in human cells. Nat Cell Biol *10*, 748-751.

Zavortink, M., Contreras, N., Addy, T., Bejsovec, A., and Saint, R. (2005). Tum/RacGAP50C provides a critical link between anaphase microtubules and the assembly of the contractile ring in Drosophila melanogaster. J Cell Sci *118*, 5381-5392.

Zhai, B., Villen, J., Beausoleil, S.A., Mintseris, J., and Gygi, S.P. (2008). Phosphoproteome analysis of Drosophila melanogaster embryos. J Proteome Res *7*, 1675-1682.

Zhao, M., Forrester, J.V., and McCaig, C.D. (1999). A small, physiological electric field orients cell division. Proc Natl Acad Sci U S A *96*, 4942-4946.

Zheng, Y., Wong, M.L., Alberts, B., and Mitchison, T. (1995). Nucleation of microtubule assembly by a gamma-tubulin-containing ring complex. Nature *378*, 578-583.

6 Appendix

6.1 Summary

In this work, immunoisolated centrosomes from *Drosophila* syncytial embryos were used to investigate biophysical properties of this organelle and for a proteomic analysis that facilitated the identification and functional characterization of centrosomal proteins. The functional analysis aimed at elucidating the role of identified proteins in the maintenance of centrosome integrity, maturation, duplication, separation and cell cycle progression. With regard to the centrosome's biophysical properties, laser-based optical manipulation of individual organelles revealed the centrosome as a negatively charged protein complex and that the centrosome structure is modulated by its own electric field in a pH-dependent manner. The MS-analysis of isolated centrosomes identified 260 centrosomal candidate proteins, which were subsequently studied by RNAi in *Drosophila* cultured cells. Immunofluorescence microscopy and FACS was used to analyze the resulting phenotypes. A set of 11 proteins was found to be critical for centrosome structure maintenance as depletion of any of these proteins in *Drosophila* SL2 cells resulted in centrosome disintegration, revealing a molecular dependency of centrosome structure on components of the protein translational machinery, actin and nuclear proteins. In total, novel centrosome related functions were assigned to 27 proteins, of which 14 were confirmed in human cells via siRNA mediated depletion of homologous proteins. Furthermore, the analysis of human orthologues revealed a high level of functional conservation for proteins implicated in centrosome duplication and separation. In addition to the whole proteome analysis of the *Drosophila* centrosome, a second proteomic study aimed at identifying centrosomal kinase substrates and elucidating their function. By enriching phosphopeptides from centrosomal preparations prior to MS analysis, 45 phosphorylation sites, of which 17 have not been described before, were identified in 27 proteins. All MS-identified phosphoproteins were functionally characterized and integrated into regulatory signaling networks with the 3 most important mitotic kinases, cdc2, polo, aur, as well as the house keeping kinase CkIIβ. Using a combinatorial RNAi strategy, novel functions for P granule, nuclear envelope and nuclear proteins in centrosome duplication, maturation and separation were revealed. For a subset of phosphoproteins, we identified previously unknown centrosome and/or spindle localization via expression of tagged fusion proteins in cultured cells. In conclusion, this work comprises a comprehensive molecular and functional description of the *Drosophila* centrosome and moreover the first inventory of *in vivo* centrosome-specific phosphorylation residues. It thereby provides an important prerequisite for future studies to gain deeper insights into the mechanisms that underlie this organelle's biogenesis and its diverse functions throughout the cell cycle and in cellular signaling.

6.2 Zusammenfassung

In der vorliegenden Arbeit wurden immun-isolierte Zentrosomen synzytialer *Drosophila*-Embryonen zur Untersuchung der biophysikalischen Beschaffenheit dieses Zellorganells verwendet. Desweiteren wurde eine Proteomanalyse zur Identifizierung und funktionellen Charakterisierung zentrosomaler Proteine durchgeführt. Die funktionelle Analyse verfolgte das Ziel, die Rolle identifizierter Proteine in der Aufrechterhaltung zentrosomaler Struktur, in zentrosomaler Reifung, Verdopplung und Separation sowie Zellzyklus-Fortschritt aufzuklären. Bezüglich der biophysikalischen Eigenschaften des Zentrosoms ergab die Laser-basierte optische Manipulation einzelner Zentrosomen, dass dieser Proteinkomplex eine negative Ladung trägt. Darüber hinaus konnte gezeigt werden, dass die Struktur des Zentrosoms in einer pH-abhängigen Weise durch das selbst erzeugte elektrische Feld moduliert wird. Die MS-Analyse isolierter Zentrosomen führte zur Identifizierung von 260 Proteinen, welche anschließend mittels RNAi in kultivierten *Drosophila*-Zellen untersucht wurden. Die daraus resultierenden Phänotypen wurden mit Immunfluoreszenz-Mikroskopie und FACS ausgewertet. Diese Analyse zeigte, dass eine Gruppe von 11 Proteinen eine kritische Rolle in der Aufrechterhaltung der zentrosomalen Struktur spielt, da ihr Abbau zum Zerfall des Proteinkomplexes führte. Hierbei wurde eine Abhängigkeit von Komponenten der Translationsmaschinerie, sowie Actin und nukleären Proteinen aufgedeckt. Insgesamt wurde 27 Proteinen eine neue Zentrosomen-bezogene Funktion zugeordnet, von denen 14 durch siRNA-vermittelten Abbau der homologen Proteine in humanen Zellen bestätigt wurden. Die Analyse humaner Orthologe zeigte zudem einen hohen Grad an funktioneller Konservierung der Proteine, die in die Verdopplung und Separation von Zentrosomen impliziert sind. Zusätzlich zu der Gesamt-Proteomanalyse des *Drosophila*-Zentrosoms sollten in einer zweiten Proteomstudie die Substrate zentrosomaler Kinasen identifiziert sowie deren Funktion aufgeklärt werden. Durch die Anreicherung von Phosphopeptiden aus zentrosomalen Präparaten und deren anschließender MS-Analyse wurden 45 Phosphorylierungsstellen in 27 Proteinen identifiziert. 17 der 45 Phosphorylierungsstellen sind bisher nicht beschrieben worden. Alle MS-identifizierten Proteine wurden im Anschluss funktionell charakterisiert und in regulatorische Signalnetzwerke mit den 3 wichtigsten mitotischen Kinasen, cdc2, polo, aur sowie der `house-keeping´-Kinase CkIIβ integriert. Eine kombinatorische RNAi-Strategie deckte neue Funktionen in der Zentrosomen-Verdopplung, -Reifung und -Separation für Proteine der nukleären Hülle, Bestandteile von `P granules´ sowie nukleäre Proteine auf. Ausgewählte Phosphoproteine wurden als getaggte Fusionsproteine in *Drosophila*-Zellen exprimiert, wodurch bisher unbekannte Lokalisationen am Zentrosom beziehungsweise an der Spindel nachgewiesen wurden. Zusammenfassend kann gesagt werden, dass diese Arbeit eine umfassende molekulare und funktionelle Beschreibung des *Drosophila*-Zentrosoms und darüber hinaus die erste Bestandsliste

Zentrosomen-spezifischer *in vivo* Phosphorylierungs-Stellen beinhaltet. Insofern stellt die vorliegende Arbeit eine wichtige Grundlage für zukünftige Studien dar, die ein besseres molekulares Verständnis der Mechanismen der Zentrosomenbiogenese und der verschiedenen zentrosomalen Funktionen im Zellzyklus sowie in zellulären Signalwegen ermöglichen wird.

6.3 Curriculum vitae

For reasons of privacy protection, a complete CV is not included in the electronic version of the thesis.

6.4 Acknowledgements

First of all, I want to thank Bodo Lange for his excellent supervision, support and patience throughout the past years. Though there were times when it seemed there was no light at the end of the tunnel, he always pulled through.

I wish to also thank Prof Schuster from the FU for reviewing this thesis. I'm grateful too to Hans Lehrach for giving me opportunity to work in his department.

Thanks to the people at Centro Nacional de Biotecnología in Madrid for a pleasant and productive collaboration. Special thanks to the High Content Screening group at the FMP in Buch for assistance on the phosphoproteome project. Even though I was a temporary fixture in their lab for several months I never felt like a stranger.

A big shout out to all members of the Lange group. Thanks for making the day-to-day routine a pleasant one. Getting up out of bed in the morning never felt like a chore at least in a work context. I'm particularly thankful to Hannah Müller and Verena Lehmann who contributed enormously to this work. I couldn’t have done it without you!

To all the colleagues and friends I made over my time at the institute. Cheers for the memories, nights out, hangovers, spring/summer/autumn and winter parties, bbq's & AWB's. Great to know we can all work by day and freak out when we need to.

Also to my friends outside the lab, thanks for being around when I needed a bit of fresh air. To my parents for being simply that, standing tall and firm behind me. Thanks for having me, and making me into the person I am.

6.5 Selbständigkeitserklärung

Hiermit erkläre ich, dass ich diese Arbeit selbst verfasst habe sowie keine anderen als die angegebenen Quellen und Hilfsmittel in Anspruch genommen habe. Ich versichere, dass diese Arbeit in dieser oder anderer Form keiner anderen Prüfungsbehörde vorgelegt wurde.

Karin Habermann Berlin, April 2010